INVESTIGATING THE ROLE OF SEROTONIN IN OLFACTORY GUIDED BEHAVIOR AND NEUROPHYSIOLOGY

A Dissertation

Presented to the Faculty of the Graduate School

of Cornell University

In Partial Fulfillment of the Requirements for the Degree of

Doctor of Philosophy

by

Matt Lewis

December 2017

INVESTIGATING THE ROLE OF SEROTONIN IN OLFACTORY GUIDED BEHAVIOR AND NEUROPHYSIOLOGY

Matt Lewis, Ph. D.

Cornell University 2017

The work presented in this thesis is a series of investigations relating to how serotonin (5-HT) modulates for olfactory behavior and network physiology. 5-HT is a neuromodulator which has been associated with a variety of neural functions including rhythmic pattern generation, reward processing, and sensory processing. I first focused my attention on how 5-HT may modulate olfactory guided behavior using a behavioral pharmacological approach. Within the habituation task we found that infusion of a 5-HT2 receptor antagonist, cinanserin, impaired habituation memory at low (0.001 Pa) odor concentrations, and impaired spontaneous discrimination at all odor concentrations test (0.001, 0.01, and 0.1 Pa). Within the forced choice discrimination task we found a significant reduction in task performance following cinanserin infusion. When sampling behavior and decision times were analyzed, we found that cinanserin infusion significantly increased decision latencies only at one carbon difference tests at 0.01 and 0.1 Pa concentrations. While rats were slower to choose the odor pots at these odor concentrations they were equivalent in accuracy in the task. Put in a speed/accuracy tradeoff context, we found that when animals were asked to discriminate between similar odorants, accuracy is maintained and the expense of speed. Later in my Ph.D. work I moved to studying how 5-HT modulates the olfactory bulb network activity using an extracellular multi-electrode array. Utilizing a horizontal brain slice preparation, I performed extracellular recordings following

serotonin application and the use the 5-HT2 receptor antagonist, cinanserin. Using signal processing techniques, we analyzed the effects of 5-HT on multiunit activity (MUA) and local field potentials (LFP). Within the LFP we focused our analysis on two frequency bands, theta (1-10 Hz) and gamma (20-55 Hz). We found that 5-HT increased MUA and increased power in both the theta and gamma bands. These effects were shown to be 5-HT2 receptor dependent because they were not detected when slices were first perfused with cinanserin. These behavioral and physiological results demonstrate that 5-HT2 receptors are necessary for non-associative and associative odor memory and that 5-HT plays an important role in the modulation of olfactory bulb network dynamics.

BIOGRAPHICAL SKETCH

Matt Lewis received his Bachelor of Science at the University of Minnesota in 2009 with a double major in biochemistry and neuroscience. There the well-rounded education in the biological science lead to a deep interest in animal behavior and neuroscience. At the University of Minnesota, Matt performed undergraduate research, studying both the chemical ecology of bark beetles and neuroethology of the medicinal leech. These undergraduate research experiences helped pursuade him that academic science was his path forward.

After graduating from the University of Minnesota, Matt entered the graduate program of the Department of Neurobiology and Behavior at Cornell University where, in, 2010, he joined the lab of Dr. Christiane Linster. While completing his doctoral research in Dr. Linster's lab, Matt spent six years as a teaching assistant for both general biology and Neurobiology specific courses. Upon obtaining his Ph.D. in the summer of 2017, Matt will be joining the Lab of Dr. Jeremiah Cohen at Johns Hopkins University as a Postdoctoral Scholar.

ACKNOWLEDGEMENTS

This thesis would not have been possible without the assistance of a large number of people. First I would like to acknowledge my lab mates, Dr. Sasha Devore, Dr. Shane Peace, and Matt Einhorn. Without their hard work and friendship a lot of this may not have been possible. Secondly I would like to acknowledge the members of the Bass lab, notably Drs. Ni Feng and Andy Bass, for their strong material and intellectual support throughout my time in graduate school. I would also like to thank the staff of NBB for their professionalism during my time here in the department. Lastly, I would like to acknowledge my parents, Robert and Cheryl Lewis, for their unconditional support during my studies.

TABLE OF CONTENTS

LIST OF FIGURES

CHAPTER 1

INTRODUCTION

Neuromodulation is a biophysical process through which chemicals released from neurons, known as neuromodulators, modify and tune cellular, synaptic, and neural network properties dependent on task demands and behavioral state of the animal. Neuromodulatory neurons may either be intrinsic to an affected neural circuit or located in distal brain regions providing centrifugal inputs to many brain regions. concurrently. Rather than transmitting information about ongoing stimuli, neuromodulatory inputs instead are thought to dynamically alter neural representations in a manner related to environmental events and/or the brains internal state (Hurley et al. 2004; Devore and Linster 2012). Serotonin (5-HT) is an important mediator of these functional changes; its function and characteristics will be reviewed in detail in this chapter.

Serotonergic neuromodulation of sensory processing

In vertebrates, the majority of sensory circuits receive centrifugal serotonergic inputs from the median raphé (MRN) and dorsal raphé nuclei (DRN) located along the midline of the brainstem. Interestingly, DRN neurons receive inputs from many sensory processing regions, including the retina and vestibular nuclei (Kawano et al.1996; Ye and Kim 2001). It should be noted that the majority of DRN inputs are not from sensory structures but instead from other raphé nuclei, midbrain, and cortical structures (Hornung 2010, Ogawa et al. 2014). Tonic DRN activity is tied to the phase of the sleep-wake cycle, with activity highest during the waking state. Compared to alert waking states, DRN neurons show decreased tonic activity during quiet waking

states, even less activity during slow-wave sleep, and are completely silent during rapid-eye movement (REM) sleep (Jacobs and Fornal 1999). DRN neurons also respond transiently to particular types of sensory stimuli (Heym et al.1982; Ranade and Mainen 2009). Lastly, recent work has suggested that DRN neurons may be transmitting signals related to features of behavioral paradigms such as reward, aversion, and executive control (Miyazaki et al. 2011; Nakamura 2008).

5-HT has been shown to modulate sensory responses across a number of neural structures across species and sensory modalities (Andersen et al. 1982; Kloppenburg and Erber 1995; Mooneyet al.1996; Hurley and Pollak 1999; Xiang and Prince 2003; Kloppenburg and Mercer 2008; Dacks et al.2009). In many regions of the brain, patterns of neuromodulatory input are highly heterogeneous and differentially target particular neuron types within specific sensory circuits (McLean and Shipley 1979; Klepper and Herbert 1991; Mooney et al.1996; Kang et al.2001; Paspalas and Papadopoulos 2001). Through complex innervation patterns and the multitude of 5-HTRs expressed within sensory circuits, 5-HT induces a variety of effects on sensory representations from gross attenuation (Petzold et al. 2009) or enhancement (Hurley and Pollak 2001; Deemyad et al. 2013) to alteration of receptive field structure (Hurley and Pollak 1999; Dacks et al 2009) and changes in neural sensitivity to environmental cues (Kloppenburg and Mercer 2008; Yokogawa et al. 2012).

In this thesis I present work looking at how serotonin modulates olfactory behavior and neurophysiology. To begin I will provide a short review of olfactory processing within the olfactory bulb and how neuromodulators affect these proposed circuit mechanisms.

Olfactory Processing

Olfactory stimuli are transduced by olfactory sensory neurons (OSNs) which reside within the nasal epithelium. Odorants taken in via respiration dissolve into the mucus layer of the nasal epithelium and interact with extracellular domains of olfactory receptor proteins (ORs), a group of G-protein coupled receptors. These interactions trigger intracellular signaling cascades that lead to depolarization of the OSN and evoke action potentials, where the number of action potentials is a function of the intensity of the odorant evoked depolarization (Pifferi et al. 2010, Rospars et al. 2000). The axons of OSNs project directly into the telencephalon and innervate glomeruli within the main olfactory bulb (MOB). OSNs expressing the same OR gene converge on discrete structures of neuropil known as glomeruli (Fig. 1) Within a single glomerulus, OSN axons interact with MOB principal cells, the mitral/tufted cells (MTCs) and three distinct interneuron types: external tufted cells (ETCs), and periglomerular cells (PGCs) and short-axon cells (SACs). ETCs are glutamatergic and have a single dendrite which branches widely within one glomerulus, an axon projecting out of the glomerular layer (GL), and generate bursts of action potentials (Hayer et al. 2004, Pinching and Powell, 1971). PGCs are GABAergic and inhibit mitral cells. SACs receive little direct OSN input and instead are mostly innervated by ETCs (Kiyokage et al. 2010). SACs have dendrites in 2-4 glomeruli and project neural processes up to 1 mm in length across the GL (Aungst et al. 2003). SACs have been shown to be both dopaminergic and GABAergic (Kiyokage et al. 2010). The glomerulus is the first site of synaptic integration within the MOB and can be conceived as the first stage of computation within the MOB (Cleland 2010).

GL circuits at this stage have been proposed to regulate contrast and create concentration invariant representations of olfactory stimuli (Cleland and Linster, 2006; Cleland and Setupathy, 2003) and recent experimental evidence has provided strong

support for these claims (Banerjee 2015, Fukanaga et al. 2014). Unlike in the visual and auditory systems, olfactory representations in the GL are not arranged in a topographical manner that is predictive of their receptive field (Soucy et al. 2009), suggesting that nearest-neighbor or proximity-dependent inter-glomerular synaptic interactions, akin to lateral inhibition in the retina, are unable to effectively decorrelate overlapping neural representations (Cleland et al. 2010). Instead, intra-glomerular synaptic interactions have been proposed to perform decorrelation of olfactory representations. This circuit algorithm is known as non-topographical contrast enhancement (Cleland and Sethupathy 2006). Briefly, a population of inhibitory PGCs which receive direct input from OSNs inhibit MTCs in a feed-forward manner. Due to the increased input resistance of PGCs compared to MTCs, PGCs will become more depolarized than MTCs to the incoming OSN activity. This increased inhibition leads to a hyperpolarization of the MTC apical dendrite and prevents MTC firing. Only when the incoming sensory input is of a high enough activity level will MTCs become activated. This process leads to a ligand-affinity based receptive field. When odorants have a moderate affinity for ORs, PGCs will win out and inhibit MTCs, and when odorants have a high affinity for the activated OR, excitation of MTCs will win out and MTCs will fire action potentials. When odorants have very low affinity for ORs, no incoming signal reaches the glomerulus or it is of a small enough intensity that there is no effect on both PGCs and MTCs. It is important to note that PGCs do not need to fire action potentials to inhibit MTCs allowing for graded inhibition of MTCs in response to incoming OSN input (Cleland and Sethupathy, 2006, Cleland et al. 2010).

Along with performing contrast enhancement, glomerular circuits are thought to perform global normalization. As odor concentrations increase, olfactory representations get broader and OSNs fire more action potentials but MTCs do not

Figure 1

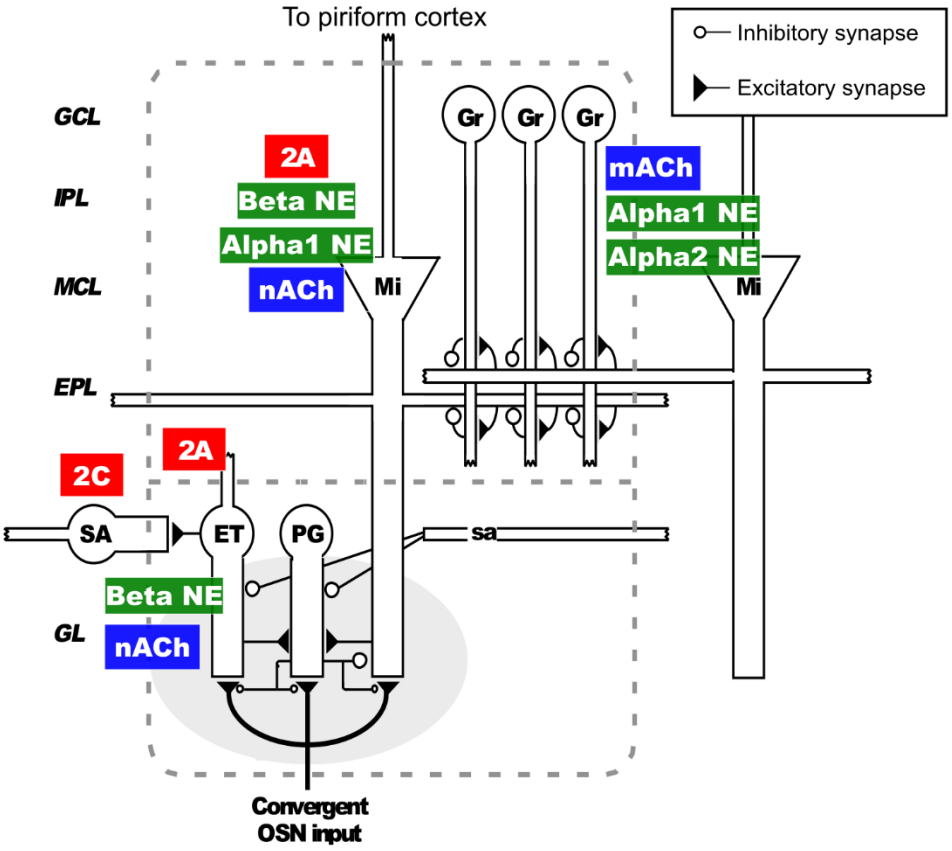
To piriform cortex
Inhibitory synapse
Excitatory synapse
GCL
IPL
MCL
EPL
GL
2A
Beta NE
Alpha1 NE
nACh
Mi
Gr
Gr
Gr
mACh
Alpha1 NE
Alpha2 NE
Mi
2A
2C
SA
ET
PG
sa
Beta NE
nACh
Convergent
OSN input

Figure 1.. A. Olfactory bulb. Sensory information, transduced by olfactory sensory neurons in the olfactory epithelium (OE) is projected to target neurons in the glomerular layer (GL) of the OB. Local microcircuits, comprised of periglomerular (PG), external tufted (ET) and short axon (SA) cells process the incoming information. This layer of bulbar processing is thought to be involved in contrast and normalization processes. The resulting activity of mitral cells (Mi) is then further processed in the external plexiform layer (EPL), where Mi cells interact with granule cells (Gr). The mutual interactions between these groups of cells and additional interneurons not depicted here are thought to create oscillatory dynamics that serve to synchronize Mi cell outputs towards olfactory secondary cortices. Receptors for ACh, NE and 5HT are numerous and organized in a laminar fashion throughout the bulbar layers including GL, EPL, internal plexiform layer (IPL) and granule cell layer (GCL) (nACh: nicotinic, mACh: muscarinic).

follow this pattern. This stability of bulbar output in response to changing glomerular inputs requires gain control mechanisms in early olfactory processing. Theoretical modeling (Cleland et al. 2007) and now neurophysiology data (Banerjee et al. 2014) suggest that this computation is occurring within the GL via extensive interglomerular connectivity mediated by SACs. ET cells, driven by afferent OSN activity activate SACs which themselves project widely across the GL and are thought to project a global average of activity across the bulb. While the precise circuit details remain to be figured out, SACs have been shown to inhibit MTCs across the GL and ablation of SACs increased correlations of MTCs to odors, and MTCs showed much reduced concentration invariance. Following synaptic integration in the GL, MTCs project further to a second stage of processing with a second group of local interneurons, predominantly with inhibitory granule cells (GCs) within the external plexiform layer (EPL). The EPL is a synaptic layer within the MOB, and is the site of dendrodendritic connections between MTCs and GCs. (Shepherd 1972). Neurobiologists have proposed that these dendrodenritic connections perform decorrelation of olfactory bulb representations via a process very similar to lateral inhibition in the retina. Briefly, following depolarization and spike generation within MTCs in response to sufficient feedforward odor input, evoked action potentials travel along the long, lateral dendrites of MTCs which in turn activate the GC dendrites (Egger and Urban, 2002). These inhibitory GCs then become depolarized and inhibit the lateral dendrite providing a source of negative feedback but also may inhibit neighboring lateral dendrites. This idea has been long held within the field of olfactory neurobiology, but it suffers from at least two limitations. First MTC lateral dendrites extend widely across the EPL and do not solely interact with granule cells within a close proximity (Willhite et al. 2006). Secondly, modeling work suggests that, while granule cells inhibit MTCs, they are insufficient to block action potential generation in the soma of

MTCs and instead are only able to delay action potential propagation along MTC lateral dendrites through shunting inhibition (David et al. 2008; McIntyre and Cleland 2016).

While nearest neighbor lateral inhibition is unlikely to occur for the reasons mentioned above, the role of synaptic connections within the EPL in bulbar computations is not completely understood and could decorrelate inputs by modulating spiking timing and synchronization (Cleland 2010, Devore and Linster 2014). The circuitry of the EPL has been shown to be an important component of the circuit activity producing gamma oscillations within the MOB (Bathellier et al. 2006, Friedman and Strowbridge 2003, Fukanaga et al. 2014, Lagier et al. 2004, Lepousez et al. 2013, Neville and Haberly, 2003). Gamma oscillations are oscillations within extracellular waveforms at frequency ranges *in vivo* between ~40-100 Hz, and 20-55 Hz *in vitro* recorded in the local field potential (LFP). A proposed circuit mechanism for the generation of gamma oscillations is as follows: incoming afferent input from OSNs depolarizes MTCs and evokes action potentials; these action potentials travel along lateral dendrites and depolarize GCs. The activated GCs provide negative feedback to MTCs and decrease MTC excitation. This resultant inhibition of MTCs then leads to GCs losing their excitatory drive and repolarizing. When the olfactory nerve is firing repeatedly, this process repeats, producing gamma oscillations. (Rojas-Libano and Kay 2008).

While gamma oscillations have been studied for quite a while, the functional significance of gamma oscillations within the vertebrate olfactory bulb is still not well understood, but some studies have begun to make headway on the issue. Nusser et al. 2001 used a genetic mouse model that lacks the **β3** subunit of the $GABA_A$ receptor. GCs are the only cells in the MOB that express the **β3** subunit. Compared to wild type control, these mutant mice showed increased gamma power within the LFP and

showed better discrimination ability between two similar odors. Interestingly the same study showed that β3-null mutants actually performed worse than controls when discriminating odor mixtures, suggesting that positive modulation of gamma is not always associated with increased task performance. Later work by Beshel et al (2007) showed that gamma oscillations increased in power when rats were making fine odor discriminations compared to when rats were making coarse discriminations. The mechanism for this increase in gamma power in response to task demands is not at all understood. Recent work has provided more evidence for the finding that "more gamma" is not always better for sensory discriminations. Lepousez and Lledo (2013) reported that following infusion of $GABA_A$ antagonists into the bulb, gamma oscillations decreased in power, as would be predicted from the model described above. Intriguingly they found that 40-50 min post infusion, gamma power was greatly increased from baseline levels. When mice were tested on a sensory discrimination task during these pharmacologically increased gamma periods, they performed worse than non-manipulated mice. These findings suggest that neural circuits within the EPL have strong effects on gamma range oscillatory power but the relationship between these oscillations and cognition is far from clear

Neuromodulation of olfactory processing

As mentioned above, neuromodulators can manipulate sensory responses in a variety of ways. This is also true within the olfactory bulb (Fig. 1). Within the olfactory bulb, neuromodulators play a critical role in modifying contrast enhancement, signal-to-noise, and experience dependent plasticity (Fletcher and Chen 2010, Linster and Fontanini 2014). Here I will briefly review the literature regarding the role of acetylcholine (ACh) and norepinephrine (NE) as neuromodulators in the olfactory bulb. ACh has been shown to modulate the behavioral discrimination of

perceptually and chemically similar odors, and it is suggested it occurs though modulation of the circuitry underlying contrast enhancement within the GL (Devore and Linster 2014). Using an olfactory habituation paradigm, rats infused with a nicotinic acetylcholine receptor antagonist showed impaired spontaneous discrimination of novel odorants following repeated presentation of a structurally similar odor. Conversely when, an acetylcholinesterase inhibitor, a drug which inhibits the breakdown of ACh, is infused into the bulb prior to testing, spontaneous discrimination of structurally similar odorants was increased (Mandairon et al. 2006). Nicotinic ACh receptors (nAChRs) are present within the GL and are expressed in both MTCs and PGCs (Castillo et al. 1999) and *in vivo* neurophysiology results showed that manipulations of nAChRs enhanced the selectivity of mitral cells to odorants (Chaudhury et al. 2009). Recent behavioral evidence supports this idea. Using a two-alternative forced choice (2AFC) task, rats were impaired in odor learning following nAChR antagonist infusion only when they had to discriminate between structurally similar odorants (Devore e al. 2014).

Muscarinic acetylcholine receptors (mAChRs) are in the granule cell layer (GCL) of the MOB and have been implicated in modulating synchronization of mitral cell activity (Devore and Linster et al. 2014) Behaviorally, muscarinic receptors have been shown to be important during a delayed match-to-sample task (Ravel et al. 1994), and in the same 2AFC task mentioned above, rats showed broad decrements in odor learning following intrabulbar infusion of a mAChR antagonist. At a mechanistic level, mAChRs have been shown to flip afterhyperpolarizations to afterdepolarizations within granule cells, making them more excitable (Pressler et al. 2007).

Norepinephrine (NE) has been associated with modulation of signal-to-noise within the MOB. Behaviorally, intrabular infusion of NA decreased odor detection thresholds (Escanilla et al. 2010). Mice infused with a combination of **α and β NA**

antagonists impaired their ability to discriminate perceptually similar odorants in a Go/No-Go task (Doucette et al. 2008). NE has also been shown to slow the acquisition of odor-reward learning in a forced choice discrimination task (Mandairon et al. 2008). Within the bulb, NA has been shown to increase responsiveness of MTCs to stimuli just below threshold and to decrease spontaneous mitral cell spontaneous activity (Jiang et al. 1996). Evidence suggests that this effect is due to direct excitation of mitral cells via noradrenergic **α1** receptors (Ciombor et al. 1999). NA also affects excitability of granule cells through both **α1 and α2 r**eceptor based mechanisms (see review by Linster et al. 2011 for further information).

Compared to ACh and NE, serotonin's actions in the MOB are not well understood. Within the MOB, serotonergic fibers are preferentially found within the GL and to a lesser degree in the EPL and GCL. Molecular work has shown that a variety of 5-HT receptors (5-HTRs) are found within the olfactory bulb (Mclean et al. 1995, Wright et al. 1995) but to date, known physiological effects are associated with 5-HT_2 receptors. In neonatal rats, release of 5-HT has been shown to be important for odor preference learning. Both chemical lesioning of 5-HT neurons and direct injection of a 5-HT_2 receptor antagonist into the neonatal MOB blocked the acquisition of an odor preference (McLean et al. 1993, 1996), but later it was found that memory odor preference learning is still possible in 5-HT depleted pups if the noradrenergic system is potently activated (Langdon et al. 1997). Compared to neonates, very little is known about the effects of 5-HT on odor perception in adult rodents. Studies using chemical lesioning methods showed that following 5-HT depletion, adult rats showed deficits in odor learning. In this one case chemical

lesioning methods lead to a significant period of cell death and loss of MOB volume. It is possible that the chemical lesioning effect was not truly 5-HT specific and that both other neuromodulatory and intrinsic bulbar circuitry was affected (Moriizumi et al. 1994).

At the neurophysiological level relatively more is known about the actions of 5-HT within the MOB, and as mentioned above the majority of the work implicates the 5-HT2 receptor as the source of most of its effects. Work performed *in vitro* has shown that 5-HT was found to directly depolarize some mitral cells via 5-HT_{2A} receptors, but in the same report the authors noted that some neurons were inhibited following 5-HT application. The authors argued that the detected inhibition was via GABAergic interneurons rather than a direct inhibitory effect (Hardy et al. 2005). In brain slices, 5-HT has been shown to modify intrinsic membrane properties of mitral cells via a 5-HT_{2A} mediated mechanism (Brill et al. 2016). 5-HT lead to the closure of a K^+ channel that increased membrane resistance and increased spontaneous firing. This same paper showed that 5-HT increased GABA release from SAC cells independent of action potential firing and that 5-HT does not have a direct effect on PGCs (Brill et al. 2016). ETCs have also been shown to be directly modulated by 5-HT also through a 5-HT_{2A} mechanism. In response to 5-HT ETCs showed increased burst firing and burst frequency, but unlike MTCs, this effect was not due to the closure of a K^+ channel but the activation of a non-selective cation TRP channel (Liu et al. 2012).

In vivo, using imaging methods, Petzold et al. (2009) found that after prolonged (minutes) stimulation of the DRN, GABAergic juxtaglomerular neurons

were excited by 5-HT, and this increased GABAergic tone led to presynaptic inhibition of OSNs via a GABAB-mediated mechanism. The authors claim that the juxtaglomerular neurons were affected via activity at the 5-HT_{2C} receptor but the identity of those neurons is not yet known. Given the report that PGCs are not directly sensitive to 5-HT (Brill et al. 2016), it is entirely possible that the cells which were activated by raphe stimulation were short axon cells. Two recent papers have increased our knowledge of 5-HT's affects *in vivo*, with similar results. Kapoor et al. (2016) showed that 3 pulse, 200 ms stimulation of the DRN sensitized medial tufted cells responses and decorrelated the population responses of mitral cells. This was the first paper to differentiate the effects of 5-HT between the two principal output neurons of the MOB. Brunert et al. (2016) gave longer stimulation of the DRN (1-4 Hz for 4 s)) and reported that serotonin increased Ca2+ transients evoked in response to ambient air in SACs and PGCs and a using glutamate reporter, iGluSnFR, expressed in PGCs and SACs showed that DRN stimulation increased glutamatergic input to these neurons. The source of this input is most likely from ETCs. MTCs showed modest increases in Ca2+ transients with only slight enhancement of inhalation-linked responses to odors. This result was quite interesting because it suggests that 5-HT may increase the degree to which ETC excitation and increased inhibition from SACs and PGs shapes olfactory output and decreases the effect of incoming OSN activity. Increased interglomerular and feedforward inhibition may modulate how mitral cell responses in a manner that facilitates fine odor discrimination.

To better understand the effects of 5-HT on olfactory behavior and neurophysiology I took a two pronged approach using both behavioral pharmacology and extracellular neurophysiology. First, using behavioral pharmacological methods and behavioral tasks I found that infusion of the 5-HT_2 antagonist cinanserin impaired odor non-associative learning in the olfactory habituation task. This effect was only detected at the lowest odor concentration tested. Within the same behavioral paradigm, I found that cinanserin infusion impaired spontaneous discrimination of structurally similar odorants. In the same chapter I report that unlike previous reports looking at NA and ACh in the forced choice discrimination task, I found a significant decrease in task performance following cinanserin infusion. I further analyzed data from the forced choice discrimination task and found that cinanserin infusion led to a slowing of decision making in the rat. This effect was found when rats were tested at high and medium odor concentrations. Finally, I present neurophysiology experiments that show that 5-HT application to horizontal mouse slices induces both gamma (20-55Hz) and theta range (1-10 Hz) oscillations within olfactory bulb slices along with strong increases in multiunit activity.

CHAPTER 2

5-HT2 RECEPTOR ANTAGONISM IMPAIRS OLFACTORY HABITUATION LEARNING AND OLFACTORY DISCRIMINATION LEARNING

INTRODUCTION

Animals must efficiently process sensory stimuli to adaptively shape behavioral responses to the demands of their environment. Sensory processing within neural systems varies with behavioral and neurochemical state, shaped in part by neuromodulators such as serotonin (5-HT), acetylcholine (ACh), and noradrenaline (NA). Cholinergic modulation is tightly linked to both attention and memory processes (Hasselmo and Starter, 2011) while noradrenaline plays a crucial role in modulating signal-to-noise ratios within sensory and reward related neural structures during behavior (Devore and Linster, 2012; Ashton-Jones and Cohen, 2005). To date, the functional role of serotonergic fibers from the median (MRN) and dorsal raphe nuclei (DRN) in sensory brain regions remains less understood in comparison. This is in part due to the complex anatomy of serotonergic innervation patterns, the diversity of serotonin receptors (5-HTRs), with seven distinct receptor classes (5-HT1-5-HT7), and the details of the microcircuits expressing 5-HTRs.

Early theories describing the role of 5-HT in behavioral control postulated an inhibitory role for 5-HT within sensory areas of the central nervous system (Jacobs and Fornal, 1999), yet recent work shows that 5-HT signaling provides a dynamic filter for particular sensory features, by acting either directly on sensory receptors or post-synaptically on major output neurons of sensory structures that relay information

to the central nervous system (Hurley et al. 2004, Petzold et al. 2009, Deemyad et al. 2013. Here, we investigate the functional role of serotonergic activity within the main olfactory bulb (MOB) of the adult rat.

The MOB is the first relay station for olfactory information in vertebrates. Briefly, olfactory sensory neurons (OSNs) terminate in the MOB with OSNs expressing a particular olfactory receptor protein converging on neuropil structures known as glomeruli. Neuronal circuits in the MOB consist of principal neurons, mitral/tufted (M/T) cells, and a number of excitatory and inhibitory interneurons that mediate both feed forward and feedback neurotransmission via chemical and electrical synapses at a variety of spatial scales (Wachowiak and Shipley 2006, Linster and Cleland 2009, Cleland 2010). The DRN and MRN project serotonergic fibers throughout the forebrain including the MOB and olfactory cortical areas (Jacobs and Azmitia 1992; McLean and Shipley 1987). Within the MOB, serotonergic fibers are preferentially found within the glomerular layer (GL) with fibers found to a lesser degree in the external plexiform layer (EPL) and granule cell layers (GCL). *In situ* hybridization studies have localized 5-$HT1_A$, 5-$HT2_A$, and 5-$HT2_C$ receptors within the olfactory bulb. 5-$HT1_A$ receptors are predominantly found in the EPL on mitral and granule cell dendrites. 5-HT_{2A} receptors are present in the mitral cell layer (MCL) and EPL along with expression in external tufted (ET) cells and M/T cells in the glomerular layer. 5-HT_{2C} receptors are present in GABAergic periglomerular neurons (PG) within the GL, and present in the GCL. Electrical stimulation of the DRN produces a $GABA_B$ receptor mediated presynaptic inhibition of OSN axon terminals, thought to reflect the direct excitation of PG cells via the 5-HT_{2C} receptor (Petzold et

al. 2009). This result is consistent with slice studies showing a direct depolarizing effect of 5-HT in ~30% of juxtaglomerular neurons. The same group found that 5-HT directly depolarized approximately half of M/T cells while indirectly hyperpolarizing the remaining half, perhaps due to inhibition from neighboring PG cells (Hardy et al. 2005). Most recently, 5-HT has been shown to directly depolarize ET cells through a 5-HT2_A receptor-mediated increase in a non-selective cation channel conductance leading to an increase in spontaneous bursting frequency in weakly activated cells (Liu et al. 2012). Although these findings provide strong evidence for 5-HT modulation of neuronal activity within the MOB, how this modulation affects olfactory memory and perception remains unexplored.

The role of bulbar 5-HT signaling in olfactory-mediated learning and memory has only been studied with respect to neonatal olfactory learning, and to date no studies have examined the roles of specific 5-HT receptor types in the behavior of an adult rodent during an olfactory perceptual task. Here, we used the 5-HT_2 antagonist cinanserin in two olfactory behavioral paradigms, cross-habituation and forced-choice discrimination tasks, across three odor concentrations (Cleland et al. 2002; Mandairon et al. 2006; Mandairon et al. 2008; Chaudhury et al. 2009). These behavioral paradigms allowed us to probe the role of 5-HT_2 receptor-mediated serotonergic action in the formation of both associative and non-associative odor learning across the two stimulus parameters, odor concentration and chemical similarity. We found that 5-HT_2 receptor blockade following bilateral infusion in the MOB impaired odor habituation memory formation, with the greatest effect at the lowest odor concentration tested (0.001 Pa), and attenuated spontaneous discrimination of novel odorants at 0.001 and

0.01 Pa. 5-HT2 blockade was also shown to impair performance in the forced choice discrimination task across odor concentrations. Thus, bulbar 5-HT_2 receptors play an important role in the expression of two different types of olfactory-guided behavior in adult mammals

MATERIALS AND METHODS

Subjects

Male Sprague-Dawley rats (250-300 g) were obtained from Charles River Laboratories (Wilmington, MA, USA). Rats were housed individually in standard laboratory cages on a 12 h reversed light/dark cycle (lights on at 21:00 h), with behavioral testing performed during the dark hours under red light. Rats were given access to water *ad libitum* throughout the experiment. During the habituation experiments (Experiment 1, see below), rats were fed 20g of rodent diet (Harlan Teklad 7912 irradiated rodent diet Madison, WI) daily following experiments. During the discrimination experiments (Experiment 2, see below), rats were maintained on a food-deprivation schedule to keep them 85-90% of their free-feeding body weight over the course of behavioral testing. All procedures were approved by the Cornell University Institutional Animal Care and Use Committee.

Cannulation Surgery

Rats were anesthetized using 5% isoflurane anesthesia and quickly transferred to and secured in a stereotaxic instrument (Kopf Instruments, Tujunga, CA, USA), and maintained at 1-3% isoflurane for the remainder of the surgery. Infusion cannulae (22-

gauge; Plastics One, Roanoke, VA, USA) were inserted bilaterally at the following coordinates with respect to bregma: AP +8.0 mm. ML +/- 1.9 mm, DV -4.5 mm and affixed to the skull with stainless steel bone screws and dental acrylic. The tips of the guide cannulae were positioned 1 mm dorsal to the target infusion site, with infusion needles extending 1 mm beyond the tip (**Fig. 1A**). To prevent blockage, dummy cannulae were place into the guide cannulae. Following surgery, rats were allowed to recover for 7-9 days before experiments.

Drug administration

The 5-HT_2 receptor antagonist, cinanserin HCl (Tocris Biosciences, Bristol, UK) was infused into the main olfactory bulbs at 6 mM, 6 μL delivered per MOB. The dosages were determined based on previously published studies of intracerebral infusions of cinanserin for behavioral experimentation. Cinanserin was dissolved in 0.9% saline and prepared freshly each day. All rats received both saline and cinanserin+saline infusions. For drug administration, two infusion cannulae were fitted into the guide cannulae so that their tips protruded 1.0 mm beyond the ends of the guide cannulae into the MOB. Two 10 μL Hamilton Syringes (Hamilton Company, Reno, NV) containing either drug solutions or vehicle were attached to the cannulae with a polyethylene tube and driven with a two-syringe infusion pump (Harvard Apparatus, Holliston, MA, USA). Drugs were delivered bilaterally into awake, freely moving rats at a rate of 1 μL/min. The infusion cannulae remained in place for one additional minute after the infusion ended in order to minimize backflow. Following removal of infusion needles and tubing, dummy cannulae were replaced and behavioral testing

began 20 minutes after drug administration (**Fig. 1A**). Following the experiments rats were infused with 1% methylene blue saline solution and euthanized 20 minutes following infusion. Blue dye was restricted to the MOB upon inspection.

Experiment 1: Olfactory cross-habituation and spontaneous discrimination

Experiment 1 odor sets

Two odor sets were used for the cross-habituation experiment. All odorants were diluted in mineral oil to emit an approximate steady-state vapor partial pressure of 0.001, 0.01, or 0.1 Pa (Cleland et al., 2002). Each odor set consisted of a homologous odor series with unbranched carbon chains plus one chemically unrelated odorant. Within each odor set, odors were selected so that odorants differed by one carbon chain difference, two carbon chain differences, and different functional group (Table 1). Odors were presented by pipetting 60 uL of diluted odorant onto a piece of filter paper contained within a weighing dish, which was then inverted and placed onto the cage top.

Experiment 1 behavioral testing

Rats were tested for olfactory habituation/spontaneous discrimination using methods published previously (Cleland et al. 2002, Mandairon et al. 2006). This behavioral task tests for non-associative odor memory formation and specificity by first habituating rats to a given odor (memory formation) and subsequently testing cross-habituation among structurally similar and dissimilar odorants (memory specificity).

During testing, rats were removed from their home cages and placed in a clean plastic cage (46 cm x 22 cm x 25 cm) with a wire frame cage top. A rat was only

tested once every 24 hours. A daily test session comprised of six, 50 s investigation trials (**Fig. 1B**). Each test session was begun with a mineral oil presentation to habituate animals to the behavioral setup, followed by three 50 s presentations of the habituation odor (Ohab), followed by two 50 s presentations of test odorants (T1 and T2), with all odor presentations separated by 5 min intervals (**Fig. 1B**). Each odor set comprised four test odorants (**Table 1**), which were tested in groups of two: 1C / 2C, and zero carbon difference / different functional group (**Fig. 1B**). The order of testing was pseudo-randomized and the order of test odorant presentation was counterbalanced within each test group. As a consequence, rats were habituated to the same odorant on two separate days. Rats were tested at three odor concentrations and all odors presented within one experimental day were of the same odor concentration. At each odor concentration, on separate experimental days, rats were infused with saline vehicle or vehicle plus 5-HT_2 antagonist, cinanserin. Presentation of test odors was counterbalanced across the two drug treatment conditions so that each odor set was tested an equal number of times per drug treatment. In total, for each rat, data was collected over 12 experimental sessions: twice per each drug treatment over three odor concentrations. Rats were sequentially tested at increasing odor concentrations (0.001 Pa to 0.1 Pa). Within each odor concentration, the four experimental tests were performed in a pseudo-randomized order. Each trial was video recorded (30 Hz frame rate) and analyzed using custom developed analysis software (Labview). The amount of time that rats spent actively investigating each presented odorant was recorded off line. Active investigation was defined as sniffing within 1 cm of the odor source while reared on the two hind legs.

FIGURE 1

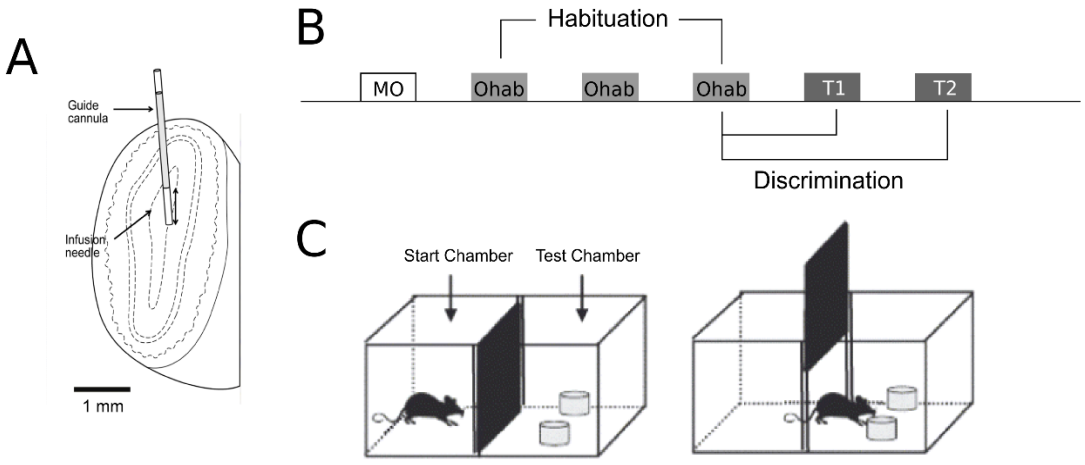
A
Guide cannula
Infusion needle
1 mm
B
Habituation
MO
Ohab
Ohab
Ohab
T1
T2
Discrimination
C
Start Chamber
Test Chamber

Figure 1. Experimental approach. A. Rats were implanted bilaterally with cannulae to allow for intrabulbar infusion of saline and saline + cinanserin. **B.** Habituation protocol (see methods). Investigation time was measured at six over trials a day. Experiments began with a mineral oil (MO) blank and were then followed by three presentations of the habituation odor. Following habituation trials, rats were presented two of four test odors. Rats were either presented the with a fourth trial of the habituated odor (zero CD), or an odorant from a different functional group (Diff. F.G.) On a separate day the rats were tested in the same manner but the rats were instead presented odors differing in one carbon chain length (1C) or two carbon chain lengths (2C). The order of presentation of the either the zero carbon difference and Diff. F.G. and the 1C and 2C tests were counterbalanced across rats. Habituation was measured by calculating a habituation index (see methods) using the first and third habituation trials. Spontaneous discrimination was measured by calculating a discrimination index between the third habituation trial and the test trial. **C**. Forced choice discrimination task. Rats were tested in an experimental chamber with two odor scented pots. One pot contained a food reward. Rats were trained to dig in pots for food prior to testing. Each pot was scented with an individual odor and the two odors varied systematically in chemical similarity from 1C, 2C, 4C, and a different functional group. Both the habituation experiment (**B**) and forced-choice discrimination experiment (**C**) were tested at three odor concentrations (0.001, 0.01, and 0.1 Pa).

Habituation Experiment Odors

Odor Set	**Ohab**	***0C***	***1C***	***2C***	***Diff. F.G.***
A (Acids)	Butanoic Acid	Butanoic Acid	Pentanoic Acid	Hexanoic Acid	(+)-Limonene
B (Alcohols)	Hexanol	Hexanol	Heptanol	Octanol	(+)-Carvone

Discrimination Experiment Odors
0.001 Pa

Odor Set	**1C**	**2C**	**4C**	**Diff. F.G.**
A (Acids)	Propanoic Acid/ ButanoicAcid	Hexanoic Acid/ Octanoic Acid	Pentanoic Acid/ Nonanoic Acid	Heptanoic Acid/ Ethyl Butyrate
B (Alcohols)	Propanol / Butanol	Hexanol/ Octanol	Pentanol/ Nonanol	Heptanol/ Neryl Acetate

0.01 Pa

Odor Set	**1C**	**2C**	**4C**	**Diff. F.G.**
A (Acids)	Octanoic Acid / Nonanoic Acid	Butanoic Acid/ Hexanoic Acid	Propanoic Acid/ Heptanoic Acid	Pentanoic Acid/ Propyl Butyrate
B (Alcohols)	Pentanol/ Hexanol	Heptanol/ Nonanol	Butanol/ Octanol	Propanol/ Pentyl Acetate

0.1 Pa

Odor Set	**1C**	**2C**	**4C**	**Diff. F.G.**
A (Acids)	Pentanoic Acid/ Hexanoic Acid	Heptanoic Acid/ Nonanoic Acid	Butanoic Acid/ Octanoic Acid	Propanoic Acid/ Hexyl Acetate
B (Alcohols)	Octanol/ Nonanol	Butanol/ Hexanol	Propanol/ Heptanol	Pentanol/ Butyl Butyrate

Experiment 1 data analysis

Data analyses were performed using JMP statistical software (JMP, SAS Institute Inc., Cary, NC). Within each odor trial, outlier values that deviated from the trial mean by more than two standard deviations were excluded from analysis.

Overall analysis: A mixed-effect model (MEM) was used to test for changes in investigation time over the main fixed effects of drug treatment (i.e. cinanserin vs. saline; "drug"), odor trial (e.g. habituation odor; "trial"), odor concentration (i.e. 0.001 Pa, 0.01 Pa, 0.1 Pa; "concentration"), as well as drug* trial, drug*concentration, trial*concentration, and drug*trial*concentration interactions. Rat identity was modeled as a random effect.

Habituation memory formation: To test if drug treatment and odor concentration affected memory formation, a mixed-effect model was performed on investigation time with the fixed effects of drug, trial, concentration, as well as drug*trial, drug*concentration, trial*concentration, and drug*concentration*trial interactions. Rat was modeled as a random effect.

Previously, the formation of memory to a habituated odor was measured as a significant decrease in time spent investigating the odor between the first and third habituation trials (Hab1 and Hab3, respectively. (Wilson and Linster 2008)). Here, we incorporate this criterion into a habituation index (HI), measured as the ratio of investigation time difference between Hab1 and Hab3 normalized by total investigation time over these trials: HI = (Hab1-Hab3)/(Hab1+Hab3). Therefore, HI is positive when there is a decrease in investigation time between Hab1 and Hab3, with

higher HI values representing stronger habituation memory formation. HI values were then compared using a mixed-effect model with drug, odor concentration, and drug*concentration as fixed effects and rat as a random effect. Tukey's HSD test was used to test for significant effect of drug treatment at each odor concentration (significance set at $p<0.05$). Additionally, custom hypothesis post-hoc tests were performed on HI values to test for the presence or absence of olfactory habituation utilizing the Holm-Bonferroni multiple comparison correction. In this test, we considered rats as habituated if the mean HI was statistically greater than zero.

Spontaneous discrimination: After habituation trials, we tested the specificity of the habituated odor memory by presenting rats with novel odors differing by one carbon (1C), two carbon (2C), functional group (DF), or a fourth presentation of the habituation odor (Hab4). The degree of specificity was represented by the discrimination index (DI), measured as the ratio of the difference between the test trial and the third habituation trial normalized to the sum of the two odor trials: DI = (Test – Hab3)/(Test + Hab3). We interpreted positive DI values as a positive discrimination of the test odor. DI values were then analyzed using a mixed-effect model with the following fixed effects: drug, test odor carbon difference (1C, 2C, DF, Hab4), odor concentration, drug*carbon difference, drug*concentration, carbon difference*concentration, and drug*carbon difference*concentration. Tukey's HSD post-hoc tests were performed to determine drug effects at a given carbon difference and odor concentration. Furthermore, we tested for the presence or absence of spontaneous discrimination of novel odorants by using a custom hypothesis test with

Holm-Bonferroni multiple comparison corrections. In this test, rats were able to discriminate test odors if mean DI values were significantly greater than zero.

Experiment 1 odor detection control experiment:

A separate group of rats (N=8) were used to test for effects of the 5-HT2 antagonist, cinanserin, on odor detection, to ensure any deficit in habituation and/or discrimination was not due to an altered detection threshold. Rats were habituated first to mineral oil (MO) followed by presentation of different odorants at 0.001, 0.01, or 0.1 Pa. This modified habituation protocol consisted of eight 50 sec odor presentation periods separated by five minute intervals. MO was first presented three times, followed by presentation of the habituation odorant, then two test trials (1C and 2C odorants). A detection index value was measured as the ratio of the difference of the first Ohab trial (Hab1) and the third mineral oil trial and the sum of the two trials. Detection index = (Hab1-MO3)/(Hab1+MO3). Data were analyzed using a mixed-effect model with drug treatment, odor concentration, and drug*concentration interaction as fixed effects and rat as a random effect. Tukey's HSD post-hoc tests were used to test for drug treatment effects at each odor concentration. A custom hypothesis test with Holm-Bonferroni multiple comparison corrections tested whether mean detection index values were significantly greater than zero, which indicated successful detection.

Experiment 2: olfactory forced choice digging task

Experiment 2 odor sets

Two odor sets were used for reinforced olfactory discrimination experiments, each composed of four odor pairs (**Table 1**). All odorants were diluted in mineral oil to a steady-state vapor-phase partial pressure of 0.001 Pa, 0.01 Pa, or 0.1 Pa. Rewarded vs. non-rewarded odor pairs were either structurally similar (1C or 2C difference) or very different (4C or functional group difference). Rats were sequentially tested at increasing odor concentrations (0.001 Pa to 0.1 Pa). Within each odor concentration, rats were tested eight times: four times per drug group, once at each carbon difference (1C, 2C, 4C, diff FG). The order of testing within an odor concentration was pseudorandomized for each rat.

Experiment 2 task training

Following cannulation surgery and Experiment 1, rats were trained to perform a digging task used for the forced-choice discrimination trials. Over several days of acclimation, rats were introduced to the two chambered experimental box and taught to retrieve a reward (Tootie Fruities, Malt-O-Meal, Minneapolis, MN, pre-exposed to >3 hr heat and air to reduce odor) by digging in a single dish filled with corncob bedding (Bed-O-Cobs, The Andersons, Maumee, OH, USA). Rats were then trained on the forced-choice discrimination task as follows. At the start of each experiment, the rat was placed in the start chamber that was separated from the experimental chamber by a plastic divider. Two ceramic dishes (9 cm diameter, 4.5 cm height) were then placed in the test chamber to present odorants and hide the reward. Each dish contained 60 µL of diluted odorant that was added to the top of 60 mL bedding and lightly mixed to scent the bedding.

Training took place over a course of five-six days, with (+)-limonene and mineral oil as training odorants, one of which was paired with a food reward. This odorant-reward association was consistent for any given rat but was counterbalanced across rats. After the rat and odor dishes were appropriately placed, the plastic divider was released, allowing the rat to approach and dig in both odor dishes until the reward was retrieved. In early training trials, the reward was intentionally placed near the top of the bedding and slowly buried deeper within the bedding over subsequent training days. Each day consisted of 20 trials and training continued over 5-6 days until rats were able to appropriately identify the rewarded dish and retrieve deeply buried rewards. To control for the possibility that the rats could smell the reward directly, 10 mL of crushed food reward was added to every liter of corncob bedding.

Experiment 2 behavioral testing

A rewarded, forced-choice odor-discrimination task is a commonly used perceptual task in sensory neuroscience (Cleland et al. 2002). Here, it was used to test to the role of bulbar 5-HT_2 receptors in the acquisition and precision of associative olfactory memory. Each rat was tested under each drug condition with a different pair of odorants (Table 1), so each rat was exposed to a particular odor pair only once throughout the experiment. Similar to training trials, experiments took place in identical cages to those used in training and each experimental session consisted of 20 consecutive trials using a given odorant pair. Trials began 20 min after drug infusion and each test session was completed within 15 min. During each trial, the dish in

which the rat first dug was recorded. Rats were not allowed to self-correct after digging in the unrewarded odor dish (**Fig. 1C**).

Experiment 2 data analysis

Data analyses were performed using JMP. A mixed-effect model was performed to analyze how task performance, measured as the fraction of trials correct, was dependent on the following fixed effects: drug treatment, carbon difference between the two odorized pots (1C, 2C, 4C, diff FG), odor concentration (0.001 Pa, 0.01 Pa, 0.1 Pa), drug*carbon difference, drug*concentration, concentration*carbon difference, and drug*concentration*carbon difference. Rat was modeled as a random effect. Tukey's HSD was used for post-hoc multiple comparisons between experimental groups.

RESULTS

Experiment 1: Habituation and spontaneous discrimination

Overall results

We examined the role of serotonergic activity at the 5-HT2 receptor in the main OB on odor habituation behavior by infusing the serotonergic antagonist, cinanserin directly into the OB prior to testing the animal in our habituation protocol. We tested for an effect of 5-HT2 antagonism on odor habituation at three odor concentrations (0.001 Pa, 0.01 Pa, 0.1 Pa). Utilizing the habituation protocol, we also investigated if 5-HT2 antagonist infusion affected spontaneous discrimination behavior, measured as a discrimination index. Here we tested spontaneous discrimination between a novel

test odorant and the habituated odor using four test odorants (three novel, one non-novel) in both drug conditions (see Methods).

We found that investigation time was significantly changed by blocking 5-HT2 action in the olfactory bulb. A mixed-model analysis of investigation time values from all 50-sec trials showed significant effects of odor trial ($F_{7,520.3} = 25.7$, $p < 0.0001$) and odor concentration*odor trial interaction ($F_{14,520.4} = 2.8428$, $p = 0.0004$) on investigation behavior during odor presentations across the experiment (data set consisted of all data from **Fig. 2,3,** and **4**). Investigation time also showed a significant odor concentration x drug treatment interaction ($F_{2,524.2} = 3.6362$, $p = 0.0270$) and an odor concentration x drug treatment x odor trial three-way interaction ($F_{14,520.3} = 1.7910$, $p=0.0369$), demonstrating that both odor concentration and drug treatment altered investigation behavior over successive odor presentations. We then analyzed data from habituation trials and test trials separately in order to assess odor memory formation and spontaneous discrimination, respectively.

Memory formation: In the habituation task used here, odor memory formation is defined as a significant decrease in investigation time over the course of habituation trials (Cleland et al. 2002; Mandairon et al. 2006). Across the three habituation trials, a mixed-effect model detected three significant effects on odor investigation time: (1) odor investigation time significantly varied across habituation trials ($F_{2,263.8}=26.55$, $p<0.0001$), with a decrease in total time investigating with repeated odor presentation; (2) blockade of 5-HT2 receptors significantly altered how odor investigation changed with repeated odor presentation (drug*trial; $F_{2,263.8}=5.9085$, $p = 0.0031$), with cinanserin infused animals showing longer investigation times during the second and

third habituation trials; (3) there was a significant drug treatment*odor concentration interaction on odor investigation time during habituation trials ($F_{2,266.6}$=4.5181, p =

FIGURE 2

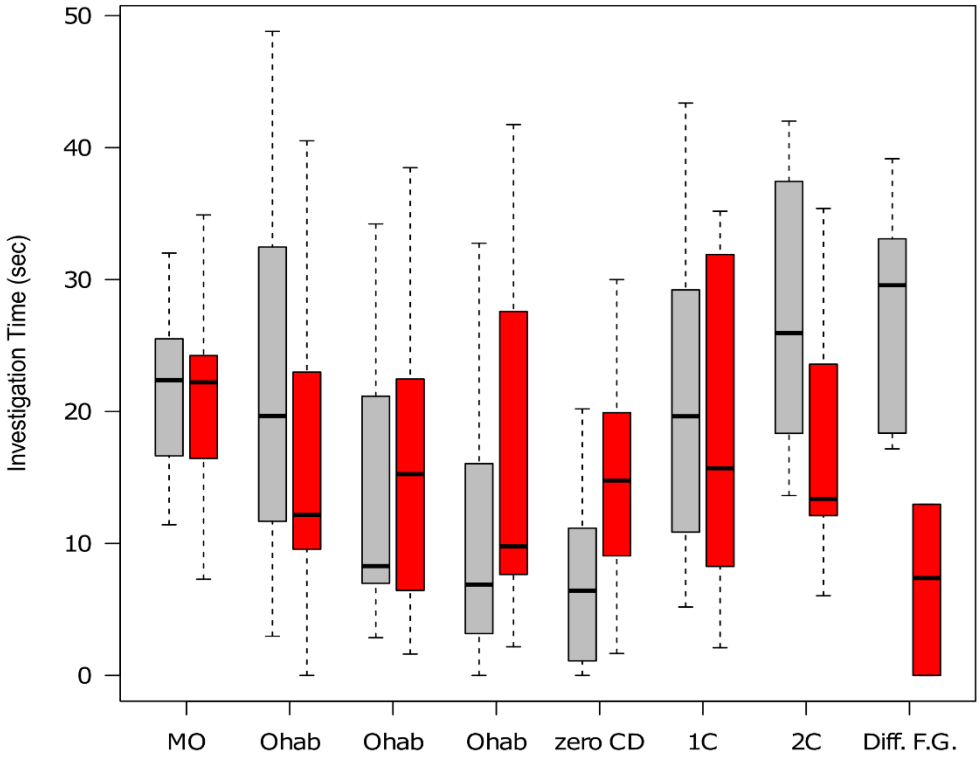

Figure 2. Investigation time over all odor presentations at 0.001 Pa. Investigation time is depicted as box plots. Trials following saline infusion are shown in gray, trials following cinanserin infusion in red. The x-axis depicts the order of odor presentation. During all trials rats began the session with a mineral oil trial followed by three presentations of the habituation odor. Following the habituation trials, rats were presented with two test odors, either a fourth trial with the habituation odor(zero CD) and an odor from different chemical functional group or an odor one carbon-chain length different (1C) from the habituated odor and an odor two-carbon chain lengths different (2C) from the habituated odor.

FIGURE 3

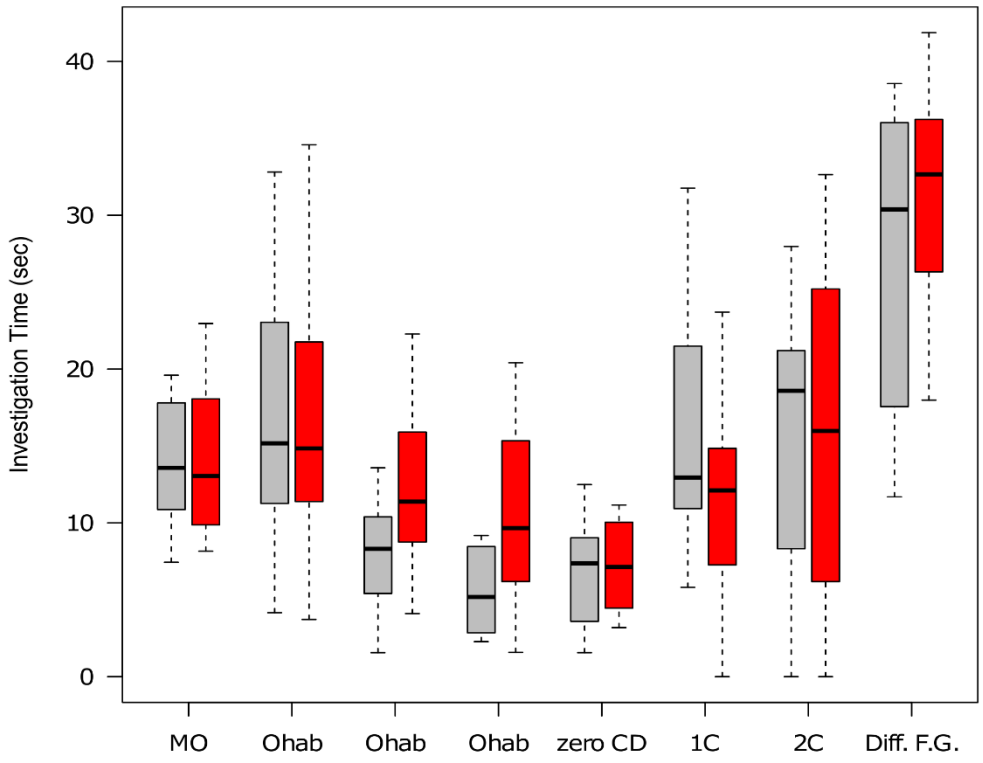
Investigation Time (sec)
0
10
20
30
40
MO
Ohab
Ohab
Ohab
zero CD
1C
2C
Diff. F.G.

Figure 3. Investigation time over all odor presentations at 0.01 Pa. Investigation time is depicted as box plots. Trials following saline infusion are shown in gray, trials following cinanserin infusion in red. The x-axis depicts the order of odor presentation. During all trials rats began the session with a mineral oil trial followed by three presentations of the habituation odor. Following the habituation trials, rats were presented with two test odors, either a fourth trial with the habituation odor(zero CD) and an odor from different chemical functional group or an odor one carbon-chain length different (1C) from the habituated odor and an odor two-carbon chain lengths different (2C) from the habituated odor.

FIGURE 4

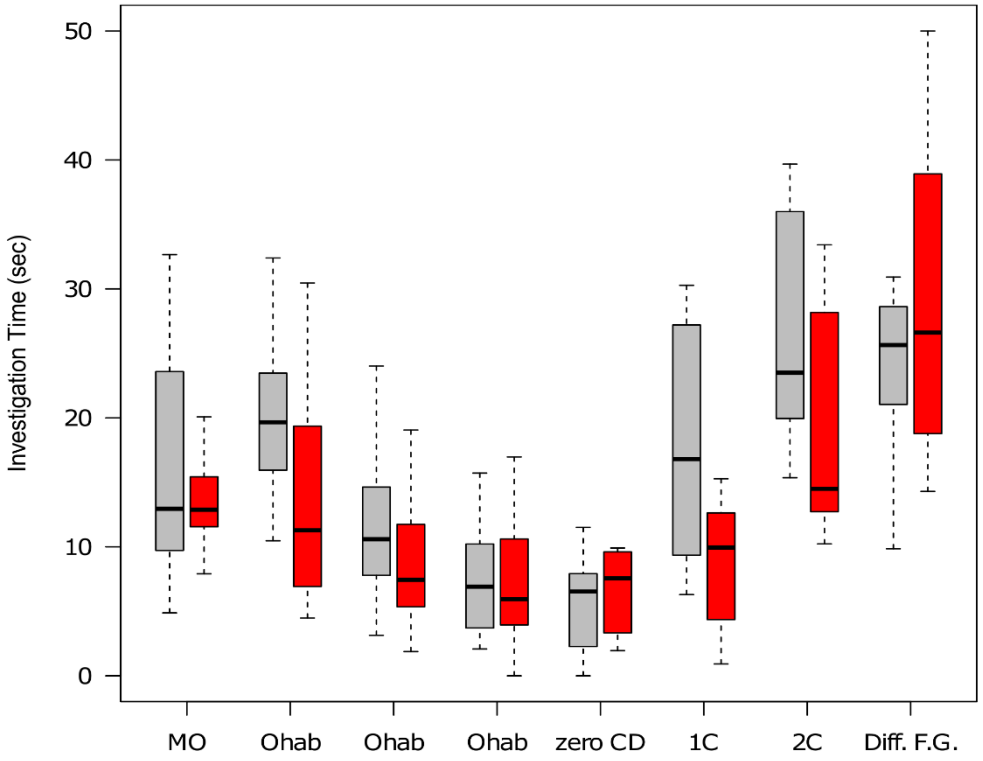
Investigation Time (sec)
0
10
20
30
40
50
MO
Ohab
Ohab
Ohab
zero CD
1C
2C
Diff. F.G.

Figure 4. Investigation time over all odor presentations at 0.1 Pa. Investigation time is depicted as box plots. Trials following saline infusion are shown in gray, trials following cinanserin infusion in red. The x-axis depicts the order of odor presentation. During all trials rats began the session with a mineral oil trial followed by three presentations of the habituation odor. Following the habituation trials, rats were presented with two test odors, either a fourth trial with the habituation odor(zero CD) and an odor from different chemical functional group or an odor one carbon-chain length different (1C) from the habituated odor and an odor two-carbon chain lengths different (2C) from the habituated odor.

0.0118). These results showed that blocking 5-HT2 in the olfactory bulb impaired memory formation in an odor concentration dependent manner.

In order to compare relative degrees of habituation across experimental conditions, a habituation index was used. This index represents the relative decrease in investigation between the first and third trial (see Methods). A mixed-effect model performed on all habituation index values detected a significant effect of drug treatment ($F_{1,81.31} = 15.0247$, $p < 0.0002$). Thus, 5-HT_2 antagonist infusion attenuated olfactory habituation between the first and third habituation trials, reaffirming the drug x trial interaction reported in the paragraph above. Post-hoc analysis utilizing a custom hypothesis test with multiple comparisons corrections highlighted that the behavioral effect of 5-HT2 antagonism is strongest at the 0.001 Pa concentration (**Fig.5**.). Except for the 0.001 Pa cinanserin group, all experimental groups exhibited olfactory habituation, measured by a mean habituation index value that is significantly greater than zero (Holm-Bonferroni Multiple Comparisons correction test). There was a significant difference in habituation index values between the saline and cinanserin drug treatments only at 0.001 Pa (**Fig.6**). Together, these results reinforced our finding that blockade of 5-HT2 receptors within the MOB impairs olfactory habituation most significantly at low odor concentrations.

Spontaneous Discrimination: The specificity of the memory formed can be assessed by comparing rats' responses to the habituated odor and novel odors during test trials. Discrimination is measured using a discrimination index (DI), a value ranging from -1

to 1 (see Methods). A mixed-effect model detected four significant effects on DI values across the experiment. Treatment with cinanserin significantly reduced DI

FIGURE 5

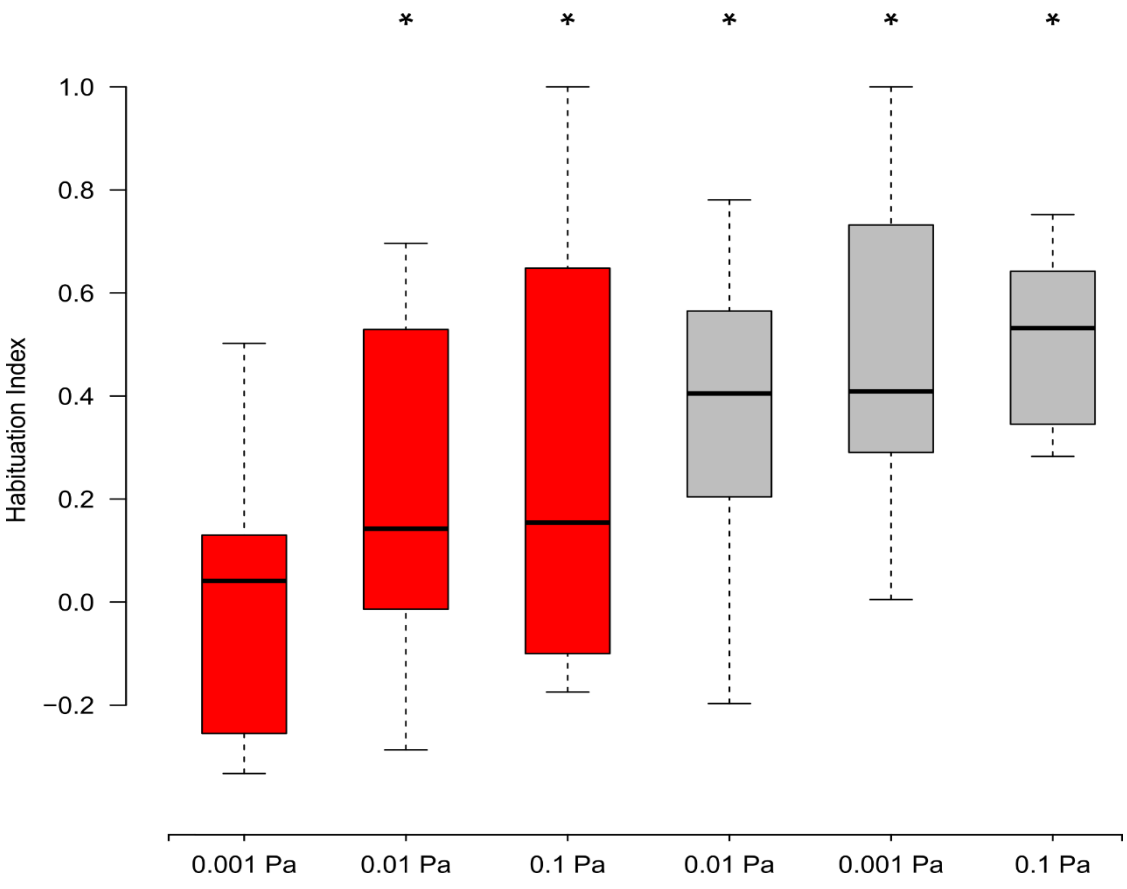

Figure 5. Cinanserin infused rats failed to habituate to repeated odor presentations at 0.001 Pa. The x-axis is arranged by increasing habituation index values. The y-axis represents habituation index values. The gray boxes represent data following saline infusion and red boxes represent data collected following cinanserin infusion. The odor concentration is labeled below the box along the x-axis of the on the figure. Here a custom hypothesis test was performed to test if habituation index values were significantly greater than zero. Habituation index values which were significantly greater than zero ($p < 0.5$) are marked with an asterisk.

FIGURE 6

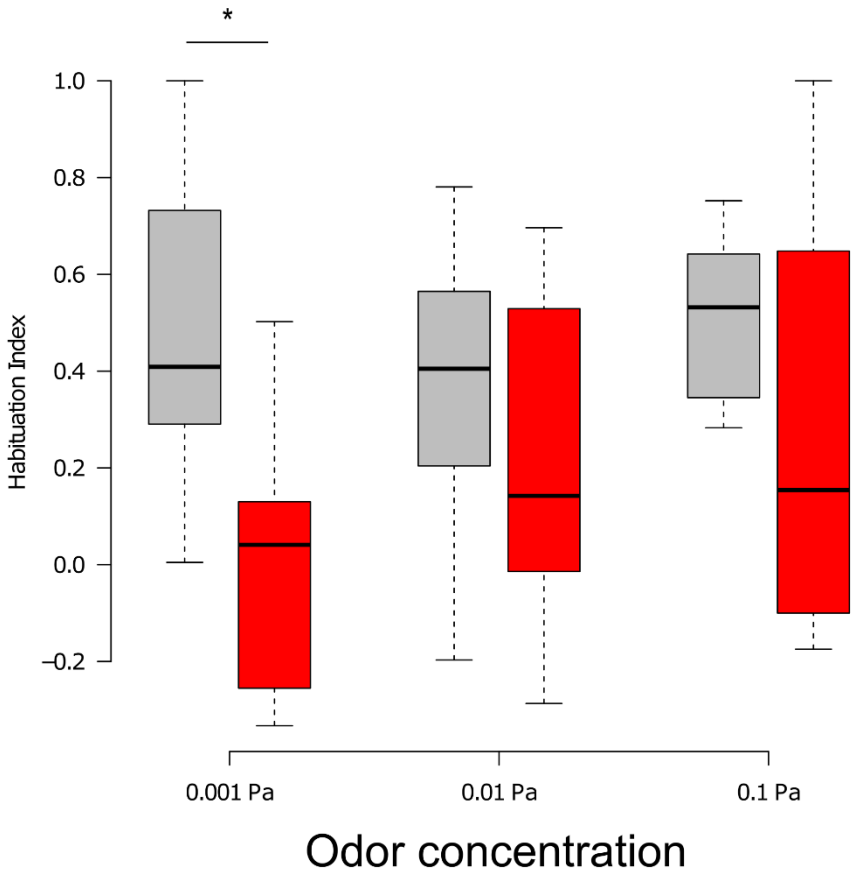
*
1.0
0.8
0.6
0.4
0.2
0.0
−0.2
Habituation Index
0.001 Pa
0.01 Pa
0.1 Pa
Odor concentration

Figure 6. Cinanserin infused rats show altered habituation to repeated odor presentation during 0.001 Pa odor trials. The x-axis represents odor concentration and the y-axis represents Habituation index. Habituation index values may be between -1 and 1 (See methods). The data here was calculated from the habituation trials over all three tested odor concentrations (Hab1, Hab2, Hab3 of figures 2, 3, and 4). Habituation index is represented as box plots, data following saline infusion in gray, data following cinanserin infusion in red.

values ($F_{1,160.7}$=10.6206, p = 0.0014) across all test odors. There was also a significant effect of the chemical difference between the habituated and test odorants on discrimination, with a monotonic rise in DI with increasing structural dissimilarity ($F_{3,160.2}$ = 10.4014). Lastly, we detected a significant three-way interaction between odor concentration, drug treatment, and odor difference ($F_{6,160.2}$=2.2056, p= 0.0451) (**Fig. 7**,**8** and **9**). Thus, the ability of rats to spontaneously discriminate a novel test odorant as it decreases in chemical similarity is dependent on both on the integrity of serotongeric signaling at 5-HT_2 receptors and the concentrations of the odorants used.

To better investigate the significant three-way interaction term, we performed post-hoc analyses within each odor concentration. First, we assessed spontaneous discrimination of the test stimuli with a custom hypothesis test with Holm-Bonferroni multiple comparison corrections (Fig. 10) **At 0.001 Pa**, saline infused animals showed spontaneous discrimination of two test odorants (2C and different functional group), as supported by mean DI values that were statistically greater than zero. However, cinanserin infused rats did not discriminate any test odorants at this odor concentration, as no DI values were statistically greater than zero (Fig. 4). Further post-hoc tests were performed to compare drug treatment effects on DI at each carbon difference. The only significant drug treatment effect on DI was found in the different functional group test **(Fig. 10**). These data showed that cinanserin greatly impairs spontaneous discrimination of all novel test odorants and that this effect is most pronounced at this low concentration. **At 0.01 Pa**, saline animals showed spontaneous

discrimination at 1C and different functional group odor tests. In contrast, cinanserin treated animals showed spontaneous discrimination of only different functional group

FIGURE 7

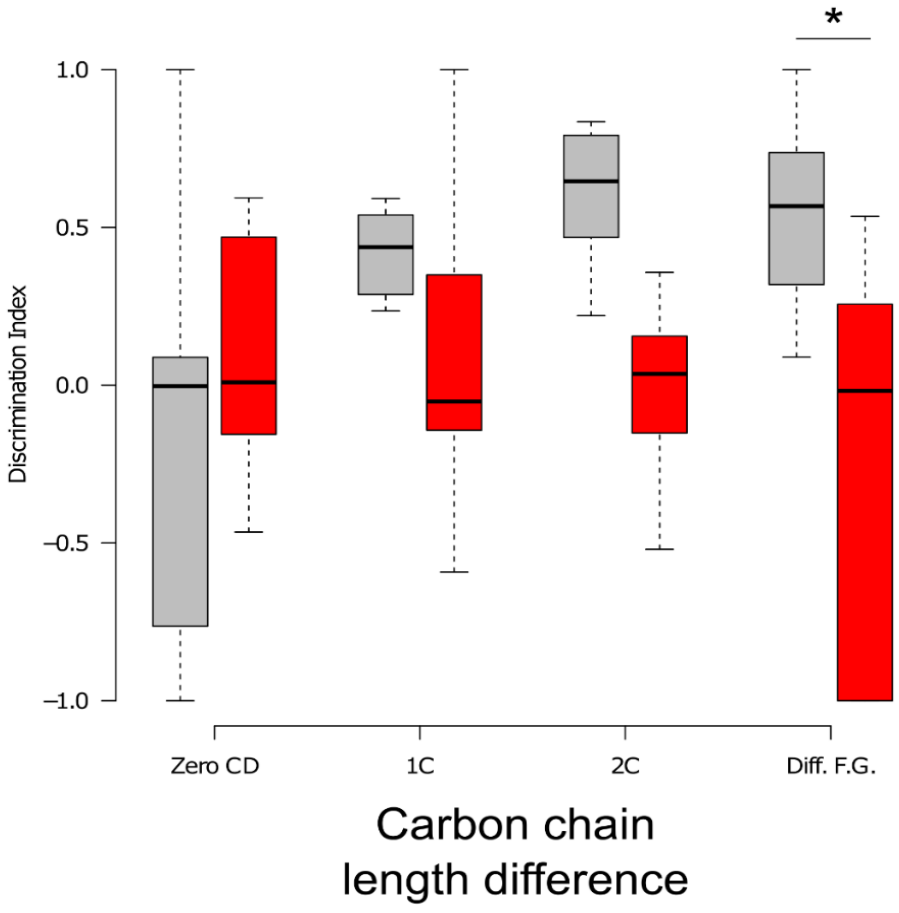

Figure 7. Discrimination index values for all test trials at 0.001 Pa. The x-axis depicts the carbon chain length difference of the test odor from the habituated odor. Discrimination index values may be between -1 and 1 (See methods). The data here was calculated from test trials at 0.001 Pa (zero CD, 1C, 2C, Diff. F.G. of Fig. 2. Discrimination index values are shown here as box plots, saline infused animals in gray and cinanserin infused animals in red. Discrimination index values were significantly different between the drug treatments in the Diff. F.G. test trials. Significance was assessed at $p<0.05$ using Tukey's HSD.

FIGURE 8

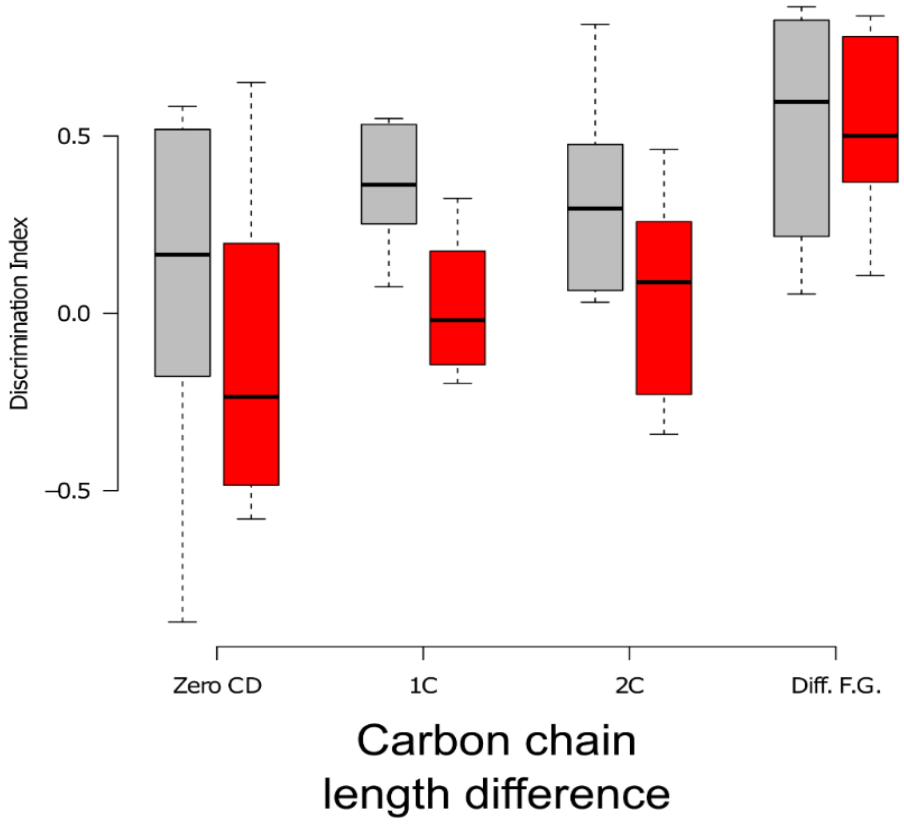
Discrimination Index
0.5
0.0
−0.5
Zero CD
1C
2C
Diff. F.G.
Carbon chain
length difference

Figure 8. Discrimination index values for all test trials at 0.01 Pa. The x-axis depicts the carbon chain length difference of the test odor from the habituated odor. Discrimination index values may be between -1 and 1 (See methods). The data here was calculated from test trials at 0.01 Pa (zero CD, 1C, 2C, Diff. F.G. of Fig. 3. Discrimination index values are shown here as box plots, saline infused animals in gray and cinanserin infused animals in red. No significant differences were found between discrimination index values at all test odors.

FIGURE 9

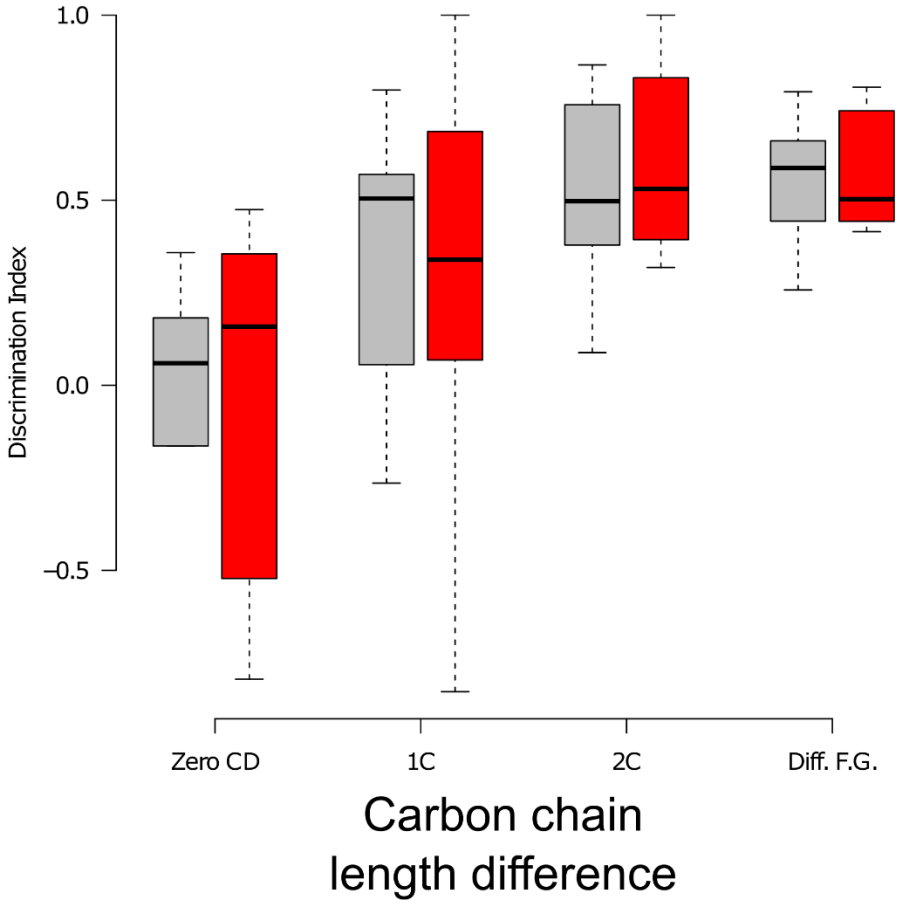
1.0
0.5
0.0
−0.5
Discrimination Index
Zero CD
1C
2C
Diff. F.G.
Carbon chain
length difference

Figure 9. Discrimination index values for all test trials at 0. 1 Pa. The x-axis depicts the carbon chain length difference of the test odor from the habituated odor. Discrimination index values may be between -1 and 1 (See methods). The data here was calculated from test trials at 0.1 Pa (zero CD, 1C, 2C, Diff. F.G. of Fig. 4. Discrimination index values are shown here as box plots, saline infused animals in gray and cinanserin infused animals in red. No significant differences were found between discrimination index values at all test odors.

odorants. These results suggest that at medium odor concentrations, 5-HT2 action is most important for discriminating between structurally similar novel odorants. We did not detect any significant differences between drug groups when DI values were compared at each carbon difference individually. Lastly, at **0.1 Pa**, both cinanserin and saline infused groups showed similar spontaneous discrimination behavior, with DI values increasing as test and habituation odorants increased in structural dissimilarity. DI values in the saline condition were statistically greater than zero in both the 2C and different functional group tests, while only the different functional group was significantly greater than zero in the cinanserin condition (**Fig. 10**.).

These results show that along with modulating odor habituation/memory, 5-HT_2 receptor blockade within the MOB also impaired the ability to spontaneously discriminate novel test stimuli as a function of chemical similarity and odor concentration.

Odor Detection Control:

To ensure the cinanserin-induced deficit in habituation and discrimination at 0.001 Pa was not due to an altered detection threshold, we tested for odor detection in a separate cohort of rats that were habituated to mineral oil. Specifically, mineral oil was presented three times, followed by test odorants presented at 0.001, 0.01, or 0.1 Pa. The change in investigation time between the last mineral oil trial and odorant trial was measured as a detection index (see Methods). Our model did not detect a significant effect of drug treatment, odor concentration or a significant interaction on DI values, suggesting that cinanserin did not impair the ability to detect odorants (**Fig. 11**). Reinforcing this result, all mean DI values were significantly greater than zero

FIGURE 10

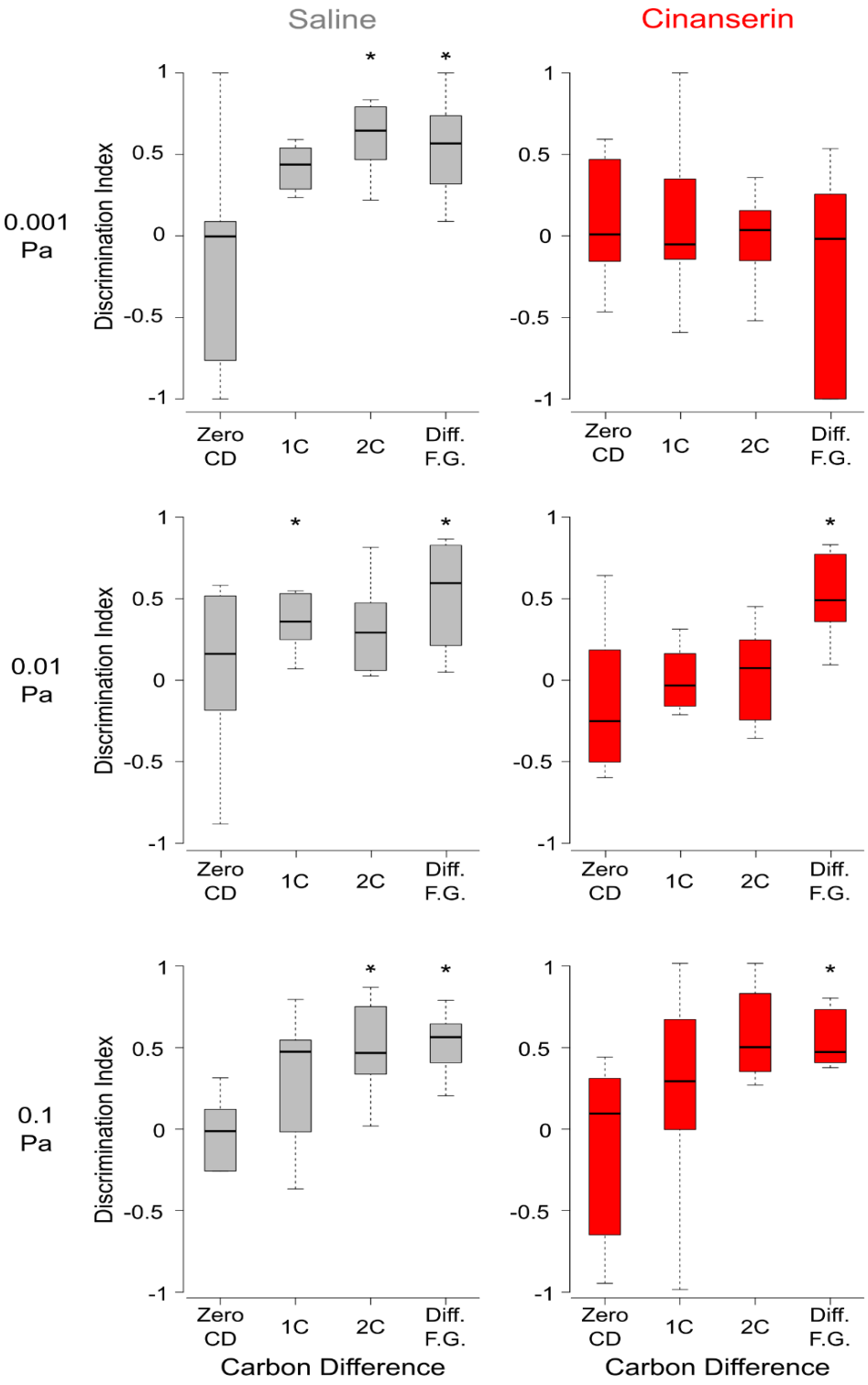
Saline
Cinanserin
0.001 Pa
0.01 Pa
0.1 Pa
Discrimination Index
1
0.5
0
-0.5
-1
*
Zero CD
1C
2C
Diff. F.G.
Carbon Difference

Figure 10. Cinanserin infused rats showed decreased spontaneous discrimination of novel odorants at all tested odor concentrations. The x-axis depicts the carbon chain length difference of the test odor from the habituated odor. The y-axis of represents the discrimination index. Discrimination index values may be between -1 and 1 (See methods). The data here is the same as in figures 7, 8, and 9, but is represented as a line graph of means rather than boxplots. Data following saline infusion is in the left column with solid lines. Data following cinanserin infusion is in the right column in dashed lines. Here a custom hypothesis test was performed to test if discrimination index values were significantly different than zero. Discrimination index values which were significantly different than zero are marked with an asterisk. Error bars represent +/- SEM.

FIGURE 11

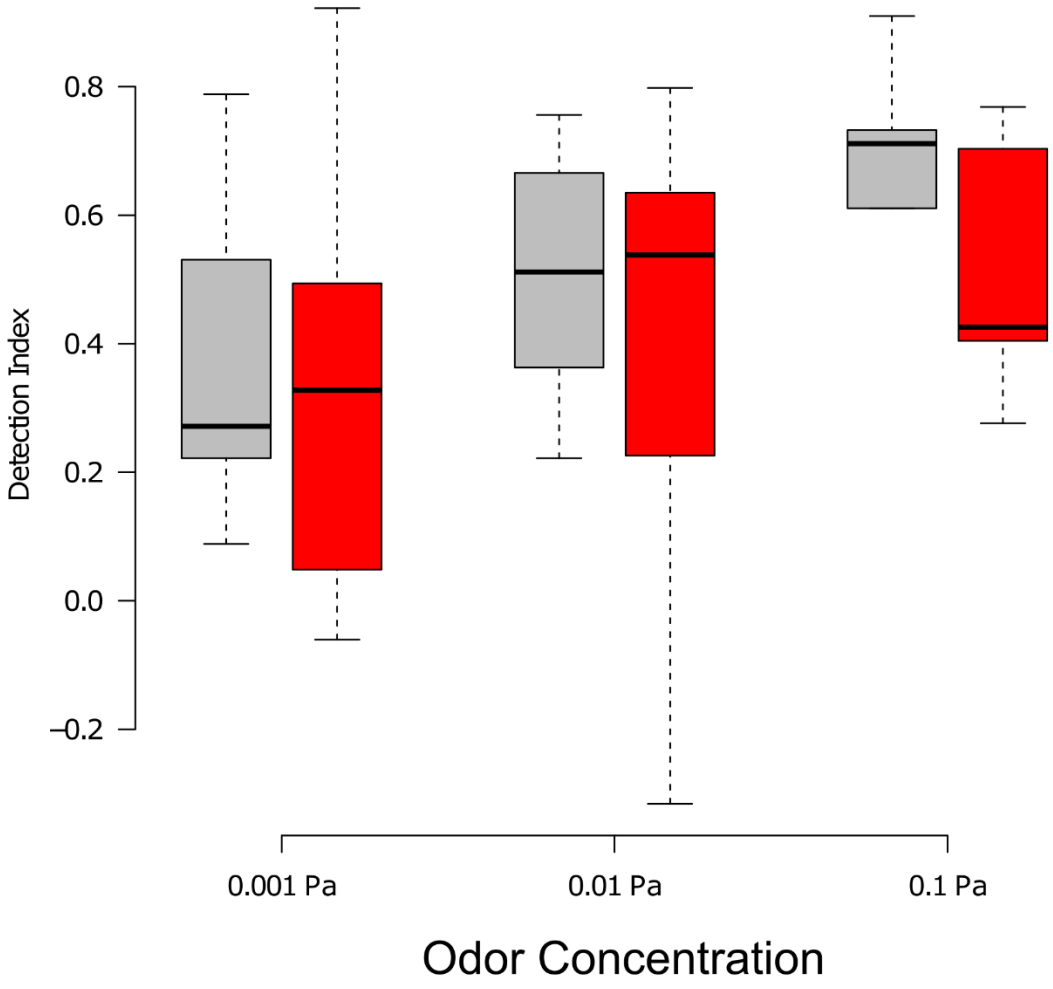
0.8
0.6
0.4
0.2
0.0
−0.2
Detection Index
0.001 Pa
0.01 Pa
0.1 Pa
Odor Concentration

Figure 11. Odor detection is not impaired by cinanserin infusion. The x-axis represents odor concentration and the y-axis represents Detection index. Detection index values may be between -1 and 1 (See methods). The data here was calculated from the rats presented three trials of mineral oil followed by one test trial. Detection index is represented as box plots, data following saline infusion in gray, data following cinanserin infusion in red. No significant differences between drug treatments were found within the data set suggesting that while rat showed impaired habituation to odors at 0.001 Pa following cinanserin infusion, they remained about to detect novel odorants from mineral oil.

following post-hoc custom hypothesis testing. Thus, while habituation and odor discrimination behavior were impaired most dramatically at 0.001 Pa (Figs. 3, 4), these effects were not due an inability to detect novel odorants within a mineral oil solution. Instead, our results suggest that the chemical processes and neural circuits underlying odor habituation memory and discrimination are modulated by both intact 5-HT_2 receptor activity and the strength of afferent input from the nasal epithelium.

Experiment 2: Forced choice discrimination task

It has previously been shown that the role of neuromodulators for discrimination between chemically similar odorants can depend on the behavioral task used (Mandairon et al. 2008). To account for differences in discrimination behavior as a function of behavioral tasks, we tested the effect of 5-HT2 receptor blockade on reward-motivated odor learning. As in the habituation experiments, rats were tested at three odor concentrations, and forced to discriminate between odorants of differing levels of similarity to obtain a sweet cereal reward. Discrimination performance, measured as the fraction of trials correct, significantly increased over 20 trials as odor concentrations increased ($F_{2,224.6} = 9.73$, $p < 0.0001$, data not shown). Similar to effects of carbon difference on spontaneous discrimination (Experiment 1), reward-motivated discrimination performance exhibited a monotonic increase with increasing structural dissimilarity between the rewarded and non-rewarded odorants ($F_{3,219.3} = 5.7357$, $p = 0.0009$). Lastly, we detected a significant effect of cinanserin treatment on discrimination performance ($F_{1,218.8} = 18.92$, $p < 0.0001$) (**Fig. 12**), but no significant interactions (treatment*carbon difference, treatment*concentration,

FIGURE 12

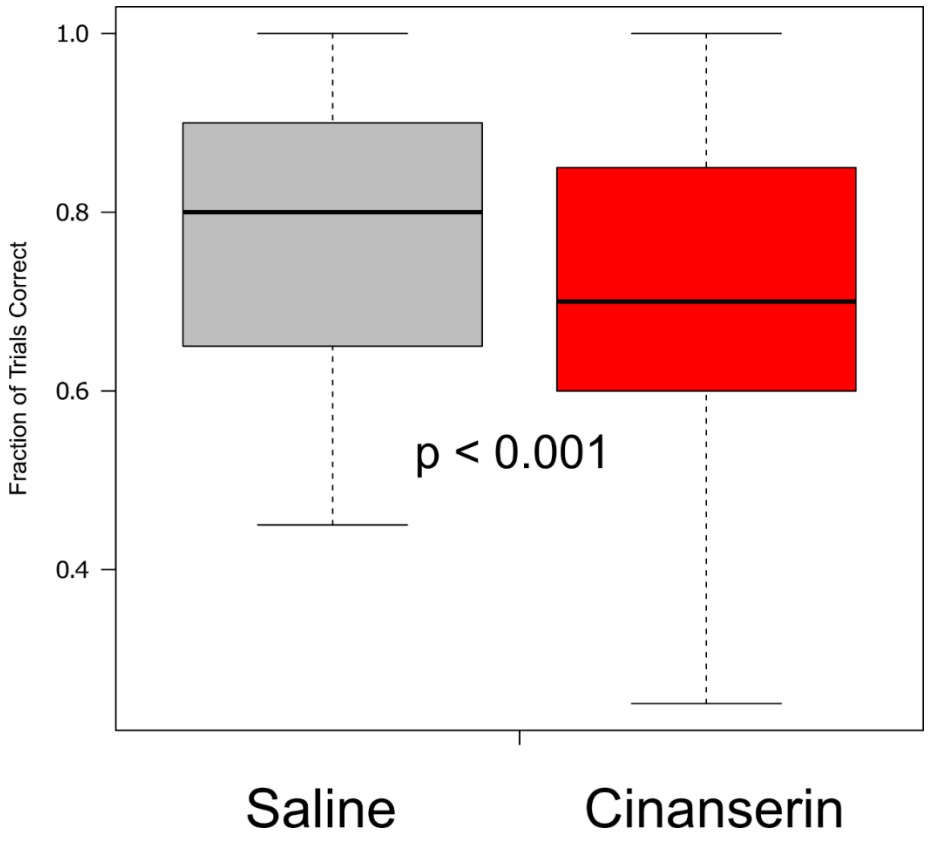
1.0
0.8
0.6
0.4
Fraction of Trials Correct
p < 0.001
Saline
Cinanserin

Figure 12. Cinanserin infusion broadly impaired odor learning in a forced choice odor discrimination task. The x-axis depicts the two drug conditions, saline and cinanserin infusion. The y-axis is the fraction of trials correct over 20 trials. Pooling all the data from all carbon difference tests from all odor concentrations showed that cinanserin infused rats performed statistically less well than saline controls. The p-value from the F-test performed on fixed effects within the linear mixed model is shown on the figure. No significant two-way or three-way interaction terms between drug treatment, odor concentration, and carbon difference were found.

treatment*concentration*carbon difference). The strong drug effect with no significant interaction terms, suggests that unlike our results from spontaneous discrimination (Experiment 1), cinanserin infusion broadly impaired discrimination behavior across all odor concentrations and structural differences between odorants, suggesting a general role of 5-HT2 receptors in olfactory reward learning.

DISCUSSION

While serotonergic modulation has been shown to be critical for olfactory learning in neonatal rodent pups, little data exists on how serotonin affects olfactory learning and perception in adult rodents. Here, we investigated the role of 5-HT2-mediated serotonin action in the MOB on olfactory-guided behavior in two distinct perceptual paradigms: the non-associative odor cross-habituation paradigm (Experiment 1) and the reward-motivated two-alternative choice digging discrimination paradigm (Experiment 2). Rats infused with the 5-HT2 antagonist, cinanserin, showed significant deficits in both tasks. Within the olfactory habituation task, cinanserin treatment significantly impaired habituation to odor stimuli. This deficit was only apparent at the 0.001 Pa odor concentration, where cinanserin treated animals showed no detectable change in investigation time over the three habituation trials. Cinanserin also impaired the rats' responses to novel stimuli during test trials designed to test whether they could discriminate between novel odors and the habituated odor. Importantly, the extent of their behavioral discrimination impairment was dependent on both the structural similarity between the habituation and test odorants as well as the concentration at which these odorants were presented. At low odor concentrations

(0.001 Pa), unlike saline controls, cinanserin infused rats did not show increases in investigation behavior during any of the novel odor test trials. Furthermore, at 0.01 Pa, 5-HT2 antagonism induced impairments for structurally more similar odorants, but not for structurally dissimilar odorants. At 0.1 Pa, 5-HT2 antagonism did not induce measurable deficits in spontaneous discrimination of novel odorants. These results support an important role for 5-HT2 receptor-mediated serotonin action in non-associative olfactory memory and perceptual processes.

In addition to causing deficits in spontaneous, non-associative odor discrimination, 5-HT2 receptor blockade also impaired odor discrimination in a reward-associated forced-choice task. However, unlike the effect in the non-associative task, the effect of 5-HT2 antagonism was not dependent on odor concentration or the chemical difference between the two odors. Instead, there was a significant decrease in discrimination performancewhen data was pooled across all odor concentrations and carbon difference tests. Thus, serotonergic modulation within the MOB is important for both non-associative and associative learning and odor discrimination.

Our finding that 5-HT2 receptors are important for olfactory perceptual and memory processes is consistent with other studies that have blocked serotonergic activity within the MOB either through receptor specific neuropharmacology or neurochemical lesioning (McLean et al., 1996; McLean and Harley, 2004; Yuan et al., 2003). In neonatal rat pups, systemic or intrabulbar infusion of a 5-HT2 antagonists impaired the acquisition of odor preference learning (McLean et al., 1996). Interestingly, this deficit could be overcome by simultaneous infusion of high doses of

isoproterenol, a β-adrenoceptor agonist. Alone, isoproterenol infusion has been shown to increase bulbar cAMP levels and was sufficient to induce olfactory preference learning. While 5-HT2 receptors do not directly control intracellular cAMP levels, *in vitro* and *in vivo* data from the rat cortex and neonatal MOB respectively showed that 5-HT2A receptor activation enhanced cAMP levels generated by isoproterenol activation of the β-adrenoceptor (Morin et al., 1992; Yuan et al., 2003). β-adrenoceptors and 5-HT2A receptors have been found co-localized within mitral cells, but mechanism of how the 5-HT2A receptor enhances the increase in cAMP concentrations resultant from β-adrenoceptor activation is unclear (Yuan et al., 2003). These studies demonstrated an important functional link between serotonergic and noradrenergic signaling pathways in the acquisition of olfactory preference memories (McLean and Harley, 2004). In adult rats, Moriizumi et al. (1994) found a loss of olfactory avoidance memory following the neurochemical lesioning of MOB serotonergic fibers by 5,7-DHT infusion. Interestingly, this behavioral deficit was concomitant with a significant decrease in volume of the glomerular layer, suggesting that bulbar serotonin is necessary to maintain structural integrity of olfactory circuits within the MOB (Moriizumi et al., 1994). 5-HT is also important for olfactory-guided behavior in non-rodent mammalian species. In the greater short-nosed fruit bat, *Cynopterus sphinx*, depletion of bulbar serotonin induced deficits in the acquisition of odor-guided feeding behaviors (Ganesh et al., 2010). Our finding that blockade of 5-HT_2 receptors impairs the formation of non-associative odor habituation memory and the acquisition of reward-odor associations in conjunction with previous studies

suggests that serotonergic activity via 5-HT_2 receptors within the main olfactory bulb regulates the expression of odor-guided behaviors in the adult rat.

How do the effects of 5-HT2 antagonism compare to the antagonism of cholinergic and noradrenergic receptors within the MOB? Previous work from our and other laboratories has shown that the neuromodulators, acetylcholine (ACh) and noradrenaline (NA), modulate olfactory perception and learning in a variety of behavioral paradigms (Doucette et al. 2007; Guérin et al. 2008; Mandairon et al. 2006; Mandairon et al. 2008; Devore et al 2014). Using the non-associative odor habituation paradigm, it was shown that infusion into the MOB of antagonists of either a nicotinic acetylcholine receptor (nAchR) or the α1 noradrenaline receptor impaired spontaneous discrimination of structurally similar, but not dissimilar odorants (Mandairon et al. 2006; Mandairon et al. 2008). Our results showed a similar effect on spontaneous discrimination behavior following 5-HT2 antagonism. Unlike the current study, these earlier studies did not report an effect of ACh or NE receptor blockade on the formation of odor habituation memory. However, when ACh and NA blockers were used, odors were not presented at0.001 Pa as we have done in the current study, and it is unclear whether ACh and NA may be important for habituation at low odor concentrations. The present results demonstrated that 5HT modulation of habituation memory formation is strongest at odor concentrations near the detection threshold.

While NA, ACh, and 5-HT have all been shown to modulate spontaneous discrimination behavior, our finding that a 5-HT2 antagonist impaired reward-motivated discrimination behavior was inconsistent with the effects of blocking NA or

ACh receptors in an identical paradigm. Utilizing our forced-choice digging paradigm, Mandairon et al. 2008 showed that while NA receptor blockade impairs performance during the first quarter of the 20 discrimination trials, the overall mean performance was not different from saline controls. Similar negative results were found following the infusion of cholinergic receptor antagonists (Mandairon et al. 2006). This marked difference between the results following blockade of 5-HT2 and that of NA or Ach suggests that 5-HT2-mediated serotonergic action plays an indispensible role in shaping bulbar odor representations, which may in turn modulate downstream processing regions such as the piriform cortex to guide behavioral choice.

While previous studies have not detected effects of NA or ACh receptor antagonism on odor discrimination in our digging task, NA and ACh have been shown to play important roles in less ethological behavioral paradigms such as the "Go-No Go" task (Doucette et al. 2008) and the two-alternative forced choice operant conditioning paradigm (Devore et al. 2014). Thus, the outcomes of manipulating major bulbar neurodmodulator pathways greatly depend on the nature of the task to be solved by the animal, as observed for 5-HT action using our two discrimination paradigms. Given these task contingencies, future studies utilizing multiple behavioral paradigms in the same animal will better elucidate how neuromodulators affect odor representations at downstream processing regions to guide discrimination behavior.

5-HT has been shown to depolarize mitral cells in brain slices (Brill et al. 2016) and increase the firing rate of mitral cells in response to odor inputs *in vivo*. 5-HT has also been shown to increase the firing rate and burst frequency of ET cells

within the glomerular layer. Both of these effects could enhance odor responses at lower odor concentrations and could explain the behavioral result within the habituation experiment. These cellular level effects could also explain the observed differences in spontaneous and forced-choice discriminations. Contrast enhancement is thought to occur within the glomerular layer of the MOB. Direct excitation of mitral cells or increased monosynaptic excitation of mitral cells via ET cells would increase excitatory drive and the co-occuring increase in ET to PG and ET to SA activity would increase glomerular level inhibition. A recent imaging study reported that DRN stimulation decorrelated mitral cell odor responses (Kapoor et al., 2016). This network level result suggesting a "gain of function" following 5-HT release is consistent with loss of function behavioral effects following 5-HT2 receptor antagonist infusion, decreased investigation of structurally similar odors during test trials within the habituation paradigm and decreased learning in the forced-choice discrimination task. Future experiments performed pairing behavioral pharmacology and awake-behaving neurophysiological approaches in both the habituation and forced-choice discrimination tasks would greatly aid in the understanding how 5-HT modulates cellular and network activity within the MOB and shapes odor responses across a variety of odors, odor concentrations, and environmental contexts or behavioral demands.

Serotonergic fibers emanating from the MRN and DRN have been hypothesized to serve important functions in arousal, sensory processing, reward, and learning and memory in a variety of species and experimental paradigms (Cohen et al. 2015; Hurley and Hall 2011; Jacobs and Fornal, 1999; Liu et al. 2014; Yokogawa et

al. 2012). Our results are consistent with the idea that 5-HT plays an essential role in modulating sensory representations within dedicated sensory structures and gating memory processes

CHAPTER 3

5-HT2 RECEPTOR ANTAGONISM SLOWS ODOR DISCRIMINATION IN RATS

Introduction

Laboratory studies investigating rodent olfactory behavior are essential to the field of olfactory neuroscience because they constrain and inform hypotheses regarding the functional significance of olfactory computations and mechanisms proposed to occur within the olfactory bulb and olfactory cortices. Olfactory discrimination learning is a classic behavioral paradigm to assess the sensory abilities of animals in response to a variety of experimental manipulations, both of internal (i.e. pharmacological manipulations of neural tissue) and external variables (i.e. odor quality, odor concentration, task difficulty/demands). One common approach to test for the dependence of olfactory decision-making on experimental manipulations is the study of reaction times, and their covariance with animal performance (Abraham et al. 2004, Abraham et al. 2006, Nunes and Kuner 2015, Rinberg et al. 2006, Uchida and Mainen 2003). Studies of reaction times across species and sensory modalities have informed theoretical models of decision-making, leading to a series of widely employed models known as integrator or evidence accumulation models (Gold and Shadlen 2007, Heitz 2014). These models can account for several commonly observed relationships between the accuracy and timing of perceptual decisions in both human and animal studies. First, when task difficulty is increased, reaction times increase. Secondly, when stimulus exposure and sampling is controlled, performance increases with increased sampling duration. Lastly, for a given behavioral task, subjects can change their "speed-accuracy tradeoff" (SAT), responding more

accurately and incurring the cost of slower responses, or more quickly and incurring the cost of reduced accuracy. Along with accounting for numerous experimental human and animal data, neurophysiological recordings collected in animals performing perceptual decision-making tasks have shown neural correlates of variables described within temporal integration/evidence accumulation models (Gold and Shadlen 2007).

Within the past 15 years, studies utilizing rigorous psychophysical experimental approaches have proposed conflicting views regarding the relationship between animal task performance, sampling time, and task difficulty in the olfactory modality. Uchida and Mainen (2003) trained rats to discriminate two pure odorants and their mixtures in an operant conditioning paradigm, varying the task difficulty by changing the relative concentrations of components in the binary odor mixtures. Rats were trained to first poke their noses into a center port where odors were delivered. Rats then sniffed the odor stimulus, and based on a learned association moved to the left or the right port for a water reward. This behavioral paradigm is commonly referred to as the two alternative forced choice paradigm (2AFC). As one might expect, they reported that rats perform with lower accuracy on more difficult tasks, yet their sampling behavior was shown to be independent of task difficulty. Rinberg et al. (2006) performed a similar study utilizing the 2AFC paradigm in mice, but unlike the study by Uchida and Mainen, Rinberg et al. utilized a "go signal" to train animals to sample for an arbitrarily long amount of time. Mice were trained to hold their nose within an odor port until the "go signal", an auditory buzz, sounded. When forced to sample the stimulus for a longer amount of time, mice performed better, but did not choose longer sampling times on their own in the absence of the "go signal", suggesting that while sampling does affect performance this relationship may not be naturally expressed. Further work by the lab of Dr. Zachary Mainen and colleagues has suggested that

rodents are sampling optimally and that increasing sampling time does not lead to increased accuracy within this behavioral task. They suggest that temporal integration is limited to one or two sniffs following odor delivery (Zariwala et al. 2013).

In contrast to the studies above, voluntary modulation of sampling times in response to experimental variables has been reported in both mice and rats. Abraham et al. (2004) trained mice in a Go/No-Go paradigm (GNG) where mice were trained to lick for a water reward delivered within an odor port in response to one odor (S+) and withdraw their heads from the port in response to a second odor (S-). Mice were rewarded on correct S+ responses and reaction times were collected when an overt behavioral response was produced on correct S- responses. Within this paradigm, mice were tested with both monomolecular odorants and binary mixtures, and mice increased sampling for hard discriminations of binary mixtures when compared to monomolecular odor trials. Experiments performed with rats showed that they improved their task performance as sampling time increased when they performed discriminations of odor mixtures (Rojas-Libano et al. 2012). Recent work has shown that longer sampling times are associated with increased performance in both GNG and 2AFC paradigms when rats have to make difficult discriminations between odor mixtures (Frederick et al. 2017). These results suggest that animals may be temporally integrating sensory evidence for their decision across two to six sniffs and highlight the importance of task selection when performing reaction time analyses. As of yet, no neural correlate of evidence accumulation has been found within the olfactory system and it is possible that longer sampling times lead to improved decision accuracy through some other decision-making mechanism.

One feature common to all of the studies mentioned above is that they report reaction times from rodents exhibiting stereotyped responses after extensive behavioral training: it is not clear how reaction times may be modulated by stimulus

parameters during the acquisition of odor discrimination behavior. Testing mice in a GNG paradigm, Slotnick (2007) reported a significant correlation between sampling time and accuracy as performance increased on S+ trials over the acquisition period. Sampling times on S- trials did not show significant differences over learning. In the same study, increased sampling time was detected with abrupt transitions between odor sets and stimulus conditions such as odor flow rate, used as a proxy for odor concentration. Building off the results reported by Abraham et al. (2004) and Rinberg et al. (2006), Slotnick (2007) reported that sampling time increased during the acquisition phase of the harder discrimination odor sets.

A second feature common to the studies mentioned above is that the researchers only made manipulations to external variables such as reward/punishment schedule, task demands, odor concentrations, and odor quality. How might internal variables such as neuromodulatory tone or particular olfactory microcircuits play a role in reaction times? Neuromodulators within the MOB are known to act on nearly every cell type within the MOB and have been shown to alter olfactory perception and neurophysiology (Chaudhury et al. 2009, Devore et al. 2014, Linster and Fontanini 2014, Mandairon et al 2008). Compared to acetylcholine and noradrenaline, the physiological and behavioral effects of serotonin (5-HT) within the MOB are poorly understood. Recent neurophysiology experiments have shown that 5-HT modulates both intrinsic and synaptic properties of glomerular layer interneurons and projection neurons *in vitro* (Brill et al. 2016, Hardy et al. 2005, Liu et al. 2012, Schmidt and Strowbridge 2014); it also modulates olfactory tuning of projection neurons and decorrelates mitral cell population activity *in vivo* (Brunert et al. 2016, Kapoor et al. 2016). To investigate how 5-HT might modulate olfactory decision behavior, I analyzed rat behavior in a forced choice discrimination task, as described by Cleland et al. 2002, to assess olfactory discrimination learning after blocking serotonergic

receptors via bilateral infusion the 5-HT_2 receptor (5-HT_2R) antagonist, cinanserin. Within this task, cinanserin infused rats were slowed in latency to make a decision (digging latency) in only the most difficult discrimination at medium and high odor concentrations, but remained statistically equivalent in performance when compared to their own saline controls suggesting that 5HT2 receptors within the MOB play an important role in the optimization of olfactory decision making.

Methods

Rats were videotaped (30-Hz acquisition frame rate) while performing the forced choice odor discrimination task following bilateral infusion of either 0.9% saline or 0.9% saline with 6 mM, 5-HT_2 receptor (5-HT_2R) antagonist, cinanserin into the main olfactory bulb. Rats were tested for a total of 24 experimental days with 20 trials per day. Each day consisted of a unique combination of odor concentration, carbon chain difference, and drug treatment. The rats were tested at three levels of odor concentrations (0.001 Pa, 0.01 Pa, 0.1 Pa), four carbon differences (1C, 2C, 4C, different functional group) and in the two aforementioned drug conditions. Video analysis with custom software (LabView) was used to measure the latency to digging in an odor pot. The start of the trial was scored as the time when the rat's head crossed from the intertrial interval half of the chamber into the experimental half of the chamber following the removal of the divider by the experimenter. The end of the trial was defined as the time when the rat began digging into an odor pot. Consistent with previous reports of sampling time during olfactory behavior, the sampling times were measured from trials in which rats chose the rewarded ("correct") odor (Uchida and Mainen 2003)

Digging times were analyzed using a linear mixed modeling approach using the lme4 package in R (Bates et al. 2015). Due to the non-normal distribution of raw digging latency values, the natural log of digging latency was used as the dependent

variable in the statistical model. Linear mixed models (LMMs) include both fixed and random effects. The inclusion of random effects allows for subject-specific modeling of the data that better accounts for the correlated nature of the experimental data. This LMM consisted of two random effects, Rat ID and odor set, and eight fixed effects. Seven of the fixed effects were discrete experimental predictors: carbon difference, drug treatment, odor concentration and all two- and three-way interactions between carbon difference, drug treatment, and odor concentration. The eighth fixed effect, trial number, was modeled as a continuous predictor. The significance of each fixed effect was assessed with F tests with Kenward-Rogers approximation using the lmerTest package in R (Kuznetsova et al. 2014). Post-hoc comparisons were performed on least square means of the LMM utilizing the Tukey's HSD test to account of multiple comparisons. Post-hoc significance was assessed at a threshold of $p < 0.05$. In the presented data figures, all least square means have back transformed from ln(seconds) to seconds.

Results

Response times and their covariance with task performance are key measures in the study of olfactory perception. Previous studies of sampling duration during olfactory discrimination tasks have utilized rigorously controlled psychophysical experiments where rodents become highly stereotyped in their behavior and undergo extensive behavioral training before data is analyzed. Here I report response times in a less behaviorally constrained odor discrimination learning task (Cleland et al. 2002) during the first 20 acquisition trials, measured as latency to dig. To assess how infusion of 5-HT_2R antagonist, cinanserin, affected odor-guided behavior during a discrimination learning paradigm, we used video analysis to monitor both choice behavior and sampling behavior during the task. Here we varied olfactory stimuli by

altering odor concentration and the structural similarity between test odors by varying carbon difference and altered neuromodulatory tone through the bilateral infusion of a selective 5-HT_2R antagonist, cinanserin, into the MOB.

Rats showed a large distribution of digging latencies on correct trials (range: 266 ms to 30.1 s; Fig. 1A). A LMM statistical analysis detected significant variation in digging latencies across the experimental data. A significant effect of trial number was found on digging latency in correct trials ($F_{1,3220.4} = 47.363$, $p < 7.058e\text{-}12$) (Fig. 1B). The beta coefficient of the LMM model term "trial number (equivalent to the slope) here modeled as a continuous predictor, was -0.0102. When properly correcting for the dependent variable being log transformed, a beta coefficient -0.0102 signifies a 1.015% decrease in digging latency for every increase in trial number. This effect is small in size, but very significant in this statistical analysis and shows that increased learning modestly decreases latency to make a decision. When trial number was removed from the LMM to produce a reduced model which was then compared to the original model, I found a significant difference in log-likelihood ratio, suggesting trial number should remain included in the LMM. The statistical model detected a significant three-way interaction between odor concentration, carbon difference, and drug treatment ($F_{6,3212.7} = 3.149$, $p = .0044$), suggesting the latency to dig was non-homogenous across stimulus conditions. Following detection of the three-way interaction term, post-hoc tests were performed to test for differences between drug conditions in each stimulus parameter combination. Within tests at 0.001 Pa, post-hoc tests showed no significant differences between digging latencies between saline and cinanserin conditions at any carbon differences. In contrast, when analyzing data collected in experiments at 0.01 and 0.1 Pa, post-hoc tests detected significant differences between digging latencies at the 1C difference, but not at 2C, 4C and

different functional group tests (Tukey's HSD, 0.01 Pa, saline vs. cinanserin 1C, p =2.38e-12; 0.1 Pa. saline vs. cinanserin 1C, p = 1.75e-6) (Fig. 2). In 1C tests at 0.01

FIGURE 1

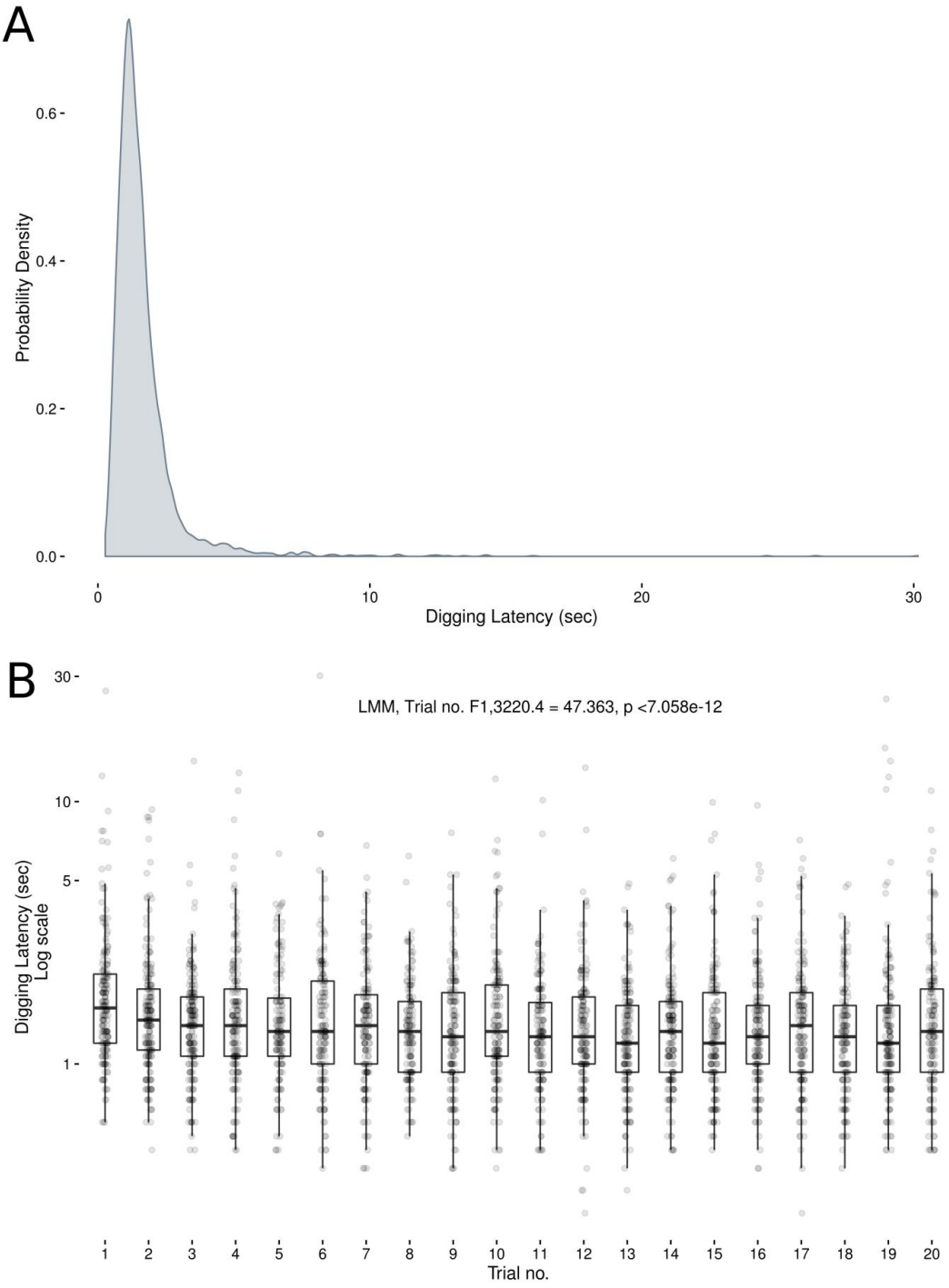

Figure 1. Digging latencies. Summary statistics are in the results. **A.** Probability density of digging latencies across all correct trials. Digging latencies were non-normally distributed and log-transformed for statistical analysis. **B**. Trial number was a significant fixed effect in a LMM of digging latency. The beta coefficient for trial was -0.010202, which translates into a 1.015% decrease in digging latency for one increase in trial number. For each trial, individual data points are plotted on top of box and whisker plots of data.

Pa, cinanserin treated animals took on average 771 msec longer to begin digging when compared to saline control. At 0.1 Pa, cinanserin animals were slower by an average of 659 msec. As odor concentrations increased, the digging latency of cinanserin infused rats during 1C tests also increased (Fig. 3A). This result was also found in digging latency data when looking at data from all carbon differences (Fig. 3B). This result was not found in rats following saline infusion, instead saline animals showed a non-monotonic curve in sampling time as odor concentration increased but no significant differences were detected between saline groups across concentrations in both 1C and all carbon difference tests. (Fig. 3A and 3B).

Within 0.01 and 0.1 Pa odor concentrations, and very similar odors (1C) rats are performing the same in terms of fraction of food rewards gained per twenty trials with no significant differences in fraction of trials correct between drug groups but took on average over half a second longer when correctly choosing the odor pot if 5-HT2 receptors were blocked in the MOB. Accuracy was maintained at the expense of speed as has been reported in mice performing a GNG task (Abraham et al. 2004). This discrepancy highlights the importance of measuring reaction times in perceptual tasks and suggests a possible speed accuracy trade-off in the higher odor concentration, 1C tests (Fig. 3).

Discussion

Here I studied the speed of decision making in an odor discrimination learning task following manipulation of serotonergic neurochemistry within the main olfactory bulb. Using a linear mixed modeling approach to study the effect of experimental variables on sampling behavior I found a significant effect of trial number, and a

significant three-way interaction between drug treatment, carbon difference, and odor concentration. This three-way interaction was due to the slowing digging latencies

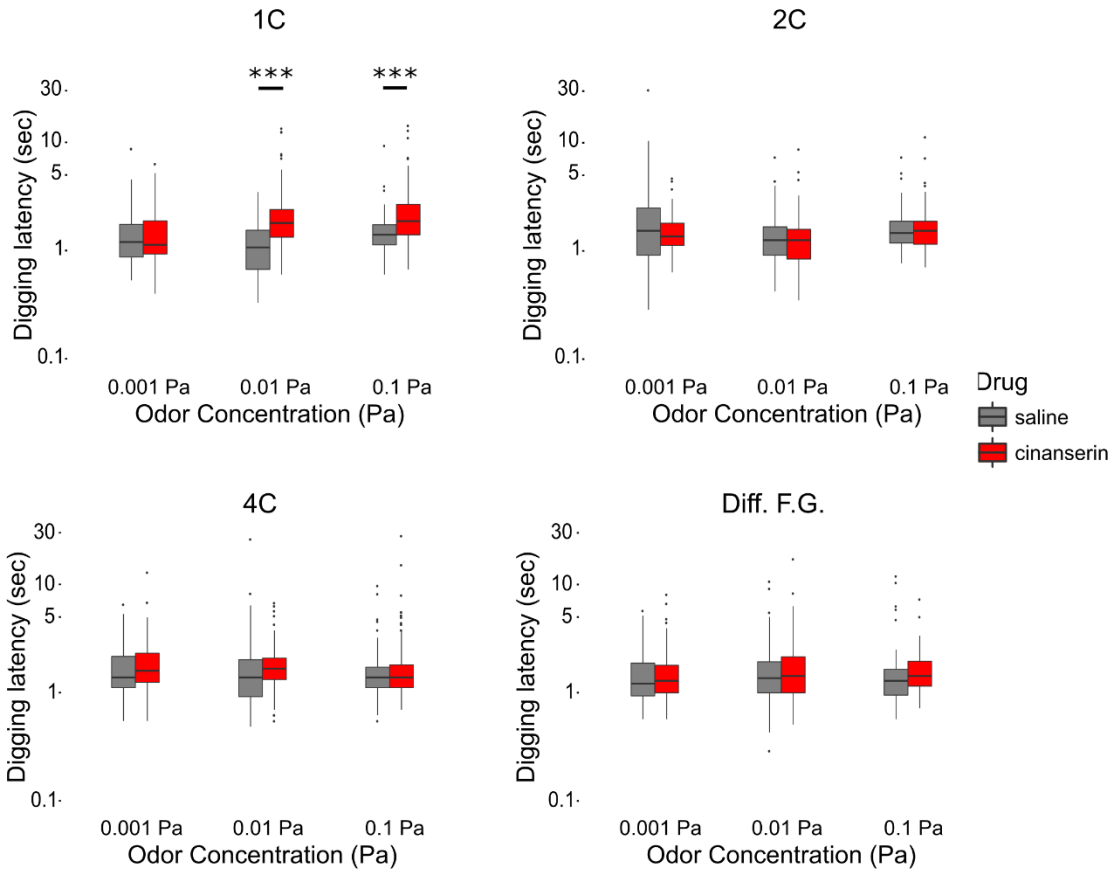

Figure 2. 5-HT_2 antagonist infusion slows digging latency in 1C tests at higher odor concentrations. Digging latency is presented from all carbon difference tests: 1C, 2C, 4C, and different functional group. The x-axis of each graph is odor concentration, increasing from left to right. The y-axis, is digging latency is depicted in log scale. Saline vehicle data is shown in gray, 5-HT_2 antagonist, cinanserin. A linear mixed model analysis found a significant three-way interaction between drug treatment, carbon difference and odor concentration. Significant post-hoc differences are depicted when found, *** signifies a p-value of <0.0001. Digging latencies were significantly different between drug groups only during 1C carbon difference tests at concentrations of 0.01 and 0.1 Pa.

FIGURE 3

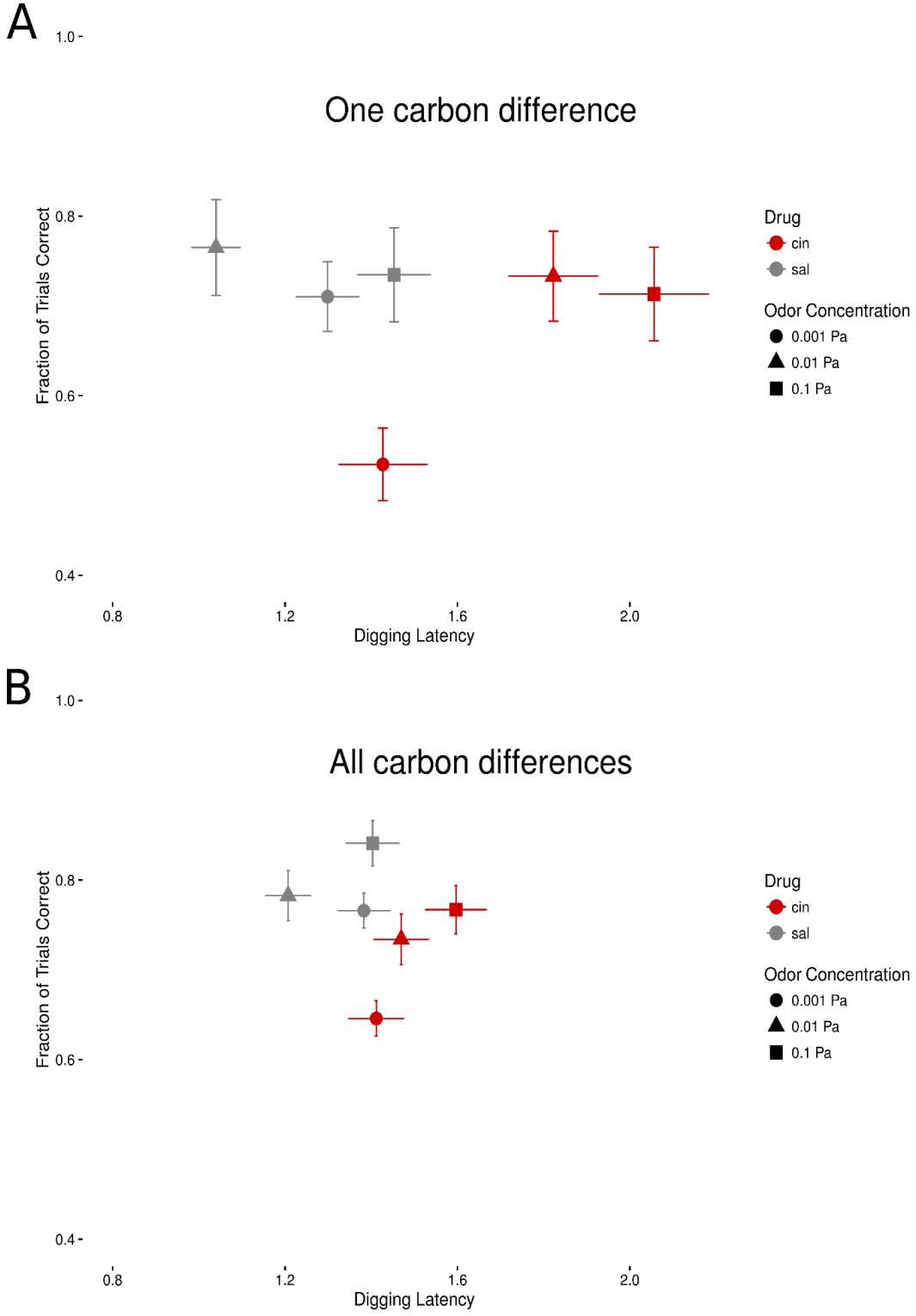
A
One carbon difference
Fraction of Trials Correct
1.0
0.8
0.6
0.4
0.8
1.2
1.6
2.0
Digging Latency
Drug
cin
sal
Odor Concentration
0.001 Pa
0.01 Pa
0.1 Pa
B
All carbon differences
Fraction of Trials Correct
1.0
0.8
0.6
0.4
0.8
1.2
1.6
2.0
Digging Latency
Drug
cin
sal
Odor Concentration
0.001 Pa
0.01 Pa
0.1 Pa

Figure 3. Speed-Accuracy trade off relationship following 5-HT_2 antagonist infusion. In both **A** and **B**, data from saline trials is shown in gray and 5-HT_2 antagonist, cinanserin, in red. Odor concentration Swas denoted by point shape. **A.** Speed-accuracy relationship during 1C difference tests. At 0.01 and 0.1 Pa, 5-HT_2 antagonist (red) infused animals were slower to initiate digging than saline controls (gray), but showed no deficits in task performance. In these trials rats maintained accuracy at the expense of speed. While rats performed most poorly in 1C tests at 0.001 Pa, both a linear and generalized linear model of % correct did not show a significant drug*odor concentration*carbon difference interaction ($p>0.05$) so no claims of statistically differences in trial outcome between drug groups as function odor concentration or carbon difference can be made. **B.** Speed-accuracy relationship at all carbon difference tests. Similar to **A**, detected a significant two-way interaction between drug and odor concentration in the digging latency data ($F_{2,3225.9} = 8.219$, $p < 0.000275$), but we did not detect a significant two-way interaction in models of % correct ($p > 0.5$). In both of the **A** and **B** above, digging latencies increased in cinanserin treated animals as odor concentrations increased. Saline animals did not show significant differences in digging latency across odor concentrations.

during the most difficult odor pairs (1C) tests at intermediate odor concentrations (0.01 and 0.1 Pa). This result is consistent with the idea that intact 5-HT_2R signaling improves discrimination of similar stimuli, but may not be needed for more dissimilar stimuli. While rats were not slowed during 1C tests at 0.001 Pa, they did perform the most poorly during that test when compared to all carbon difference and odor concentration combinations. During 1C tests, at 0.01 and 0.1 Pa, rats infused with cinanserin were statistically equivalent in choosing the correct odor while taking 771 and 659 msec longer to initiate digging, respectively. This maintenance of accuracy with slowing of decision behavior suggests speed accuracy trade-off (SAT) in this task. Tight experimental control of SAT conditions (stimulus duration; response deadlines) within this experiment were not made and instead animals were allowed to sample as long as they wanted. Future studies looking at serotonergic signaling within the olfactory bulb and decision making behavior would benefit from tighter experimental control of stimulus delivery and automation of task events which is not possible using the digging odor discrimination learning paradigm. .

The result that rodents show decreased speed of decisions when presented with similar olfactory stimuli is consistent with work performed in mice a Go/No-go task and showed increased response latencies during trials with binary mixtures but not monomolecular odorants (Abraham et al. 2004). While extrinsic factors such as differences between two odor stimuli modulate decision speed, intrinsic factors such as synaptic interactions between cell types and their resultant network activity also have been implicated in the modulation of olfactory response times. Two studies highlight the role of granule cells (GCs), the most numerous type of inhibitory interneuron in the main olfactory bulb, as important regulators of the olfactory reaction times (Shepherd et al. 2007; Abraham et al. 2010, Nunes and Kuner 2015).

Abraham et al. (2010) showed that in mice that have had selective deletion of the AMPA receptor subunit GluA2 in GCs show decreased response times in a GNG behavioral paradigm when discriminating between two similar odor mixtures. The presence of the GluA2 subunit in AMPA receptors renders the receptor Ca^{2+} impermeable and deletion of the subunit increased Ca^{2+} influx into granule cells following mitral cells activation and increased recurrent inhibition back onto mitral cells *in vivo* and *in vitro*. A similar study that used genetic techniques for selective deletion of receptor subunits within the granule cell layer in conjunction with a GNG behavioral paradigm reported that granule cell specific deletion of the $GABA_AR$ β3-subunit lead to the disinhibition of granule cells and decreased reaction times during difficult odor discriminations when compared to non-manipulated controls. In both studies the neurophysiological outcome of their genetic deletion was increased inhibition from granule cells onto mitral/tufted cells. How this increased inhibition speeds up olfactory decision-making is not yet clearly understood, but GC-mediated inhibition is a major player in a variety of models of odor processing (Cleland and Linster 2005, Laurent et al. 2001, Leon and Johnson 2003, Margrie and Schaefer 2003, Urban 2002) and may represent the substrate of the stimulus-dependent changes in decision behavior presented here. Through a combination of optogenetic and behavioral approaches, GC-mediated inhibition has been implicated in the process of pattern separation within the MOB *in vivo* (Gschwend et al. 2015). Pattern separation is the process through which two overlapping inputs are transformed into two less correlated output patterns. Increased GC-mediated inhibition increased pattern separation as recorded by a reduction in correlation between extracellular odor responses, and increased task performance in a discrimination task both increasing accuracy and reducing reaction times (Gschwend et al. 2015). Importantly, 5-HT has been shown to increase GC-mediated inhibition onto mitral cells (Schmidt &

Strowbridge 2014). 5-HT directly depolarizes MCs which leads to increased excitation of GCs and increased inhibitory feedback onto MCs from GCs. In an awake rodent, 5-HT may modulate MC excitability and shape the inhibitory tone of the olfactory bulb by modulating recurrent inhibition. Following cinanserin infusion *in vivo*, I would expect a decrease in synaptic inhibition onto mitral cells compared to the pre-infusion state with intact serotonergic signaling. This decrease in synaptic inhibition may be a key neural correlate for the behavioral effects presented here. The fact that digging latency was altered at 0.01 Pa and 0.1 Pa odor concentrations may be due the increased tuning width of mitral/tufted cells to odors as odor concentration increased following cinanserin infusion. 5-HT_2Rs have been shown to modulate glomerular layer circuits thought to underlie network computations such as normalization which endow mitral cells with concentration invariant responses (Banerjee et al. 2015). If both glomerular layer computations are compromised following cinanserin infusion, leading to more overlapping odor responses, increased time may be necessary before odor representations are separated enough to guide behavior.

In conclusion, bilaterial infusion of a 5-HT_2R antagonist, cinanserin, yielded higher digging latencies in tests using structurally very similar odorants at intermediate odor concentrations, with uncompromised accuracy. The occurrence of this effect would be expected for a mechanistic effect of 5-HT_2R antagonism that decreased differences between similar odor representations within the MOB. This finding, along with findings in a non-associative task, , show that 5HT_2Rs modulate odor-guided behavior not only as a function of structurally similarity of odorants but also the concentration of the odorants being used.

This study is the first report of blockade of neuromodulatory receptors within the MOB on the speed of olfactory decisions and to put into evidence that odor processing as early as in the OB modulates decision making as well as speed-acurcary trade offs. Our results suggest that when odor representations are rendered less clear due to blockade of 5-HT receptors, rats may make up for this manipulation by longer decisions times to preserve accuracy.

CHAPTER 4

SEROTONERGIC MODULATION OF OLFACTORY BULB DYNAMICS

Introduction

Neuromodulators are released in specific behavioral and state-dependent contexts and modify intrinsic and/or synaptic properties of neurons within neural circuits. Serotonin (5-HT) is an evolutionarily ancient neuromodulator implicated in myriad processes ranging from locomotion, respiration, mood and emotional regulation, neurodevelopment (Lesch and Waider 2012), and sensory processing (Hurley et al. 2004).

Rostrally-projecting serotonergic efferents originate in the dorsal raphe nuclei (DRN) and median raphe nuclei (MRN) and innervate structures throughout the forebrain (Jacobs and Azmitia). The main olfactory bulb (MOB) is one of these target forebrain structures. Serotonergic innervation of the MOB is found throughout bulbar layers, but is strongest within the glomerular layer (GL) of the MOB (McLean and Shipley 1987, Steinfeld et al. 2015, Suzuki et al. 2015). *In vitro* studies have provided evidence for direct actions of 5-HT on MOB glutamatergic neurons, external tufted (ET, local interneurons) and mitral/tufted (MT, projection neurons) cells (Brill et al. 2016, Hardy et al. 2005, Liu et al. 2015). 5-HT increases the firing and burst frequency rate of ET cells (Liu et al. 2012) and this increased ET cell spiking activity increases excitatory drive onto MT cells and GL interneurons, short axon cells (SACs), and periglomerular cells (PGCs) (Brill et al. 2016). 5-HT has also been shown to directly depolarize MT cells, rendering the MOB output more excitable.

Both of the effects of 5-HT on ET and MT cells are through a 5-HT_{2A} receptor mechanism.

In vivo work has shown that 5-HT modulates sensory-evoked responses of both MT cells and interneurons, but the effects are more variable than in *in vitro* slice preparations. Prolonged (minutes long) activation of raphe afferents has been shown to activate a population of juxtaglomerular neurons and suppress olfactory sensory neuron input to the glomerular layer. Transient (sub second) activation of raphe afferents has been shown to potentiate MT cells using imaging techniques. This fast acting effect of raphe stimulation was shown to be in part due to the release of glutamate from raphe terminals.

To date, no data has been published regarding how 5-HT may modulate neural dynamics within the MOB. To examine the role of 5-HT in rhythmogenesis and the relationship to multiunit spiking activity (MUA), I performed extracellular recordings from horizontal bulb slices using a 60-channel planar, microelectrode array (MEA). Consistent with earlier findings, I found that 5-HT application increases MUA activity within bulb slices. When examining the responses of local field potential (LFP) bands I found a significant increase in both the theta (1-10 Hz) and gamma (20-55 Hz) bands. No modulation of MUA or LFP was seen in slices in which the 5-HT_2 antagonist, cinanserin, was bath-applied prior to 5-HT application, suggesting that 5HT modulation in the MOB is mediated through 5-HT_2 receptors

Materials and Methods

Male OMP-ChR2-EYFP transgenic mice bred in house (provided to the Cleland lab by Venkatesh Murthy, Harvard University) were used for all recordings. All procedures for MEA experiments were performed under the auspices of a protocol approved by the Cornell University Institutional Animal Care and Use Committee (IACUC).

OB slice preparation: Horizontal slices (300 uM) were prepared from the olfactory bulbs of 28-42 day old mice. Mice were anesthetized with isoflurane gas and ketamine (150 mg/kg I.P.), then decapitated. Immediately after decapitation, the head was briefly placed in ice cold, oxygenated (carbogen 95% O2, 5% CO2), low-Ca^{2+}/high- Mg^{2+} artificial cerebrospinal fluid (aCSF) dissecting solution containing (in mM) NaCl 124, KCl 2.54, $NaHCO_3$ 1.23, $CaCl_2$ 1, $MgSO_4$ 3, glucose 10). After briefly chilling the tissue, the olfactory bulbs were quickly removed. Slices were cut on a vibrating microtome (Leica VT 1000S, Wetzler, Germany). Slices were incubated in oxygenated dissecting solution at 37ºC for twenty minutes, then maintained in oxygenated dissecting solution at room temperature until transfer to the recording well.

Electrophysiology recordings. During experimental recordings, slices were continuously superfused at 1 mL/minute with heated (34ºC), oxygenated aCSF (in mM: NaCl 125, KCl 3, $NaHCO_3$ 25, NaH_2PO_4 1.25, $CaCl_2$ 2, $MgCl_2$ 1, glucose 25) from a gravity-fed perfusion system. Slices were held in position by nylon webbing glued to C-shaped chrome wire weight. Extracellular signals were recorded from OB slices using a 60-channel planar microelectrode array (MEA; Multichannel Systems, Reutlingen, Germany). The electrodes were arranged in an 8x8 grid (200 μm pitch, minus the four corners); electrode 15 (column 1, row 5) was connected to ground and used a reference. Electrodes were made from titanium nitride and were 30 μm in width, with a 30-50 kΩ impedance. Each electrode on the MEA chip was individually connected to an amplifier in the MEA1060 baseplate. Signals were bandpass filtered (1Hz – 3000Hz), amplified (1200x gain), sampled (20 kHz at 16-bit resolution), and acquired using proprietary MC_RACK software.

Pharmacology. Slices were stimulated by pipetting 200 μL of 200 μM Serotonin creatinine sulfate monohydrate (Sigma-Aldrich, St. Louis, MO, USA) directly into the

aCSF bath. To test if the effect of 5-HT was dependent on intact signaling at the 5-HT_2 receptors we utilized the 5-HT_2 receptor antagonist, cinanserin hydrochloride (20

FIGURE 1

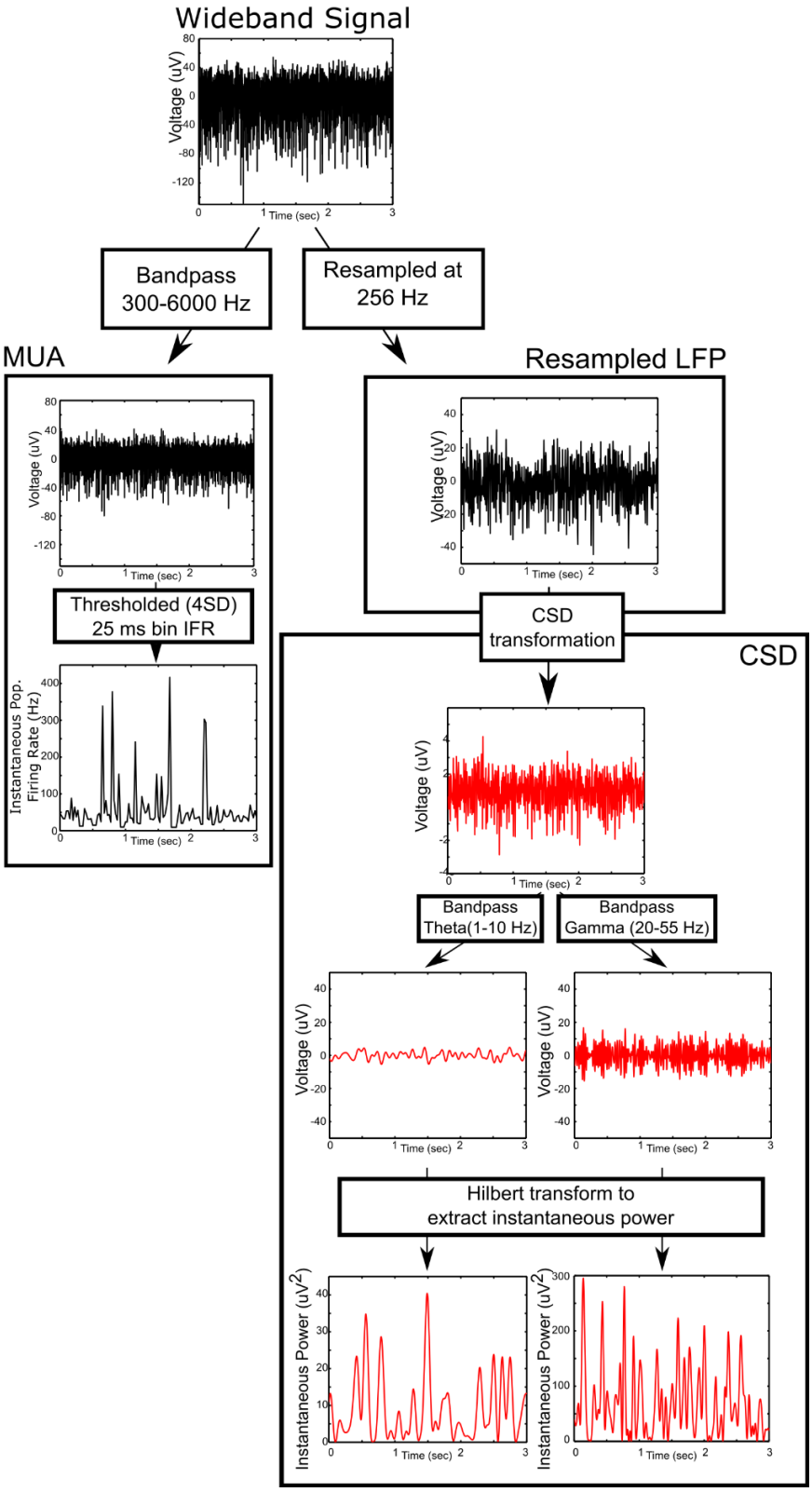

Figure 1. Workflow of signal generation and analysis. Wideband Signal. Raw, wideband data was collected at a sampling rate of 20 kHz. **MUA.** A bandpass filter between 300 and 6000 Hz was applied to the wideband data to extract a bandpassed voltage trace free of low frequency oscillations. This voltage trace was then thresholded at +/- 4SD to extract spike times. The instantaneous population firing rate was then calculated using the reciprocal of the inter-spike interval within a 25 ms bin. The data were then smoothed with a 3 point span (75 ms). **Resampled LFP.** Resampled LFP time series were produced by resampling at 256 Hz. Resampled LFP time series were then filtered into discrete LFP bands: theta (1-10 Hz) and slice gamma (20-55 Hz). The hilbert transform was applied to each filtered time series to extract instantaneous power time series. **CSD.** Current-source-density values produced from applying the 2-D CSD transformation (see methods). Similar to the resampled LFP, CSD time series were filtered into theta (1-10 Hz) and slice gamma (20-55 Hz). The hilbert transform was applied to each filtered time series to extract instantaneous power time series

μM; Tocris Biosciences, Bristol, UK). During experiments using cinanserin, slices were superfused with recording aCSF + 20 uM Cinanserin for at least 3 minutes prior to application of 5-HT via pipette. *Signal processing.* All signal processing was performed using Matlab (Mathworks, Natick, MA, USA).

Local Field Potentials. To extract a local field potential signal, raw wide-band data was resampled at 256 Hz using the resample() function. To attenuate 60-Hz interference and other non-neuronal noise, a principal component analysis based noise removal process was performed. The signal produced by resampling and denoising is referred to as "resampled LFP". Spectrograms were computed using multitaper spectral analysis methods (Chronux package) with 500 msec windows and 100 ms overlap. The time bandwidth product, TW, was equal to (0.5 sec)*(4 Hz) = 2. The number of tapers, K, utilized was calculated from 2*TW-1 = 3 **(**Bokil et al. 2010**).** Spectrograms were normalized by taking a raw spectrogram and then dividing the value at each time-frequency point (pixel in the image) by the mean power at each frequency calculated over a 20 sec baseline, pre-drug stimulation window

$$Normalized\ power(t,f) = \frac{power(t,f)}{baseline(f)}$$

where t = time, and f = frequency. Data were transformed to dB for visualization using the following equation:

$$dB(t,f) = 10 * log10\big(Normalized\ power(t,f)\big)$$

To increase the spatial precision of the localization of extracellular activity the current source density (CSD), which is the second spatial derivative, or scaled Laplacian of the LFP, was calculated by subtracting the mean of instantaneous voltages of four neighboring electrodes (separated by 200 μm) from the instantaneous voltage of that particular electrode. Specifically, for a two-dimensional (2D) microelectrode array, the CSD at coordinate (*x*,*y*) of a particular electrode is defined as (Chen et al. 2011, Dubey and Ray 2015).

$$CSD(x,y) = \left(\frac{-4\varepsilon}{d^2}\right) * \left[V(x,y) - \frac{V(x-1,y)+V(x+1,y)+V(x,y-1)+V(x,y+1)}{4}\right]$$

In line with previous published reports (Chen et al. 2011, Dubey and Ray 2015) I ignored the term ($-4\varepsilon/d^2$). This was done for the sake of simplicity and for CSD time series to have units of voltage. This CSD method uses only differences in the LFP in the lateral direction, implicitly assuming very little variation in the vertical direction. CSD values may only be calculated for electrodes which have four neighboring electrodes. This reduced the total number of recording electrodes to 35 from 59 per brain slice. More complex and advanced methods that would account for boundary layer constraints have been employed for CSD analysis, Similar to PCA denoising, the transformation of resampled LFP to CSD is a type of spatial filtering, but rather than defining weights by inter-electrode covariance, the weights are defined according to inter-electrode distance. CSD analysis increases spatial precision of extracellular signals, and is used to attenuate the effects of volume conduction and 60 Hz interference within the neural time series data (Cohen 2014). Only CSD values were analyzed within this study.

To further extract signals within known MOB LFP bands, CSD signals were filtered using finite impulse response filtering (FIR, firls() and filtfilt() functions in Matlab).

Theta rhythms were extracted by using a 1-10 Hz bandpass FIR filter. Slice gamma rhythms were extracted by using a 20-55 Hz bandpass FIR filter. Next the Hilbert transform (hilbert()) of band pass filtered data (theta, gamma) was calculated. The Hilbert transform takes a real-valued signal and transforms it into what is referred to as "analytic signal" which is a complex valued signal. Complex signals can be understood as time varying vectors directed to points on a complex 2-D plane (i.e. x = real, y = imaginary). The projection of the complex vector onto the real axis is equivalent to the originally recorded voltage value. The angle between complex vector and the real axis is the phase angle. The instantaneous power was calculated by taking the absolute value of the complex signal, or the magnitude of the vector within the complex plane, at every time point and raising it the second power. To analyze the effects of 5-HT application, I divided each recording's data into two 60-sec segments, one just prior to drug stimulation, the second immediately following drug application. In all slices, extracellular responses were detectable within 1-5 sec immediately following 5-HT application. I then calculated the mean instantaneous power from every electrode during the pre- and post-drug 60 sec time periods. The Wilcoxon signed-rank test was used to assess statistical change in power values following 5-HT application in both control and antagonist conditions. The fold change in power within both theta and gamma bands was calculated by dividing the post-drug mean by the pre-drug mean. When comparing the distributions of power changes following 5-HT application in control versus antagonist conditions, the Kolmogorov-Smirnov test was utilized. *Multiunit Activity*. To extract multiunit activity, wide-band data was filtered using a 4^{th} order Butterworth filter between 300 and 6000 Hz. Following filtering, spike detection was performed using threshold crossings at 4 standard deviations above the electrode mean. The instantaneous population firing rate (IFR) was calculated by taking the reciprocal of the inter-spike interval using a 25 ms time bin.

The IFR time series was then smoothed using a 3 point span, 75 ms, using the smooth() function.

Following creation of IFR time series, data for each electrode was broken into two 60 sec segments, one before and one after 5-HT application. The same two 60 sec segments were used for the MUA and CSD data.

Results

Serotonin application induces increased gamma band power within MOB slices

I find that an acute application of 200 μM 5-HT (6-10 sec duration) increased gamma band power within MOB slices (**Fig. 2A**). Unlike previous published reports of gamma oscillations within MOB slices, but consistent with previous work of the lab, these long lasting gamma oscillations lasted on the order of tens of seconds (**Fig 2A, 2B).** When analyzing time series from all electrodes on all recorded slices (CSD, 8 slices, 280 recording electrodes) I found a significant increase in gamma band power when comparing pre- and post-infusion 60 sec windows. (Wilcoxon signed-rank test, CSD, $p < 2.2e\text{-}16$) (**Fig. 3Ai,ii**). When slices were first superfused with the ACSF containing the 5-HT_2 receptor antagonist, cinanserin, I failed to detect a significant change in gamma-band power (Wilcoxon signed-rank test,; CSD, $p = 0.2552$), demonstrating that 5-HT acts through a 5-HT_2 receptor to induce increased network activity in the gamma range (**Fig. 3Bi,ii).** When comparing the normalized change in power in the gamma band following 5-HT application there was a significant difference between the ACSF and ACSF + cinanserin groups (KS Test, $p < 2.2e16$; Fig 3Ci,ii) with the distribution of power changes in the ACSF group exhibiting a long tail, while the ACSF+cinanserin electrodes did not show changes greater than 1.5 times that of baseline.

A

FIGURE 2

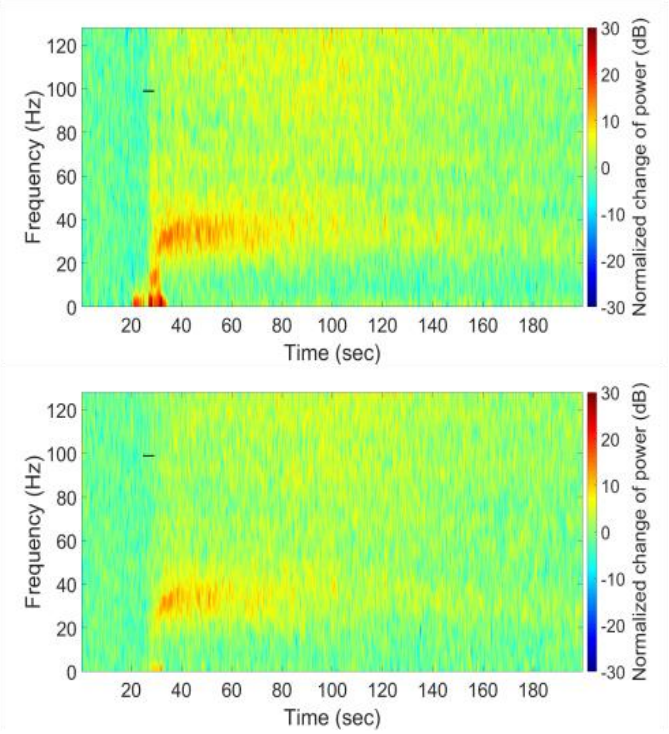
Frequency (Hz)
Time (sec)
Normalized change of power (dB)
Frequency (Hz)
Time (sec)
Normalized change of power (dB)

B

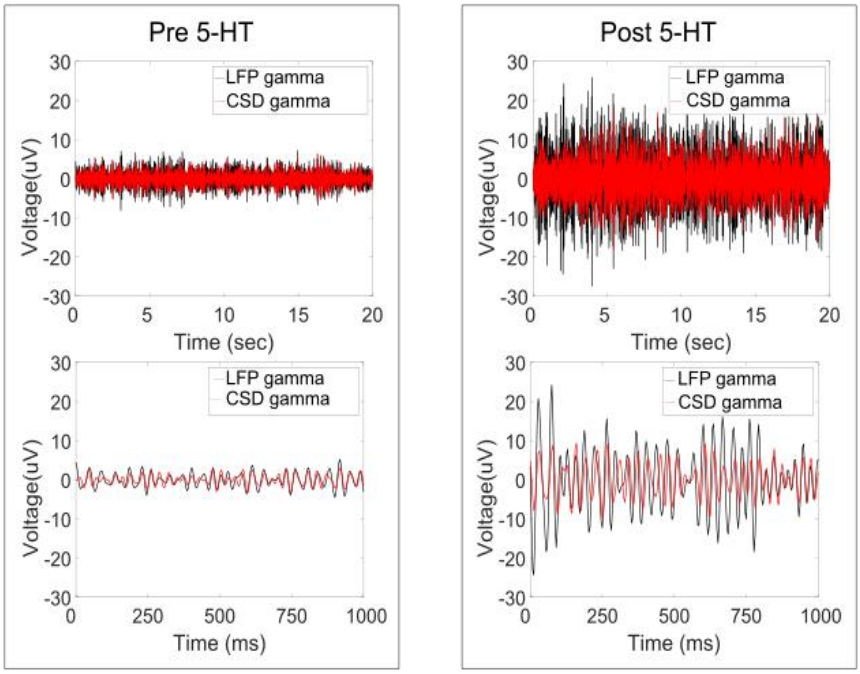
Pre 5-HT
LFP gamma
CSD gamma
Voltage(uV)
Time (sec)
LFP gamma
CSD gamma
Voltage(uV)
Time (ms)
Post 5-HT
LFP gamma
CSD gamma
Voltage(uV)
Time (sec)
LFP gamma
CSD gamma
Voltage(uV)
Time (ms)

Figure 2. 5-HT induces gamma range (20-55 Hz) oscillations. A. Top. Example normalized spectrogram of LFP signal recorded on a electrode showing strong increase in gamma power following 5-HT application (black bar). Bottom, normalized spectrogram of CSD data calculated from the LFP signal used to produce the spectrogram above. **B.** Example time series of LFP and CSD traces filtered between 20-55 Hz before ("Pre-5HT") and after 5-HT application ("Post 5-HT"). Top races are 20 sec segments and bottom traces are 1 sec in length.

FIGURE 3

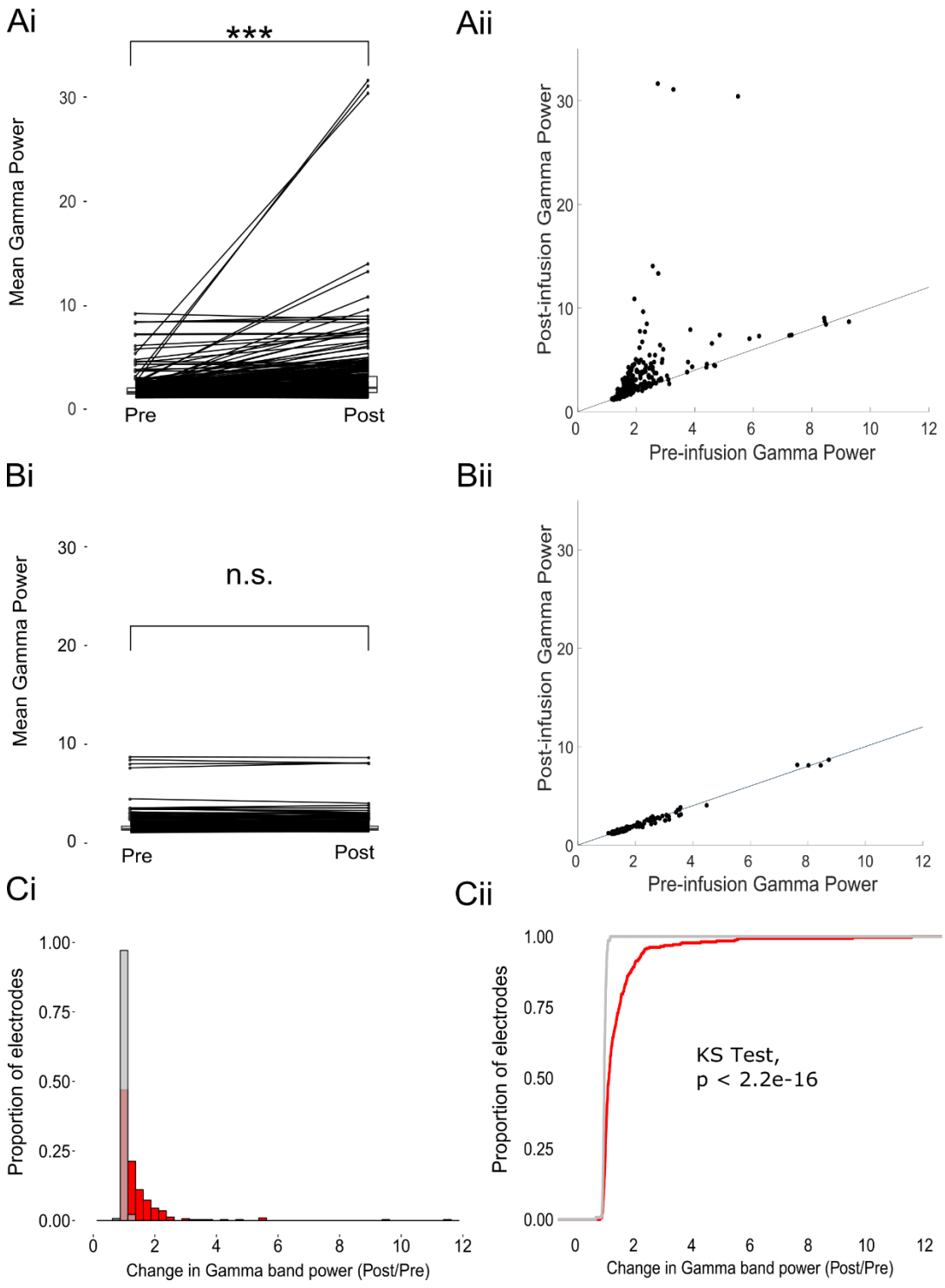
Ai
***
Mean Gamma Power
Pre
Post
Aii
Post-infusion Gamma Power
Pre-infusion Gamma Power
Bi
n.s.
Mean Gamma Power
Pre
Post
Bii
Post-infusion Gamma Power
Pre-infusion Gamma Power
Ci
Proportion of electrodes
Change in Gamma band power (Post/Pre)
Cii
Proportion of electrodes
KS Test,
p < 2.2e-16
Change in Gamma band power (Post/Pre)

Figure 3. Modulation of gamma oscillations by 5-HT requires intact signaling at 5-HT2 receptors. Ai. Results of 5-HT application in normal ACSF conditions. 5-HT increases gamma power. (*** signifies a p-value smaller than 0.00001). **Aii**. Scatter plots of the effect of 5-HT on gamma band power (comparison of 60 sec epochs before and after drug application). Each dot represents a single electrode. **Bi.** Results of 5-HT application in ACSF containing the 5-HT2 receptor antagonist (20 uM). No significant change was found following 5-HT application into the antagonist containing bath. **Bii**. Scatter plots of the effect of 5-HT application in cinanserin containing ACSF bath. **Ci.** Normalized histogram showing the normalized change of power (Post/Pre) in both 5-HT (gray) and 5-HT+Cinanserin (red) conditions. **Cii.** Empirical cumulative distribution function of the same data reported in Ci. The distributions of changes in power (60 sec epochs) following 5-HT application was statistically different from changes in power following 5-HT application into the 5-HT2 antagonist containing bath.

Serotonin application induces increased theta-band power within MOB slices

Consistent with known effects of 5-HT on ET cells and their effects in turn on theta range cellular dynamics, I detected increased theta-band power on MEA electrodes following 5-HT application (**Fig. 4A,B**). The data presented in Figure 4 was recorded from a different slice preparation presented in Figure 2. When comparing 60 sec epochs before and after 5-HT application I detected a significant increase in theta band power when comparing all electrodes (Wilcoxon signed rank test, CSD, $p < 2.2e-16$, 8 slices, 280 electrodes) (**Fig. 5Ai,ii)**. Similarly to the case with 5-HT induced increases in gamma power, increases of theta power were not detected when slices were first bathed with recording solution containing the 5-HT_2 receptor antagonist, cinanserin (Wilcoxon signed-rank test, CSD, $p = 0.051$, 6 slices, 210 electrodes) (**Fig. 5Bi,ii).** When comparing the distributions of the change in power following 5-HT application, there was a significant difference between the ACSF and ACSF+cinanserin conditions (KS test, $p<2.2e-16$, **Fig. 5Ci,ii**). In response to 5-HT the ACSF distribution showed a long tail with electrodes showing changes of power up to 5 times baseline, while the ACSF+ cinanserin distribution was tightly arranged around a normalized change of power of one. These results show that similar to changes in gamma range activity, activation of 5-HT2 receptors increases theta band power in bulb CSD time series.

Serotonin application induces increases in multiunit activity within MOB slices

To investigate population spiking activity I first thresholded the data at 4 +/- SD to extract spike times to produce multiunit spike trains. Consistent with previous work showing that 5-HT increases MT activity, I found a significant increase in

multiunit IFR from baseline following 5-HT application ($p < 2.2e-16$) (**Fig 6Ai,ii)**. On many electrodes, the IFR during the baseline period was 0 Hz, therefore 5HT induced

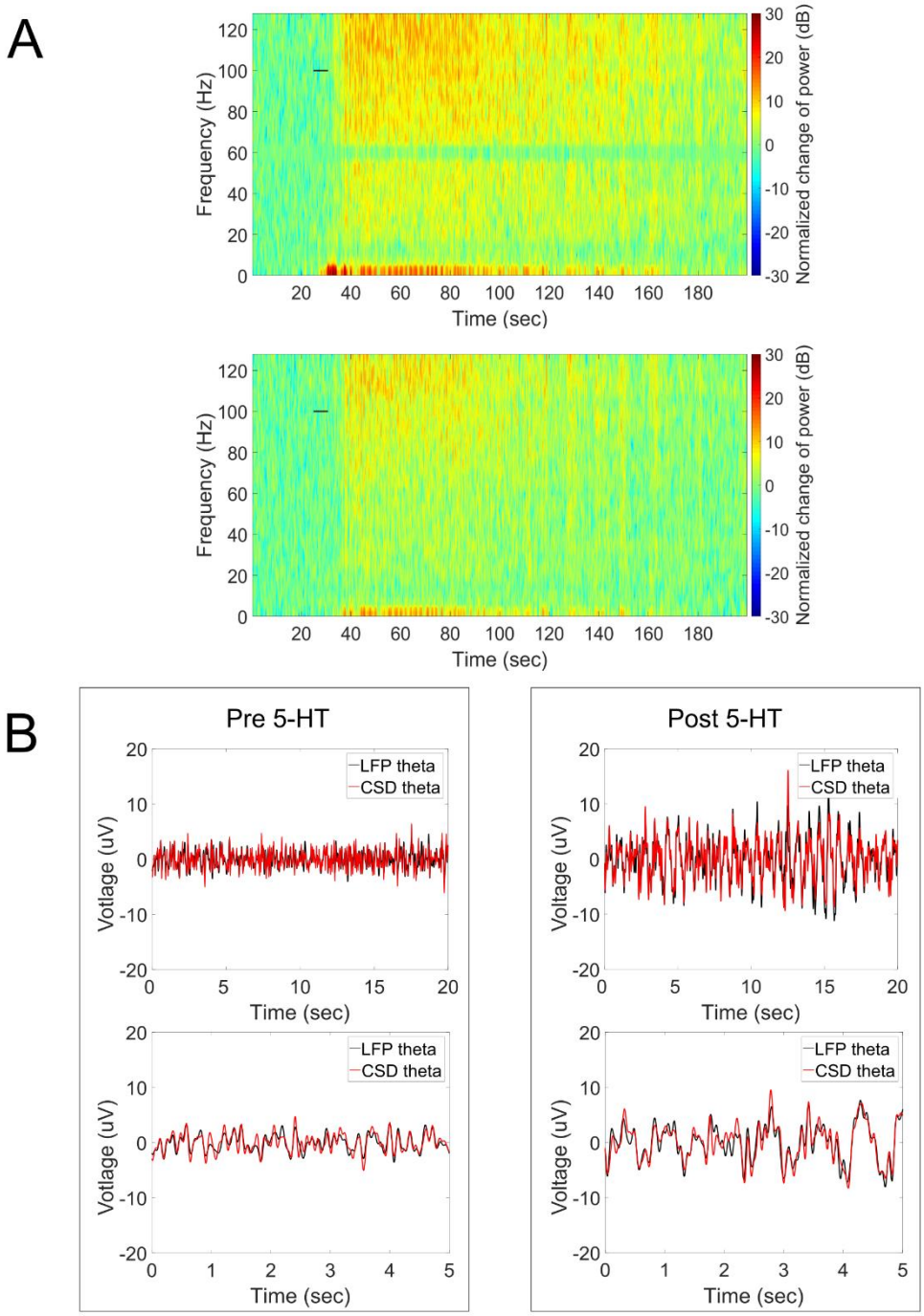

Figure 4. 5-HT induces theta range (1-10 Hz) oscillations. A. Top. Example normalized spectrogram of LFP signal recorded on a electrode showing strong increase in theta power following 5-HT application (black bar). Bottom, normalized spectrogram of CSD data calculated from the LFP signal used to produce the spectrogram above. **B.** Example time series of LFP and CSD traces filtered between 20-55 Hz before ("Pre-5HT") and after 5-HT application ("Post 5-HT"). Top races are 20 sec segments and bottom traces are 5 sec in length.

]

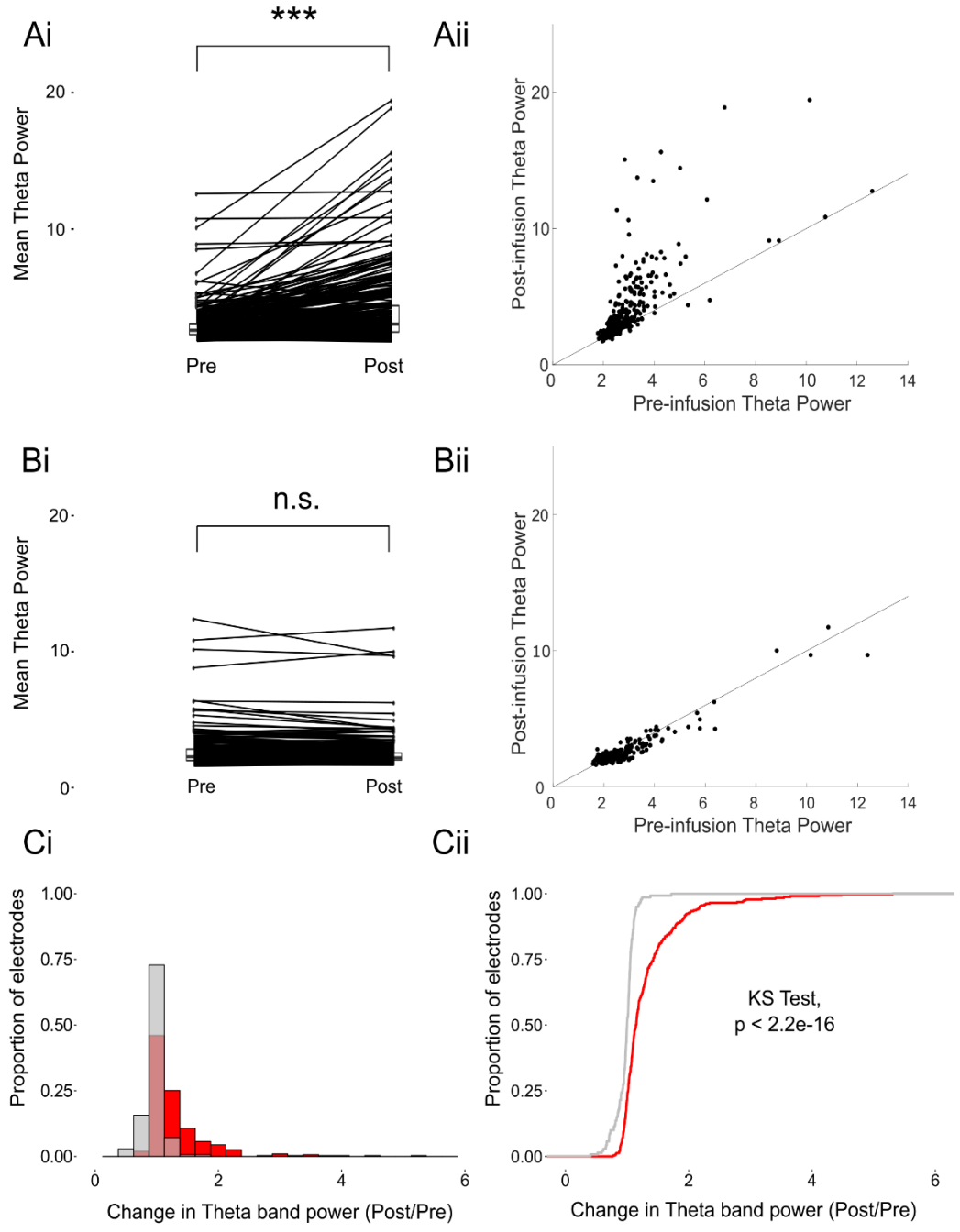
Ai
***
Mean Theta Power
20
10
Pre
Post
Aii
Post-infusion Theta Power
Pre-infusion Theta Power
0
2
4
6
8
10
12
14
Bi
n.s.
Mean Theta Power
0
Bii
Ci
Proportion of electrodes
1.00
0.75
0.50
0.25
0.00
Change in Theta band power (Post/Pre)
Cii
KS Test,
p < 2.2e-16

Figure 5. Modulation of theta oscillations by 5-HT requires intact signaling at 5-HT2 receptors. Ai. Results of 5-HT application in normal ACSF conditions (comparison of 60 sec epochs before and after drug application). 5-HT increases theta power (*** signifies a p-value smaller than 0.00001). **Aii**. Scatter plots of the effect of 5-HT on theta band power (comparison of 60 sec epochs before and after drug application). Each dot represents a single electrode. **Bi.** Results of 5-HT application in ACSF containing the 5-HT2 receptor antagonist (20 uM). No significant change was found following 5-HT application into the 5-HT2 antagonist containing bath. **Bii**. Scatter plots of the effect of 5-HT application in cinanserin containing ACSF bath. **Ci.** Normalized histogram showing the normalized change of power (Post/Pre) in both 5-HT (gray) and 5-HT+Cinanserin (red) conditions. **Cii.** Empirical cumulative distribution function of the same data reported in Ci. The distributions of changes in power (60 sec epochs) following 5-HT application was statistically different from changes in power following 5-HT application into the 5-HT2 antagonist containing bath.

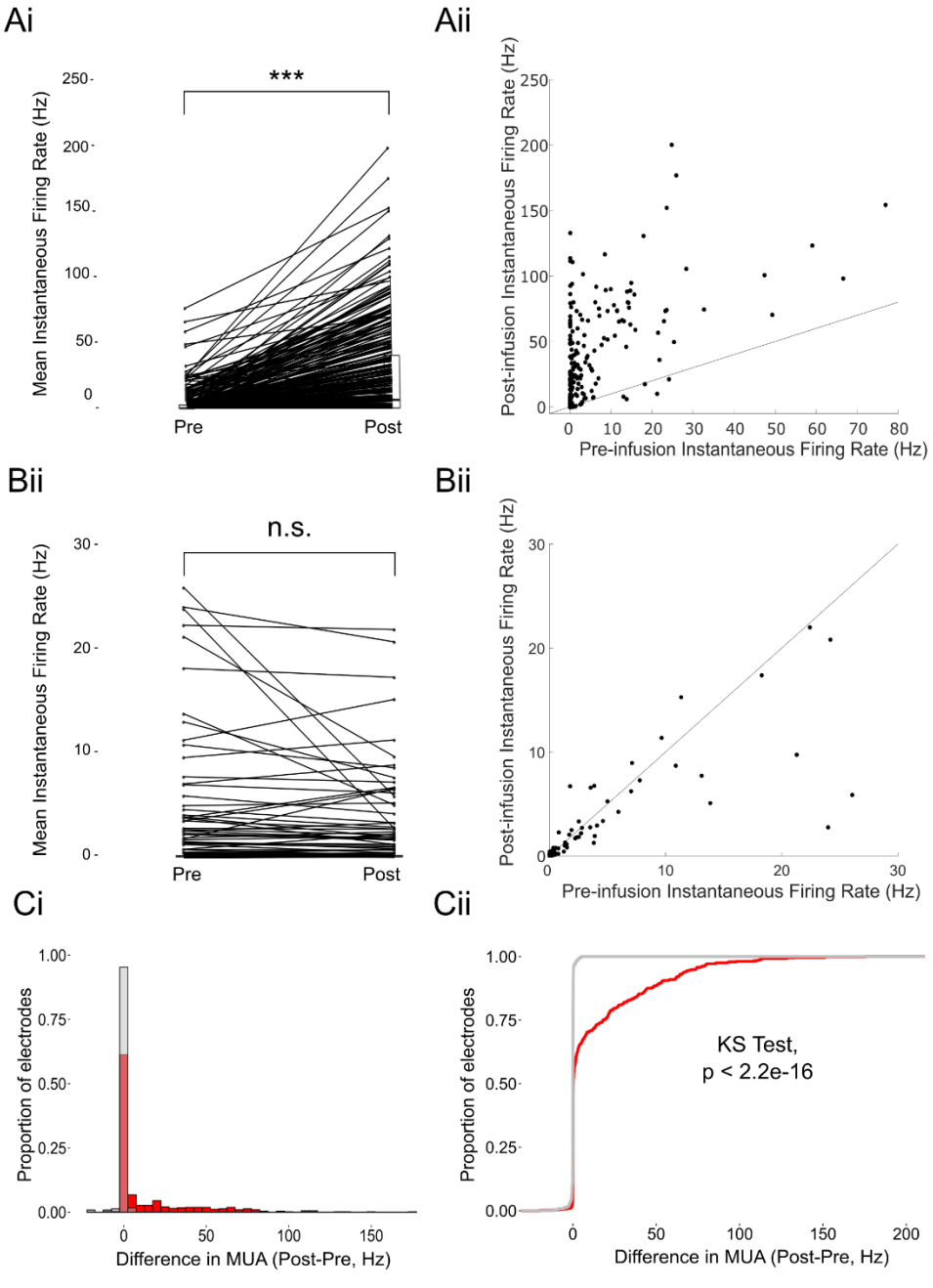
Ai
Aii
Bii
Bii
Ci
Cii
***
n.s.
Mean Instantaneous Firing Rate (Hz)
Pre
Post
Post-infusion Instantaneous Firing Rate (Hz)
Pre-infusion Instantaneous Firing Rate (Hz)
Proportion of electrodes
Difference in MUA (Post-Pre, Hz)
KS Test,
p < 2.2e-16

Figure 6. 5-HT application increases multiunit activity within horizontal bulb slices. Ai. Results of 5-HT application in normal ACSF conditions (comparison of 60 sec epochs before and after drug application). 5-HT increases the mean instantaneous firing rate (IFR) (*** signifies a p-value smaller than 0.00001). **Aii**. Scatter plots of the effect of 5-HT IFR (comparison of 60 sec epochs before and after drug application). Each dot represents a single electrode. **Bi.** Results of 5-HT application in ACSF containing the 5-HT2 receptor antagonist (20 uM). No significant change was found following 5-HT application into the 5-HT2 antagonist containing bath. **Bii**. Scatter plots of the effect of 5-HT application in cinanserin containing ACSF bath. **Ci.** Normalized histogram showing the normalized change of power (Post/Pre) in both 5-HT (gray) and 5-HT+Cinanserin (red) conditions. **Cii.** Empirical cumulative distribution function of the same data reported in Ci. The distributions of changes in power (60 sec epochs) following 5-HT application was statistically different from changes in power following 5-HT application into the 5-HT2 antagonist containing bath.

changes in IFR are shown as differences, not ratios (Fig. 4Biii). When slices were bathed in the 5-HT_2 receptor antagonist, cinanserin, prior to 5-HT application, I did not detect a significant increase in multiunit IFR (Wilcoxon signed-rank test, p-value = 0.07107) (**Fig 6Bi,ii**). When comparing the distributions of firing rate changes between the ACSF and ACSF+cinanserin groups, there was a significant difference between the distribution of changes in firing rate between the two experimental groups (KS Test, $p<2.22e-16$) This result along with the results showing no 5-HT induced changes in theta and gamma rhythms with cinanserin present in the bath suggest that 5-HT is increasing both theta and gamma rhythms within the MOB predominantly through 5-HT_2 receptor mediated mechanisms.

Relationships between CSD and MUA

Lastly, I asked how these changes in MOB network dynamics related to the MUA in response to 5-HT stimulation. In principle the modulation of power within CSD and the rate of MUA by 5-HT could reflect two distinct processes. Alternatively, changes in power within LFP/CSD frequency bands could define excitability of the local bulbar circuitry and therefore related to the MUA response to 5-HT. To distinguish between these two scenarios, I asked to what extent the 5-HT induced changes in power in the theta and gamma bands were captured by the MUA response to 5-HT. For each frequency band, I correlated the time averaged change in instantaneous firing rate (mean(IFR_{post})- mean(IFR_{pre}); Hz) with the normalized change in band-passed CSD power. For the gamma band oscillation, I found a positive correlation, indicating that a 5-HT induced increase in gamma power was associated with a stronger MUA response to 5-HT. (**Fig 7A**. Spearman's rho = 0.52, N= 280

electrodes, correlation coefficient significantly different from 0, p = 1.3564e-23).

A

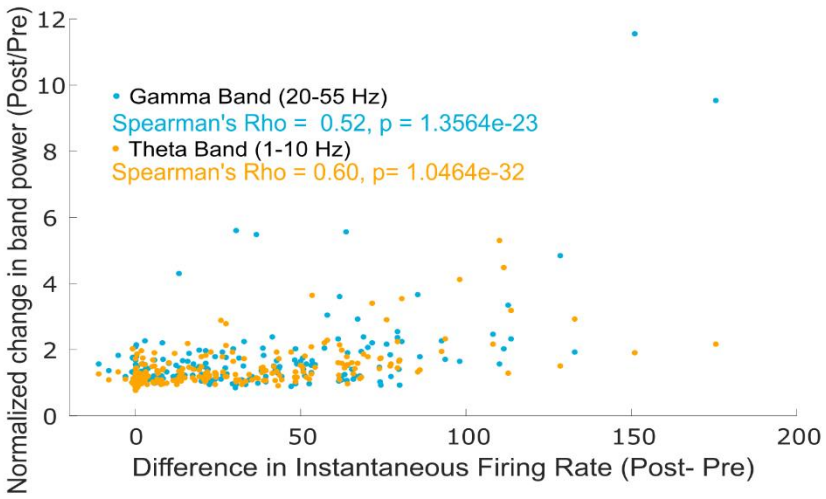

B

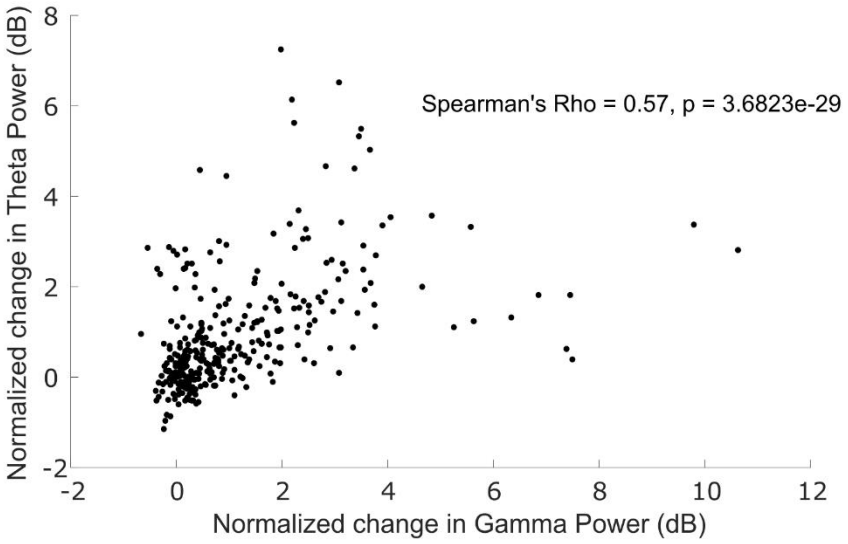

Figure 7. Relationship between LFP rhythms and MUA following 5-HT application. A. Enhancement of multiunit activity exhibited a positive correlation with enhancement of both gamma (blue) and theta (orange) band power following 5-HT application. Both measures of changes of MUA and LFP band power were made by comparing 60 sec epochs before and after 5-HT application. Each dot corresponds to a single electrode. **B.** Increases in gamma and theta power are correlated across electrodes. Enhancement of gamma power is correlated with an enhancement of theta power. Axes are decibel transformed, $dB = 10^* (\log_{10}(Post/Pre))$.

Spearman's rho = 0.60, n = 280 electrodes, correlation coefficient significantly different from 0, p =1.0464e-32). Lastly, to examine how 5-HT induced changes in theta and gamma power within an electrode may be related, I correlated the 5-HT induced change in theta power with the 5-HT induced change in gamma power. Interestingly I found a positive correlation between changes in gamma band and theta band power (Fig. 7B, Spearman's rho = 0.57, n = 280 electrodes, correlation coefficient significantly different from 0, p = 3.6823e-29). Together these results propose that measurements in CSD power in different frequency bands relate to the MUA such that both low (theta) and higher (gamma) frequencies correspond to increased MUA activity following 5-HT application. Further, rather than being two distinct phenomena, increased oscillatory power within the theta and gamma bands showed a significant correlation suggesting that increased theta and gamma band power can be detected within same regions of space within a MOB slice.

Conclusion

In this study, I identified three major effects of 5-HT on MOB network activity within brain slices: 1) an increase of gamma-band oscillations (20-55 Hz), 2) an increase in theta band (1-10 Hz) oscillations, and 3) a strong increase in firing rate of MUA. All three of these effects were shown to be dependent on serotonergic signaling at 5-HT_2 receptors as these effects were not detected when a 5-HT_2 receptor antagonist was present in the recording solution. Despite a long history of study, the mechanisms producing bulbar oscillations are still highly debated and there is very little published information regarding how neuromodulators may affect network rhythms. Studies investigating the mechanistic origin of MOB network dynamics

have focused primarily on gamma band rhythms (Friedman and Strowbridge, Lagier et al. 2004, Neville and Haberly 2003). Studies performed in vitro have relied on olfactory nerve stimulation to induce gamma oscillations within MOB slices (Friedman and Strowbridge 2003, Lagier et al. 2004), and have suggested that the circuitry involved in gamma rhythmogenesis is intrinsic to the MOB and implicated the synaptic connections between excitatory M/T cells and inhibitory GCs within the external plexiform layer of the MOB. In the present study I found a significant increase in overall activity in response to 5HT application; while I did not record intracellularly, previous work suggests that 5-HT's direct, depolarizing effect of MT cells may be the source of the increased activity and specifically the increase in gamma band power reported here. Schmidt and Strowbridge (2014) reported an increase in synchronous inhibition onto MT cells following 5-HT application. Importantly, this effect of 5-HT was seen in slices where the glomerular layer had been surgically removed, demonstrating that this increase in inhibitory synchrony is not due to inhibitory interneurons within the glomerular layer (Schmidt and Strowbridge 2014). This increased inhibitory tone onto MT cells from GCs was detected following direct depolarization of MT cells by 5-HT. 5-HT induced depolarization of MT cells and the subsequent synaptic interactions between MT cells and GCs within the external plexiform layer could be the source of increased gamma power detected with extracellular electrodes **(Fig 8**). One important point to

FIGURE 8

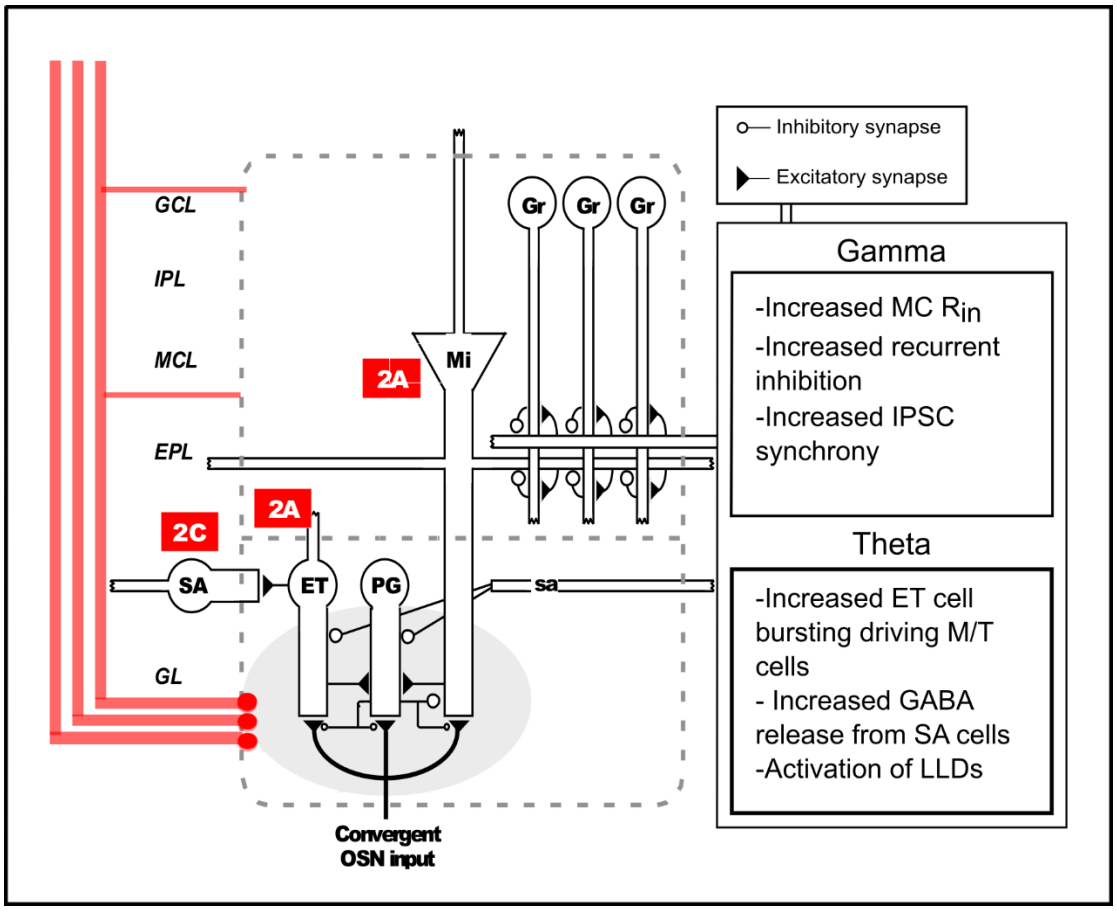
Inhibitory synapse
Excitatory synapse
GCL
IPL
MCL
EPL
GL
2A
2C
2A
Mi
Gr
Gr
Gr
SA
ET
PG
sa
Convergent
OSN input
Gamma
-Increased MC Rin
-Increased recurrent inhibition
-Increased IPSC synchrony
Theta
-Increased ET cell bursting driving M/T cells
- Increased GABA release from SA cells
-Activation of LLDs

Figure 8. Illustration of distribution of receptors in the olfactory bulb and the possible effects on MOB LFP rhythms. Rahpe terminals are shown in red, with receptor types labeled next to the cell types where physiological effects are known. Sensory information, transduced by olfactory sensory neurons(OSNs) in the olfactory epithelium is projected to target neurons in the glomerular layer (GL) of the OB. Local microcircuits, comprised of periglomerular (PG), external tufted (ET) and short axon (SA) cells process the incoming information. This layer of bulbar processing is thought to be involved in contrast and normalization processes. 5-HT has been shown to directly depolarize ET cells, increasing bursting and the frequency of bursting (Liu et al. 2012). ET cells burst within theta range and 5-HT's effects on ET cells may be an important element in the production of theta rhythms recorded within bulb slice. SA cells also play a role in shaping glomerular output, and their role in theta oscillations in vivo and in vitro is unclear, but increased GABA release in combination with increased glutamate release from ET cells may lead to increased theta range rhythmicity. The resulting activity of mitral cells (Mi) is then further processed in the external plexiform layer (EPL), where Mi cells interact with granule cells (Gr). The mutual interactions between these groups of cells and additional interneurons not depicted here are thought to create oscillatory dynamics that serve to synchronize Mi cell outputs towards olfactory secondary cortices. Previous work has shown that mitral cells are directly depolarized by 5-HT via a conductance decrease mechanism (closure of a K+ channel) and this increased excitatory tone depolarizes inhibitory granule cells, increasing recurrent inhibition back onto Mi cells. Increases in activity within these excitatory-inhibitory circuits in response to 5-HT may be the underlying mechanism producing increased gamma power within our experiments.

emphasize is that while the reciprocal synapse between MCs and GCs within the EPL is thought to be the major source of gamma range rhythmogenesis, synaptic inputs from other EPL interneurons such as PV+ interneurons () or deep short-axon cells could also be directly affected by 5-HT and modulate network state. Slice experiments utilizing whole-cell patch methods in conjunction with extracellular recording, pharmacology, and cell-type expression of optognetic reagents would allow for the measurement of both synaptic currents within a MC during a pharmacologically induced gamma oscillation while manipulating MOB interneurons. Modulation of gamma rhythms *in vivo* has been linked to modulations in olfactory discrimination performance, with both positive and negative changes in gamma power being associated with decreased accuracy (Nusser et al. 2001, Beshel et al. 2007, Lepousez and Lledo 2013.), and blocking the effects of 5-HT via a 5-HT2R antagonist may alter MOB gamma oscillations *in vivo* and be involved in the outcome of impaired performance in the behavioral tasks presented in Chapters 2 and 3.

Along with an increase in gamma band power, I detected an increase in the theta band (1-10 Hz) power following 5-HT application. *In vivo*, the theta band is highly coherent with the rhythms of respiration (Rojas-Libano et al. 2012) and interruption of nasal air flow greatly modulates theta rhythms in the LFP (Courtiol et al. 2011). While the rhythmic nature of afferent input to the MOB drives slow, theta range patterning, the intrinsic dynamics of the glomerular layer are also involved (De Sait Jan et al. 2009; Grosmaitre et al. 2007). In MOB slices, synchronized rhythmic activity occurs in mitral cells projecting to the same glomerulus. This activity can be induced by electrical stimulation of the olfactory nerve or through pharmacological manipulations of cellular excitability (Isaacson 1999; Carlson et al., 2000; Puopolo and Belluzzi, 2001; Schoppa and Westbrook, 2001; Christie et al. 2005) and there is consensus in the field that this activity is generated by glutamatergic signaling within a

glomerulus. While there are excitatory interactions between mitral cells within the glomerulus (Schoppa and Westbrook, 2002; Urban and Sakmann, 2002; Christie et al. 2005), evidence suggests that excitatory connections from ET cells to mitral cells play an important role in shaping mitral cell activity (Hayar et al. 2004, 2005; De Saint Jan et al. 2009). ET cells exhibit pacemaker activity and spontaneously generate bursts of spikes on the time scale of the theta band that are highly correlated among ET cells of the same glomerulus (Hayar et al., 2004) synchronized with mitral cell bursting (De Saint Jan et al, 2009) Thus populations of external tufted cells within a glomerulus and across the glomerular layer may act as important components of network oscillators that are entrained by incoming sensory input and ongoing network activity. Importantly, 5-HT has been shown to directly depolarize and increase burst firing in ET cells through a 5-HT_{2A} receptor dependent mechanism (Liu et al. 2012). It was shown that 5-HT also directly increases GABA release from SA cells, an inhibitory neuron within the GL (Brill et al. 2016). These neurons inhibit both ET and PG cells within the GL and while SA cells have not been shown to be involved in the generation of theta range patterning in bulb slices or *in vivo*, the 5-HT driven increase in ET cell activity coupled with increased inhibitory tone from SA cells may modulate theta range activity of mitral cell assemblies.

Within my experiments, ET cells would be depolarized by 5-HT and begin bursting within the theta range and in turn drive M/T assemblies to fire at that time scale. Rhythmic output of a glomerulus would show up in extracellular LFP recordings within the theta range. Patch recordings of ET and MC following 5-HT in combination with MEA recordings would help definitiveely prove that rhythmic activity of at the microscopic, cellular level drives rhythmic network rhythms. *In vivo*, 5-HT affecting the low frequency network activity may be very important for maintaining concentration invariant odor representations and contrast enhancement

during odor discrimination (Banerjee et al. 2015, Fukunaga et al. 2014) and is a potential mechanism to explain why rats were impaired in odor learning during a forced-choice discrimination task and showed increased latencies in olfactory decisions following the bilateral intrabulbar infusion of a 5-HT_2 antagonist (Chapter 2 and 3).

Consistent with previous reports of 5-HT increasing neural activity in MT cells in vitro and in vivo, here I detected a significant increase in MUA following 5-HT application. Interestingly, changes in MUA activity were positively correlated with changes in both theta and gamma band activity. Of the two bands tested, changes in theta power were more correlated with changes in MUA than changes in gamma power. I also detected a positive correlation between changes in gamma band and theta band power. It was possible that increased gamma and theta power were independent responses to 5-HT, and that increased MUA would either occur with increased theta or gamma, but the finding that changes in gamma and theta power are significantly correlated suggests that within the 200 micron span of each electrode, activity of both frequencies may be coupled. To date few studies have investigated the relationship between MUA and LFP power in the MOB. In primates and other mammals researchers have begun to study the relationships between MUA and LFP activity (Ray and Maunsell. 2009, Sellers et al. 2013). Working in V1 of ferrets, Sellers et al found a negative correlation between visually induced MUA and both delta (0.5-4 Hz) and alpha (8-12 Hz) rhythms and a positive correlation between MUA gamma band power (20-40 Hz) (Sellers et al. 2013). From this result the authors concluded that visual cortex alternates between two states, one with lower MUA, higher slow wave activity and higher MUA and higher gamma activity. In my data set both theta and gamma power are positively correlated with MUA activity, and the positive correlation between changes in gamma and theta power suggest that 5-HT

application produces a state where all three of these phenomena are present. One possible explanation for this finding is that there is very little spontaneous activity in the OB slice and that application of 5-HT greatly increases excitability within the slice and increases activity over a variety of time scales, rather than subtlety modifying the relative power of certain frequencies from baseline as visual input does within ferret V1. Studying the effects of 5-HT on MOB bulbar dynamics *in vivo* would help delineate between effects of 5-HT on bulb rhythms that are consistent across experiments and those that are due to artifacts of brain slice experiments.

In conclusion, here I have reported the first results of 5-HT on extracellular network dynamics in MOB slices. 5-HT application increased power in both the theta and gamma bands and increased MUA within MOB slices. Importantly these effects were not seen in slices following 5-HT application when a 5-HT2 receptor antagonist was present in the bath. These results suggest that 5-HT is an important regulator oscillatory dynamics in the MOB and serotonergic modulation of MOB rhythms may play a role in the behavioral effects reported following 5-HT_2 antagonism.

CHAPTER 5

CONCLUSIONS AND FUTURE DIRECTIONS

The main olfactory bulb (MOB) is heavily innervated by neuromodulatory structures and the actions of neuromodulators allow the nervous system to adapt to environmental demands and a variety of stimulus conditions. Compared to acetylcholine(ACh) and noradrenaline (NA), both the behavioral functions and effects of 5-HT within the MOB are less well understood. The studies presented in this thesis were motivated by this relative lack of understanding. Here I summarize my findings and suggest future experiments to better understand serotonergic modulation of the MOB.

Serotonergic modulation of olfactory habituation

I began my time in the lab looking at serotonergic modulation of olfactory habituation behavior (Chapter 2). Olfactory habituation is a behavioral paradigm used to investigate non-associative olfactory memory and perceived similarity between presented odorants. To examine this, I performed pharmacological manipulations of the MOB prior to habituation testing via infusion cannulae. Influenced by the literature regarding 5-HT's action within the antennal lobe in moths and drosophila (Mercer and Kloppenburg, 2009; Dacks et al. 2009) and previous work looking at NA in altering detection and discrimination thresholds of olfactory stimuli, I tested olfactory habituation and spontaneous discrimination at three odor concentrations. My work revealed a role of 5-HT2 signaling in the formation of olfactory habituation memory of low odor concentration stimuli. When tested at higher odor concentrations, rats infused with 5-HT2 antagonists exhibited odor habituation similar

to saline controls. At the odor concentrations where 5-HT2 antagonist infused animals exhibited olfactory habituation they showed decreased spontaneous discrimination during presentation of structurally similar odorants.

Serotonergic modulation of olfactory discrimination learning

Next I investigated the role of 5-HT in discrimination learning using a forced choice discrimination task. Here rats were conditioned to discriminate between simultaneously presented pairs of odorants, one rewarded, one non rewarded. Similar to the habituation task I manipulated olfactory bulb serotonergic chemistry by infusing a 5-HT2R antagonist directly into the MOB prior to testing. To vary the level of stimulus overlap between odorants to be learned I tested rats at three odor concentrations and four levels of difficulty (Chapter 2 and 3). This work showed that infusion of the 5-HT2 antagonist, cinanserin, significantly impaired olfactory discrimination learning over twenty trials. Importantly I did not detect three- or two-way interactions between drug treatment, odor concentration, or carbon difference, which suggests that antagonism of 5-HT2 receptors broadly impairs decision accuracy. In contrast to 5-HT2 antagonism's effects on accuracy, rats showed significant differences in the speed of correct olfactory decisions only for specific difficulty/concentration combinations: Rats showed increased latencies to dig in correct odor pots during the most difficult trials at higher concentrations. Importantly, during these trials, 5-HT2R antagonist infused rats exhibited no differences in accuracy compared to saline controls. These results suggest that 5-HT2 receptors are important for proper discrimination learning and that both the speed and accuracy of olfactory decisions can be tuned by the activity of neuromodulators.

Serotonergic modulation of neural dynamics within MOB slices

To investigate potential neural mechanisms underlying my observed behavioral results I began to study the effects of 5-HT on the neural dynamics within MOB slices recorded with an extracellular multi-electrode array. Previous work in the lab (Peace et al. in prep) found that long lasting (>60 sec) gamma oscillations could be induced by a variety of manipulations (ChR2, mGluR agonists, and carbachol). Application of 5-HT, similarly increased long lasting gamma oscillations in MOB slices. Along with increasing power within the gamma band, 5-HT was found to increase theta band oscillations within bulb slices. Theta band oscillations, while commonly studied *in vivo*, have not before been reported within the LFP of bulb slices. Both the effects of 5-HT on gamma and theta band power were dependent on signaling of 5-HT at 5-HT2 receptors. Lastly, consistent with previous reports of 5-HT increasing firing rates of mitral and external tufted cells, I detected a significant increase in multi-unit activity (MUA) following application of 5-HT. Interestingly the changes of power detected both in the theta and gamma band were significantly correlated with changes in MUA. The discovery of theta range oscillations within slice local field potentials opens a variety of questions regarding their generation and the role of other neuromodulators in their generation. The ability to measure both theta and gamma range oscillations with a MOB slice also opens questions about the temporal relationships between them and future analysis could be performed on already existing data took investigate phenomena such as phase-amplitude coupling between theta and gamma rhythms. Future analysis and experiments could be performed to formally investigate the effect of 5-HT on functional connectivity across the array (i.e. phase based connectivity, power-based connectivity).

Functional role of 5-HT in modulating olfactory processing

Over the past decade there has been increasing *in vivo* and *in vitro* neurophysiology data that supports a circuit model of serotonergic modulation that involves increased excitation of external tufted (ET) and mitral (Mi) cells within the olfactory bulb. In both cell types, 5-HT acts directly via 5-HT2A receptors. 5-HT also acts through both direct and indirect means to enhance the responses of inhibitory periglomerular (PG) and short axon (SA) cells to olfactory input (Brill et al. 2016; Brunert et al. 2016; Kapoor et al. 2016). One consequence of increased ET cell activity could be an increased weight of disynaptic excitation onto Mi cells and the resultant inhibition by PG and SA in determining bulbar output, at the expense of afferent, feedforward olfactory sensory neuron input. Increasing the weight of ET cell activity in controlling Mi cell output could facilitate odor coding in a variety of ways. The bursting response of ET cells to OSN input may increase the reliability of signal propagation and attenuate the effect of transient fluctuations in OSN input (Schoppa and Westbrook 2002, Liu and Shipley 2008). Increased ET cell activity could also increase coupling of Mi cells to the respiration rhythm and temporally sharpen Mi cells responses. Resultant changes in interglomerular and feedforward inhibition may alter Mi cell response patterns to facilitate contrast enhancement (Cleland and Sethupathy, 2006; Fukunaga et al. 2014) of overlapping odor stimuli and increase the dynamic range across odor concentrations (Banerjee et al. 2015). The combined effects of 5-HT on ET and Mi cells result in Mi cells having a membrane potential closer to firing threshold and an increased input resistance. Both of these effects would make Mi cells more sensitive to weaker olfactory inputs and the blocking of these effects via a 5-HT2 receptor antagonist could underlie effects of odor concentration on olfactory habituation behavior (Chapter 2). 5-HT also has been shown to modulate inhibitory synchrony (Schmidt and Strowbridge, 2014) and gamma rhythms (Chapter 4) within olfactory bulb slices. Modification of inhibition on Mi

cells has been shown to be involved in altering olfactory sampling behavior during discriminations of overlapping stimuli (Abraham et al. 2010), and modulation of gamma rhythms within the local field potential has been associated with both increased and decreased task performance in reward-based olfactory tasks (Beshel et al. 2007; Nusser et al. 2001; Lepousez and Lledo, 2013). From my slice data I would predict that 5-HT2 antagonism decreases gamma power within the olfactory bulb and this decrease in gamma power would impair olfactory discriminations, particularly between two overlapping stimuli. Simultaneous manipulation of serotonergic projections and recording of olfactory LFP during behavior would greatly aid in elucidating the neural mechanism(s) underlying the behavioral effects of 5-HT2 receptor antagonism reported here.

Dynamics of serotonergic release during olfactory behavior?

Two major questions regarding the nature of serotonergic neuromodulation within the MOB are when and how 5-HT is released from raphe terminals during behavior. 5-HT within the central nervous system has been shown to be involved in a variety of neural processes. Classic studies of the dorsal raphe nucleus (DRN) have suggested that serotonergic neurons exhibit tonic activity during waking which is modulated during sleep states (reviewed in Jacobs and Fornal 1999). Other theories have proposed 5-HT to be involved in processing reward and punishment (Daw et al. 2002; Maier and Watkins, 2005; Nakamura et al. 2008; Cools et al. 2011). One theory states that 5-HT regulates aversive learning in response to punishments (Soubrie 1986, Deakin and Graeff, 1991, Dayan and Huys, 2009). This theory states that 5-HT opposes the positive reinforcement and behavioral invigoration produced by dopamine. In this theory serotonergic neurons would signal punishments, and adjust future behavior and inhibit actions associated with aversive events. While this theory

benefits from support from stimulation, lesion, and pharmacological studies (Graeff and Silveira Filho, 1978; Crockett et al. 2009; Shin and Ikemoto, 2010), little evidence exists that serotonergic neurons signal punishments in awake behaving animals, and the evidence that does exist shows increased raphe activity following noxious peripheral sensory stimulation (Aghajanian et al. 1978; Schweimer and Ungless, 2010). A second theory states 5-HT is necessary for waiting for reward and intertemporal choice (Doya 2002; Miyazaki et al. 2011a, 2011b; Fonseca et al. 2015). In this theory, activation of serotonergic neurons inhibits movements that allow the animal to optimally wait for a delayed reward. This theory is similar to the one stated above in that serotonergic activity leads to behavioral inhibition but it differs in that serotonergic neurons are not thought encode aversive events or stimuli.

Recent work experimental work suggests that simple theories of serotonergic modulation require revising. Cohen et al. 2015 found three main features of serotongeric neuron activity. Measuring the activity of optically identified serotonergic neurons, they showed that a large fraction of units showed tonic firing modulation depending on state values, phasic excitation in response to punishments, and phasic excitation to reward-predicting cues. In this work many neurons were shown to be activated by both reward-predictive cues and punishment. From their results the authors propose that serotonergic neurons multiplex information regarding reward and punishment on multiple timescales.

One issue regarding theories of serotonergic function is that they make no predictions as to how 5-HT should modulate sensory encoding within sensory structures. Previous theories of 5-HT had suggested that 5-HT inhibited sensory structures at the expense of exciting locomotor areas (Jacobs and Fornal 1999). In this framework, external sensory cues would be suppressed during locomotion and one would predict that 5-HT release would attenuate sensory acuity and impair sensory

discriminations. This result stands in stark contrast to the literature and the results presented within this thesis. Instead, at least within the OB, 5-HT release excites neural circuits underlying stimulus detection and discrimination.

A secondary issue complicating the understanding of activity of 5-HT within sensory structures is the topography of projections from the raphe and the physiological location of serotonergic neurons within the raphe nuclei (Lowry et al. 2000; Vertes, 1991, Crawford et al. 2010). Quite simply, do the raphe neurons which project to the OB also project to other chemosensory structures or non-chemosensory forebrain structures or are OB-projecting raphe neurons a dedicated subpopulation amongst the larger population? Anatomical tracing of raphe neurons would greatly aid in determining the nature of raphe input to the OB. The other major issue complicating our understanding of 5-HT within the MOB is the fact that at least two regions of the raphe nuclei (the DRN, and Median Raphe Nuceleus, MRN) project to the olfactory bulb (McLean and Shipley 1987), and may preferentially target distinct layers of the olfactory bulb (Steinfeld et al. 2015). To better understand the dynamics of serotonergic neurons within the MOB, one could use fiber photometry methods to record changes in fluorescence originating from calcium transients within OB-projecting raphe neurons. Using SERT-Cre mice and following injection of a GcaMP containing AAV construct within either the DRN or MRN one could measure Ca2+ transients within the bulb from serotonergic fibers originating within each respective nucleus of the raphe nuclei. One could then possibly determine if tasked based stimuli (odors, task related cues, rewards) or contexts (discrimination difficulty, learning vs. recall, low vs. high motivation) alter serotonergic activity within the MOB during behavior.

Concluding remarks

Using both behavioral and neurophysiological approaches, I was able to provide a significant contribution to the current understanding of serotonergic function within the rodent olfactory bulb. In Chapters 2 and 3, I measured behavior following pharmacological blockade of 5-HT2 receptors within the MOB. Within the behavioral paradigms tested I found a deficit in olfactory habituation only when tested at low (0.001 Pa) odor concentrations and impaired spontaneous discrimination at all odor concentrations tested. Odor learning was also impaired in the forced choice discrimination task and interesting effects on decision times were detected. In chapter 4, I looked at how 5-HT modulates bulbar neural dynamics to uncover potential mechanisms for the behavioral results reported here. This work has provided new insights into the behavioral relevance of 5-HT within the olfactory bulb and how 5-HT modulates bulbar network dynamics, and has lead to new questions for future researchers within the field of olfactory neuroscience.

REFERNCES

Abraham, N. M., Spors, H., Carleton, A., Margrie, T. W., Kuner, T., & Schaefer, A. T. Maintaining accuracy at the expense of speed: stimulus similarity defines odor discrimination time in mice. *Neuron* **44**, 865-876 (2004).

Abraham, N. M., Egger, V., Shimshek, D. R., Renden, R., Fukunaga, I., Sprengel, R., Seeburg, P. H., Klugmann, M., Margrie, T. W., Schaefer, A. T., & Kuner, T. Synaptic inhibition in the olfactory bulb accelerates odor discrimination in mice. *Neuron* **65**, 399-411 (2010).

Aghajanian, G. K.,Wang, R. Y., & Baraban, J. Serotonergic and non-serotonergic neurons of the dorsal raphe: reciprocal changes in firing induced by peripheral nerve stimulation. *Brain Res.* **153**, 169-175 (1978)

Andersen, E. & Dafney, N. Dorsal raphe nucleus modulates sensory evoked responses in caudate and septum. *Int J Neurosci* **17**, 151-155 (1982)

Ashton-Jones, G. & Cohen, J. D. An integrative theory of locus coeruleus-norepinephrine function: adaptive gain and optimal performance. *Annu Rev Neruosci.* **28**, 403-450 (2005)

Aungst J. L., Heyward, P. M., Puche, A. C., Karnup, S. V., Hayar, A., Szabo, G., & Shipley, M.T. Centre-surround inhibition among olfactory bulb glomeruli *Nature* **426**, 623-629 (2003)

Banerjee, A., Marbach, F., Anselmi, F., Koh, M. S., Davis, M. B., Garcia da Silva, P., Delevich, K., Oyibo, H. K., Gupta, P., Li, B., & Albeanu, D. F. An interglomerular circuit gates glomerular output and implements gain control in the mouse olfactory bulb. *Neuron* **87**, 193-207 (2015).

Bates, D., Maechler, M., Bolker, B.,& Walker, S. Fitting Linear Mixed-Effects Models Using lme4. *J. Stat Softw.* **67**, 1-48 (2015)

Bathellier, B., Lagier, S., Faure, P., & Lledo, P. M. Circuit properties generating gamma oscillations in a network model of the olfactory bulb. *J Neurophysiol* **95**, 2678-2691 (2006)

Beshel, J., Kopell, N., & Kay L. M. Olfactory bulb gamma oscillations are enhanced with task demands. *J Neurosci*. **27**, 8358-8365 (2007)

Bokil, H., Andrews, P., Kulkarni, J. E., Mehta, S., & Mitra, P. P. Chronux: a platform for analyzing neural signals. *J Neurosci Methods* **192**, 146-151 (2010)

Brill, J., Shao, Z., Puche, A. C., Wachowiak, M., & Shipley, M. T. Serotonin increases synaptic activity in olfactory bulb glomeruli. *J. Neurophysiol.* **115**, 1208-1219 (2016).

Brunert, D., Tsuno, Y., Rothermel, M., Shipley, M. T., & Wachowiak, M. Cell-type-specific modulation of sensory responses in olfactory bulb circuits by serotonergic projections from the raphe nuclei. *J. Neurosci.* **36**, 6820-6835 (2016).

Carlson, G. C., Shipley, M. T., & Keller, A. Long-lasting depolarizations in mitral cells of the rat olfactory bulb. *J. Neurosci.* **20**, 2011-2021 (2000)

Castillo, P. E., Carleton, A., Vincent, J. D., & Lledo, P. M. Multipled and opposing roles of cholinergic transmission in the main olfactory bulb. *J Neurosci*. **19**, 9180-9191 (1999)

Chen, Y., Dhamala, M., Bollimunta, A., Schroeder, C. E., & Ding, M. Current source density analysis of ongoing neural activity theory and application. In: *Electrophysiological Recording Techniques, Neuromethods* (14th ed.) edited by Vertes, R. P. & Stackman, R. W. Jr, New York: Humana **54**, 27-40 (2011)

Chaudhury, D., Escanilla, O. & Linster, C. Bulbar acetylcholine enhances neural and perceptual odor discrimination. *J. Neurosci.* **29**, 52-60 (2009).

Christie, J. M., Bark, C. Hormuzdi, S. G., Helbig, I., Monyer, H. & Westbrook, G. L. Connexin36 mediates spike synchrony in olfactory bulb glomeruli. *Neuron* **46**, 761-772 (2005)

Ciombor, K. J., Ennis, M., & Shipley, M. T. Norepinephrine increases rat mitral cell excitatory response to weak olfactory nerve input via alpha-1 receptors in vitro. *Neuroscience* **90**, 595-606 (1999)

Cleland, T.A. Early transformations in odor representation. *Trends Neurosci*. **33,** 130-139 (2010)

Cleland, T.A., Johnson, B. A., Leon, M., & Linster, C. L. Relational representation in the olfactory system. *Proc Natl Acad Sci USA* **104**, 1953-1958 (2007)

Cleland, T. A., Morse, A., Yue, E. L., & Linster, C. Behavioral models of odor similiarty. *Behav. Neuerosci.* **116**, 222-231 (2002).

Cleland, T. A., & Linster, C. Computation in the olfactory system. *Chem. Senses.* **30**, 801-813 (2005).

Cleland, T. A., & Sethupathy, P. Non-topographical contrast enhancement in the olfactory bulb. *BMC Neurosci.* **24**, 7:7 (2006)

Cohen, J. Y., Amaoros, M. W., & Uchida, N. Serotonergic neurons signal reward and punishment on multiple timescales. *eLife* **4** doil: 10.7554/eLife.06346 (2015)

Cohen, M. X. Analysis of Neural Time Series Data. MIT Press: Cambridge, MA (2014)

Cools, R., Nakamura, K., & Daw, N. D. Serotonin and dopamine: unifying affective, activational, and decision functions. *Neuropsychopharmacology* **36**, 98-113 (2011)

Courtiol, E., Amat, C., Thevenet, M., Messaoudi, B., Garcia, S. & Buonviso, N. Reshaping of bulbar response by nasal flow rate in the rat. *PLoS One* **6**, e16445. Doi: 10.1371/journal.pone.0016445 (2011)

Crockett, M. J., Clark, L., & Robbins, T. W. Reconciling the role of serotonin in behavioral inhibition and aversion: acute tryptophan depletion abolishes punishment-induced inhibition in humans. *J Neurosci*. **29**, 11993-11999 (2009)

Crawford, L. K., Craige, C. P., & Beck, S. G. Increased intrinsic excitability of lateral wing serotonin neurons of the dorsal raphe: a mechanism for selective activation in stress circuits. *J Neurophysiol* **103**, 2652-2663 (2010)

Dacks, A.M., Green, D. S. Root, C. M., Nighorn A. J. & Wang, J. W. Serotonin modulates olfactory processing in the antennal lobe of Drosophila. *J Neurogenet* **23**, 366-377 (2009)

David, F., Linster, C., & Cleland, T. A. Lateral dendritic shunt inhibition can regularized mitral cell spike patterning. *J Comput Neurosci* **25**, 25-382008)

Daw, N. D., Kakade, S., & Dayan, P. Opponent interactions between serotonin and dopamine. *Neural Networks* **15**, 603-616 (2002)

Dayan, P. & Huys, Q. J. Serotonin in affective control. *Annu. Rev. Neurosci.* **32**, 95-126 (2009)

Deakin, J. F.& Graeff F. G. 5-HT and mechanism of defence. *J Psychopharmacol*. **5**, 305-315 (1991)

Deemyad, T. Metzen, M. G., Pan, Y. & Chacron, M. J. Serotonin selectively enhances perception and sensory neural responses to stimuli generated by same-sex conspecifics. *Proc Natl Acad Sci USA* **110**, 19609-19614 (2013)

De Sant Jan, D., Hirnet, D., Westbrook, G., & Charpak, S. External tufted cells drive the output of olfactory bulb glomeruli. *J. Neurosci*. **29**: 2043-2052 (2009)

Devore, S., de Almeida, L., & Linster, C. Distinct roles of bulbar muscarinic and nicotinic receptors in olfactory discrimination learning. *J. Neurosci.* **34**: 11244-11260 (2014)

Devore, S. & Linster, C. Noradrenergic and cholinergic modulation of olfactory bulb sensory processing. *Front Behaav Neurosci.* **6**, 52 (2012)

Doucette, W. Milder, J. & Restrepo, D. Adrenergic modulation of olfactory bulb circuitry affects odor discrimination. *Learn. Mem.* **14**, 539-547 (2007)

Doya, K. Metalearning and neuromodulation. *Neural Netw.* **15**, 495-506 (2002)

Dubey, A. & Ray, S. Spatial spread of local field potential is band-ass in the primary visual cortex. *J Neurophysiol.* **116**, 1986-1999 (2016)

Egger, V. & Urban, N. Dynamic connectivity in the mitral cell-granule cell microcircuit. *Semin Cell Dev Biol*. **17**, 424-432 (2006)

Escanilla, O., Arrelanos, A., Karnow, A., Ennis, M., & Linster, C. Noradrenergic modulation of behavioral odor detection and discrimination thresholds in the olfactory bulb. *Eur J Neurosci*. **32**, 458-468 (2010)

Fletcher, M. L. & Chen, W. R. Neural correlates of olfactory learning: critical role of centrifugal neurmodulation. *Learn. Mem.* **17**, 561-570 (2010)

Fonseca, M. S., Murakami, M., & Mainen, Z. F. Activation of dorsal raphe serotonergic neurons promotes waiting by is not reinforcing. *Curr. Biol.* **25**, 306-315 (2015)

Frederick, D., Brown, A., Tacopina, S., Mehta, N., Vujovic, M., Brim, E., Amina, T., Fixsen, B., & Kay, L. M. Task-dependent behavioral dynamics make the case for temporal integration in multiple strategies during odor processing. *J. Neurosci.* **37**, 4416-4426 (2017).

Friedman, D. & Strowbridge, B. W. Both electrical and chemical synapse mediate fast network oscillations in the olfactory bulb. *J Neurophysiol.* **89**, 2601-2610 (2003)

Fukunaga, I., Herb, J. T., Kollo, M., Boyden, E. S., Schaefer, A. T. Independent control of gamma and theta activity by distinct interneurons networks in the olfactory bulb. *Nat Neurosci.* **17**, 1208-1216 (2014)

Ganesh, A., Bogdanowicz, W., Haupt, M., Marimuthu, G. & Rajan, K. E. Role of olfactory bulb serotonin in olfactory learning in the grater short-nosed fruit bat, Cynopterus sphinx (Chiroptera: Pteopodidae). *Brain Res.* **1352**, 108-117 (2010)

Graeff, F. G.& Silverira Filho, N. G. Behavioral inhibition induced by electrical simulation of the median raphe nucleus of the rat. *Physiol Behav.* **21**, 477-484 (1978)

Grosmaitre, X., Santarelli, L. C., Tan, J., Luo, M., & Ma, M. Dual functions of mammalian olfactory sensory neurons as odor detectors and mechanical sensors. *Nat Neurosci* **10**, 348-354 (2007)

Gold, J. I. & Shadlen, M. N. The neural basis of decision making. *Annu. Rev. Neurosci.* **30**, 535-574 (2007)

Gschwend, O., Abraham, N. M., Lagier, S., Begnaud, F., Rodriguez, I., & Carleton, A. Neuronal pattern separation in the olfactory bulb improves odor discrimination learning. *Nat. Neurosci.* **18** 1474-1482 (2015).

Guerin, D., Peace, S. T., Didier, A., Linster, C. & Cleland, T. A. Noradrenergic neurmodulation in the olfactory bulb modulates odor habituation and spontaneous discrimination. *Behav Neurosci.* **122**: 816-826 (2008)

Hardy, A., Palouzier-Paulignan, B., Duchamp, A., Royet, J. P. & Duchamp-Viret, P. 5-Hydroxytryptamine action in the rat olfactory bulb: in vitro electrophysiological patch-clamp recordings of juxtaglomerular and mitral cells. *Neuroscience* **131**, 717-731 (2005).

Hayar, A., Karnup, S., Shipley, M. T., & Ennis, M. Olfactory bulb glomeruli: external tufted cells intrinsically burst at theta frequency and are entrained by patterned olfactory input. *J Neurosci.* **24**, 1190-1199 (2004)

Hayar A., Shipley, M. T., Ennis, M. Olfactory bulb external tufted cells are synchronized by multiple intraglomerular mechanisms. *J Neurosci*. **25**, 8197-8208 (2005)

Heitz R. P. The speed-accuracy tradeoff: history, physiology, methodology, and behavior. *Front. Neurosci.* 8:150. doi: 10.3389/fnins.2014.00150 (2014).

Heym, J., Trulson, M. E., Jacobs, B. L. Raphe unit activity in freely moving cats: effects of phasic auditory and visual stimuli. *Brain Res.* **232**: 29-39 (1982)

Hornung, J. P. The neuroanatomy of the serotonergic system. In: Handbook of Behavioral Neurobiology of Serotonin (Ed: Muler C. P. & Jacobs, B. L.) Elsevier (2010)

Hurley, L. M. & Hall, I. C. Context-dependent modulation of auditory processing by serotonin. *Hear Res*. **279**, 74-84 (2011)

Hurley, L. M. & Pollak, G. D. Serotonin differentially modulates responses to tones and frequency-modulated sweeps in the inferior colliculus. *J Neurosci.* **19**, 8071-8082 (1999)

Hurley, L. M., Devilbiss, D. M., & Waterhouse, B. D. A matter of focus: monoaminergic modulation of stimulus coding in mammalian sensory networks. *Curr Opin Neurobiol* **14:**, 488-495 (2004)

Isaacson, J. Glutamate spillover mediates excitatory transmission in the rat olfactory bulb. *Neuron* **23**, 377-384 (1999)

Jacobs, B. L. & Azmitia, E. C. Structure and function of the brain serotonin system. *Physiol Rev*. **72**, 165-229 (1992)

Jacobs, B. L. & Fornal, C. A. Activity of serotonergic neurons in behaving animals. *Neuropsychopharmacology* **21,** 9S-15S (1999)

Jiang, M., Griff, E. R., Ennis, M., Zimmer, L. A., & Shipley, M. T. Activation of locus coeruleus enhances the responses of olfactory bulb mitral cells to weak olfactory nerve input. *J Neurosci*. **16,** 6319-6329 (1996)

Kapoor, V., Provost, A. C., Agarwal, P. & Murthy, V. N. Activation of raphe nuclei triggers rapid and distinct effects of parallel olfactory bulb output channels. *Nat. Neurosci.* **19**, 271-282 (2016).

Kang, T. C., Lee, J. C., Choi, K. Y., Park, S. K., Jeong, Y. G., Jo, S. M., Won, M. H. Distribution of serotonin immunoreactivity in the main olfactory bulb of the Mongolian gerbil. *Anat Histol Embryol* **30**, 117-120 (2001)

Kawano, H., Decker, K., & Reuss, S. Is there a direct retina-raphe-suprachiasmatic nucleus pathway in the rat? *Neurosci Lett.* **212**, 143-146 (1996)

Kiyokage, E., Pan, Y. Z., Shao, Z., Kobayaski, K., Szabo, G., Yanagawa, Y., Obata, K., Okano, H, Toida, K., Puche, A. C., & Shipley, M. T. Molecular identify of periglomerular and short axon cells. *J Neurosci*. **20**, 1185-1196 (2010)

Klepper, A. & Herbert, H. Distribution and origin of noradrenergic and serotonergic fibers in the cochlear nucleus and inferior colliculus of the rat. *Brain Res.* **557**, 190-201 (1991)

Kloppenburg, P & Erber, J. The modulatory effects of serotonin and octopamine I the visual system of the honey bee (*Apis mellifera* L.) II: Electrophysiological analysis of motion-sensitive neurons in the lobula. *J Comp Physiol A* **176**, 119-129 (1995)

Kloppenburg, P. & Mercer, A. R. Serotonin modulation of moth central olfactory neurons. *Annu Rev Entomol.* **53**, 179-190 (2008)

Kuznetsova, A., Brockhoff, P. B. & Haubo Bojesen Christensen, R.. lmerTest: Tests for random and fixed effects for linear mixed effect models (lmer objects of lme4 package). R package version 2.0-6. (2014).

Lagier, S., Carleton, A., & Lledo, P. M. Interplay between local GABAergic interneurons and relay neurons generates gamma oscillations in the rat olfactory bulb. *J Neurosci.* **24**: 4382-4392 (2004)

Langdon, P. E., Harley, C. W., & McLean, J. H. Increased beta adrenoceptor activation overcomes conditioned olfactory learning deficits induced by serotonin depletion. *Brain Res Dev Brain Res.* **102**, 291-293 (1997)

Laurent, G., Stopfer, M., Friedrich, R. W., Rabinovich, M. I., Vokovskii, A. & Abarbanel, H. D. Odor encoding as an active, dynamical process: expriments, computation, and theory. *Annu. Rev. Neurosci.* **24**, 263-297 (2001).

Leon, M. & Johnson, B. A. Olfactory coding in the mammalian olfactory bulb. *Brain Res. Brain Res. Rev.* **42**, 23-32 (2003).

Lepousez, G, & Lledo, P. M. Odor discrimination requires proper olfactory fast oscillations in awake mice. *Neuron* **80**, 1010-1024 (2013)

Lesch, K. P. & Waider, J. Serotonin in the modulation of neural plasticity and networks: implications for neurodevelopmental disorders. *Neuron* **76**, 175-191 (2012)

Linster, C. & Cleland, T. A. Glomerular microcircuits in the olfactory bulb. *Neural Netw.* **22**, 1169-1173 (2009)

Linster, C. & Fontanini, A. Functional neuromodulation of chemosensation in vertebrates. *Curr. Opin. Neurobiol.***29**, 82-87 (2014).

Liu, S., Aungst, J. L., Puche, A. C. & Shipley, M. T. Serotonin modulates the population activity profile of olfactory bulb external tufted cells. *J. Neurophysiol.* **107**, 473-483 (2012).

Lowry, C. A., Rodda, J. E., Lightman, S. L. & Ingram, C. D. Corticotropin-releasing factor increases in vitro firing rates of serotonergic neurons in the rat dorsal raphe nucleus: evidence for activation of a topgraphically organized meolimbocortical serotonergic system. *J Neurosci.* **20**, 7728-7736 (2000)

Maier, S. F. & Watkins, L.R. Stressor controllability and learned helplessness: the roles of the dorsal raphe nucleus, serotonin, and corticotropin-releasing factor. *Neurosci Biobehab Rev.* **29**, 829-841 (2005)

Mandairon, N., Ferreti, C. J., Stack, C. M., Rubin, D. B., Cleland, T. A., & Linster, C. Cholinergic modulation in the olfactory bulb influences spontaneous olfactory discrimination in adult rats. *Eur Jo Neurosci.* **24**, 3234-3244 (2006)

Mandairon, N., Peace, S., Karnow, A., Kim, J., Ennis, M. & Linster, C. Noradrenergic modulation in the olfactory bulb influences spontaneous and reward-motivated discrimination, but not the formation of habituation memory. *Eur. J. Neurosci.* **27**, 1210-1219 (2008).

Margrie, T. & Schaefer, A. T. Theta oscillation coupled spike latencies yield computational vigour in a mammalian sensory system. *J. Physiol.* **546** 363-374 (2003).

McIntyre, A. B. & Cleland, T. A. Biophysical constraints on lateral inhibition in the olfactory bulb. *J Neurophsyiol* **115**, 2937-2949 (2016)

Mclean, J. H. & Harley, C. W. Olfactory learning in the rat pup: a model that may permit visualization of a mammalian memory trace. *Neuroreport* **15**, 1691-1697 (2004)

McLean, J. H. & Shipley, M. T. Serotonergic afferents to the rat olfactory bulb I. Origins and laminar specificity of serotonergic inputs to the adult rat. *J Neurosci.* **7**, 3016-3028 (1987)

McLean, J. H., Darby-King, A., Sullivan, R. M., & King, S. R. Serotonergic influence on olfactory learning in the neonate rat. *Behav. Neural Biol* **60**, 152-162 (1993)

McLean, J. H., Darby-King, A., & Paterno, G. D. Localization of 5-HT2A receptor mRNA by in situ hybridization in the olfactory bulb of the postnatal rat. *J Comp Neurol*. **353**, 371-378 (1995)

McLean, J. H., Darby-King, A., & Hodge, E. 5-HT2 receptor involvement in conditioned olfactory learning in the neonate pup. *Behav Neurosci.* **110**, 1426-1434 (1996)

Miyazaki, K., Miyazaki, K. W., & Doya, K. Activation of dorsal raphe serotonin neurons underlies waiting for delayed rewards. *J Neurosci.* **31**, 469-479 (2011a)

Miyazaki K. W., Miyazaki, K., & Doya, K. Activation of the central serotonergic system in response to delayed by not omitted rewards. *Eur J Neurosci* **33**, 153-160 (2011b)

Mooney, R. D., Huang, X., Shi, M. Y., Bennett-Clarke, C. A., & Rhoades, R. W. Serotonin modulates retinotectal and corticotectal convergence in the superior colliculus *Prog. Brain Res.* **112**, 57-69 (1996)

Morin, D., Sapena, R., Zini, R., & Tillement, J. P. Serotonin enhances the beta-adrenergic response in rat brain cortical slices. *Eur. J. Pharmacol.* **225**, 273-274 (1992)

Moriizumi, T., Tsukatani, T., Sakashita, H. & Miwa, T. Olfactory disturbance induced by deafferentation of serotonergic fibers in the olfactory bulb. *Neuroscience* **61**, 733-738 (1994)

Nakamura, K., Matsumoto, M.,& Hikosaka, O. Reward-dependent modulation of neuronal activity in the primate dorsal raphe nucleus. *J Neurosci*. **28**, 5331-5343 (2008)

Neville, K. R. & Haberly, L. B. Beta and gamma oscillations in the olfactory system of the urethane-anesthetized rat. *J Neurophysiol*. **90**, 3921-3930 (2003)

Nunes, D. & Kuner, T. Disinhibition of olfactory bulb granule cells accelerates odour discrimination in mice. *Nat. Commun.* **6**:8950 (2015).

Nusser, Z., Kay, L. M., Laurent. G., Homancis, G. E., Mody, I. Disruption of GABAA receptors on GABAergic interneurons leads to increased oscillatory power in the olfactory bulb network. *J Neurophysiol* **86**, 2823-2833 (2001)

Ogawa, S. K., Cohen, J. Y., Hwang, D., Uchida, N., Watabe-Uchida, M. Organization of monsynaptic inputs to the serotonin and dopamine neuromodulatory systems. *Cell Rep*. **8**, 1105-1118 (2014)

Paspalas, C. D., & Papadopoulos, G. C. Serotonergic afferents preferentially innervate distinct subclasses of peptidergic interneurons in the rat visual cortex. *Brain Res*. **891**, 158-167 (2001)

Petzold, G., Hagiwara, A., & Murthy, V. N. Serotonergic modulation of odor input ot the mammalian olfactory bulb. *Nat Neurosci*. **12**, 784-791 (2009)

Pifferi, S., Memini, A., & Kurahashi, T., Signal transduction in vertebrate olfactory cilia. In: The Neurobilogy of Olfaction. Boca Raton (FL): CRC Press/Taylor & Francis (2010)

Pinching, A. J. & Powell, T. P. The neuron types of the glomerular layer of the olfactory bulb. *J Cell Sci.* **9**, 305-345 (1971)

Pressler, R. T., Inoue, T. & Strowbridge, B. W. Muscarinic receptor activation modulates granule cell excitability and potentiates inhibition onto mitral cells in the rat olfactory bulb. *J Neurosci.* **27**, 10969-10981 (2007)

Puopolo, M., & Belluzzi, O. NMDA-dependent, network-driven oscillatory activity induced by bicuculline or removal of Mg2+ in rat olfactory bulb neurons. *Eur. J Neurosci*. **13**, 92-102 (2001)

Nakamura, K., Matsumoto, M. & Hikosaka, O. Reward-dependent modulation of neuronal activity in the primate dorsal raphe nucleus. *J Neurosci.* **28**, 5331-5343 (2008)

Ranade, S. P. & Mainen, Z. Transient firing of dorsal raphe neurons encodes diverse and specific sensory, motor, and reward events. *J Neurophysiol* **102**, 3026-3037 (2009)

Ravel, N., Elaagouby, A., & Gervais, R. Scopolamine injection into the olfactory bulb impairs short-term olfactory memory in rats. *Behav. Neurosci.* **108**, 317-324 (1994)

Ray, S. & Maunsell, J. Different origins of gamma rhythm and high-gamma activity in macaque visual cortex. *PLoS Biol* **9**, e1000610 (2011)

Rinberg, D., Koulakov, A. & Gelperin,A. Speed-accuracy tradeoff in olfaction. *Neuron* **51,** 351-358 (2006).

Rojas-Libano, D. & Kay, L.M. **2** system gamma oscillations: the physiological dissection of a cognitive neural system. *Cogn Neurodyn* **2**, 179-194 (2008)

Rojas-Libano, D. & Kay, L.M. Interplay between sniffing and odorant sorptive properties in the rat. *J. Neurosci.* **32**, 15577-15589 (2012).

Rospars, J. P., Lanksy, P., Duchamp-Viret, P., & Duchamp, A. Spiking frequency versus odorant concentration in olfactory receptor neurons. *Biosystems **58** 133-141* (2000)

Schmidt, L. J. & Strowbridge, B. W. Modulation of olfactory bulb network activity by serotonin: synchronous inhibition of mitral cells mediated by spatially localized GABAergic microcircuits. *Learn. Mem.* **21**,40-416 (2014).

Schweimer, J. V. & Ungless, M. A. Phasic responses in dorsal raphe serotonin neurons to noxious stimuli. *Neuroscience* **171**, 1209-1215 (2010)

Schoppa, N.E. & Westbrook, G. L. Glomerulus-specific synchronization of mitral cells in the olfactory bulb. *Neuron* B31B, 639-651 (2001)

Sellers, K. K., Bennet, D V., & Frohlich, F. Frequency-band signatures of visual responses to naturalistic input in ferret primary visual cortex during free viewing. *Brain Res.* **1598**, 31-45 (2013)

Shepherd, G. Synaptic organization of the mammalian olfactory bulb. *Physiol Rev.* **52**, 864-917 (1972)

Shin, R. & Ikemoto, S. The $GABA_B$ receptor agonist baclofen administered into the median and dorsal raphe nuclei is rewarding as shown by intracranial self-administration and conditioned place preference in rats. *Psychopharmacology (Berl.)* **208**, 545-554 (2010)

Slotnick, B. Odor-sampling time of mice under different conditions. *Chem. Senses.* **32**, 445-454 (2007).

Soubrie, P. Reconciling the role of central serotonin neurons in human and animal behavior. *Behav Brain Res*. **9**, 319-364 (1986)

Soucy, E. R., Albeanu, D. F., Fantana, A. L., Murthy, V. N., & Meister, M. Precision and diversity in an odor map on the olfactory bulb. *Nat. Neurosci*. **12**, 210-220 (2009)

Suzuki, Y., Kiyokage, E., Sohn, J., Hioki, H., & Toida, K. Structural basis for serotonergic regulation of neural circuits in the mouse olfactory bulb. *J Comp Neurol.* **523**, 262-280 (2015)

Steinfeld, R., Herb, J. T., Sprengel, R., Schaefer, A. T., & Fukunaga, I. Divergent innervation of the olfactory bulb by distinct raphe nuclei. *J Comp Neurol*. **523**, 805-813 (2015)

Uchida, N. & Mainen, Z. F. Speed and accuracy of olfactory discrimination in the rat. *Nat. Neurosci.* **6**, 1224-1229 (2003).

Urban, N. Lateral inhibition in the olfactory bulb and in olfaction. *Physiol. Behav.* **77**

Vertes, R. P. A PHA-L analysis of ascending projections of the dorsal raphe nucleus in the rat. *J Comp Neurol* **313**, 643-668 (1991)

Wachowiak, M. & Shipley, M. Coding and synaptic processing of sensory information in the glomerular layer of the olfactory bulb. *Semin Cell Dev Biol* **17**,411-423 (2006)

Willhite, D. C., Nguyen, K. T., Masurkar, A. V., Greer, C. A., Shepherd, G. M., Chen, W. R. Viral tracing identifies distributed columnar organization in the olfactory bulb. *Proc Natl Acad USA* **103**, 12592-12597 (2006)

Wright, D. E., Seroogy, K. B., Lundgren K. H., Davis, B. M. & Jennes, L. Comparative localization of serotonin1A, 1C, and 2 receptor subtype mRNAs in rat brain. *J Comp Neurol*. **351**, 357-373 (1995)

Xiang, Z., & Prince, D. A. Heterogeneous actions of serotonin on interneurons in rat visual cortex. *J Neurophysiol*. **89**, 1278-1287 (2003)

Ye, Y. & Kim, D. O. Connections between the dorsal raphe nucleus and a hindbrain region consisting of the cochlear nucleus and neighboring structures. *Acta Otolaryngol*. **121**, 284-288 (2001)

Yokogawa T., Hannan, M. C., & Burgess, H. A. The dorsal raphe modulates sensory responsiveness during arousal in zebrafish *J Neurosci*. **32**, 15205-15215 (2012)

Yuan, Q., Harley, C. W., & McLean, J. H. Mitral cell beta1 and 5-HT2A receptor colocalization and cAMP coregulation: a new model of norepinephrine-induced learning in the olfactory bulb. *Learn Mem.* **10**, 5-15 (2003)

Zariwala, H., Kepecs, A., Uchida, N., Hirokawa, J. & Mainen, Z. F. The limits of deliberation in a perceptual decision task. et al. 2013 *Neuron* **78**, 339-351 (2013).